EXPERIMENTAL INVESTIGATION INTO PERFORMANCE OF ELECTROCHEMICAL JET MACHINING (EJM) FOR IMPROVEMENT OF SURFACE FINISH OF Ti6Al4V

By

ARINDAM MAITY

B.E. Mechanical Engineering

Jadavpur University

Kol-700032

Examination Roll No-**M4PRD23006**

Registration No.-**147684 (2018-2019)**

THESIS

SUBMITTED IN PARTIAL FULFILLMENT OF THE REQUIREMENT FOR THE AWARD OF THE DEGREE OF MASTER OF PRODUCTION ENGINEERING IN THE FACULTY OF ENGINEERING AND TECHNOLOGY,

JADAVPUR UNIVERSITY

DEPARTMENT OF PRODUCTION ENGINEERING

JADAVPUR UNIVERSITY

KOLKATA-700032

JADAVPUR UNIVERSITY FACULTY OF ENGINEERING AND TECHNOLOGY

CERTIFICATE OF RECOMMENDATION

I HEREBY RECOMMEND THAT THE THESIS ENTITLED "**EXPERIMENTAL INVESTIGATION INTO PERFORMANCE OF ELECTROCHEMICAL JET MACHINING (EJM) FOR IMPROVEMENT OF SURFACE FINISH OF Ti6Al4V**" CARRIED OUT UNDER MY/OUR GUIDANCE BY MR. ARINDAM MAITY MAY BE ACCEPTED IN THE PARTIAL FULFILLMENT OF THE REQUIREMENTS FOR THE DEGREE OF "MASTER OF PRODUCTION ENGINEERING".

Countersigned

Thesis Advisors

_____

(Prof. Bijoy Bhattacharya)
Professor,
Dept. of Production Engineering
Jadavpur University
Kolkata-700032

_____

HEAD,
Dept. of Production Engineering
Jadavpur University
Kolkata-700032

_____

(Prof. Souren Mitra)
Professor,
Dept. of Production Engineering
Jadavpur University
Kolkata-700032

_____

DEAN,
Faculty of Engineering and Technology
Jadavpur University
Kolkata-700032

JADAVPUR UNIVERSITY

FACULTY OF ENGINEERING AND TECHNOLOGY

CERTIFICATE OF APPROVAL*

The foregoing thesis is hereby approved as a creditable study of an engineering subject carried out and presented in a manner satisfactory to warrant its acceptance as a prerequisite to the degree for which it has been submitted. It is understood that by this approval, the undersigned do not necessarily endorse or approve any statement made, opinion expressed and conclusion drawn therein but thesis only for the purpose for which it has been submitted.

_____

(External Examiner)

COMMITTEE ON FINAL EXAMINATION FOR EVALUATION OF THE THESIS

_____

_____

(Internal Examiner)

*only in case the recommendation is concurred in

ACKNOWLEDGEMENT

I would like to express my heartfelt gratitude and appreciation to everyone who has contributed to the completion of my thesis. Their guidance, support, and encouragement have been instrumental in making this journey a fulfilling one.

First and foremost, I extend my deepest thanks to my esteemed guides, Prof. Bijoy Bhattacharya and Prof. Souren Mitra . Your expertise, patience, and unwavering commitment to excellence have been invaluable throughout this research endeavor. Your guidance and insightful feedback have shaped my understanding and enhanced the quality of my work. I am truly grateful for your mentorship and the trust you placed in me.

I would also like to extend my sincere appreciation to the fellow PhD scholars who have been an integral part of my academic journey. Your camaraderie, discussions, and exchange of ideas have been intellectually stimulating and have broadened my perspectives. I am thankful for your support and for being a part of this remarkable community.

Furthermore, I would like to offer a special note of gratitude to my parents Mr. Sukanta Maity and Mrs Pampa Maity. Their unwavering support, love, and belief in my abilities have been the driving force behind my accomplishments. Their sacrifices and encouragement throughout my academic pursuits have been the cornerstone of my success. I am eternally grateful for their constant motivation and for instilling in me the values of perseverance and determination.

Lastly, I would like to express my appreciation to all the individuals who have provided assistance, whether directly or indirectly, in the completion of this thesis. Your contributions, whether through insightful discussions, technical support, or moral encouragement, have been immensely valuable.

To everyone mentioned above and to those who may not be named but have played a significant role in shaping my academic journey, I extend my deepest appreciation. Your support has been invaluable, and I am truly grateful for your presence during my project.

ARINDAM MAITY
CLASS ROLL NO- **002111702004**
Examination Roll No-**M4PRD23006**

TABLE OF CONTENT

CHAPTER 1

1. INTRODUCTION

Electrochemical jet machining (EJM) is a non-traditional machining process that uses electrochemical dissolution to remove material from a workpiece. In EJM, a high-pressure jet of electrolyte is directed at the workpiece, and an electric current is passed through the electrolyte. The current causes the workpiece material to anodically dissolve,

at the point of impact of the jet, and the material is carried away by the electrolyte. EJM is a versatile process that can be used to machine a wide variety of materials, including metals and metal composites. It is particularly well-suited for machining complex shapes and for machining materials that are difficult to machine using traditional methods. EJM has a number of advantages over traditional machining methods. It is a non-contact process, which means that there is no wear on the cutting tools. It is also a very precise process, and it can be used to produce very fine finishes. EJM is a relatively new process, but it is rapidly gaining popularity in a wide range of industries.

1.1 Overview of Electrochemical Machining Process

Electrochemical machining (ECM) is a machining process that operates on the principles of Faraday's electrolysis, without requiring direct contact between the tool and workpiece. For ECM to work effectively, both the tool and workpiece must possess electrical conductivity. The tool functions as the cathode and is connected to the negative terminal, while the workpiece serves as the anode and is connected to the positive terminal during the electrolysis process.

By applying a specific voltage across the tool and workpiece interface in the presence of an electrolyte, material removal occurs through anodic dissolution. The metal from the workpiece dissolves into the electrolytic solution at the anode in the form of atoms. As the tool approaches the workpiece, it erodes the workpiece's negative shape, resulting in the machined profile acquiring the inverse shape of the tool.Notably, the material removal in ECM takes place primarily through the dissolution of the workpiece with the assistance of the electrolyte, eliminating the need for mechanical forces or physical contact during the machining process.

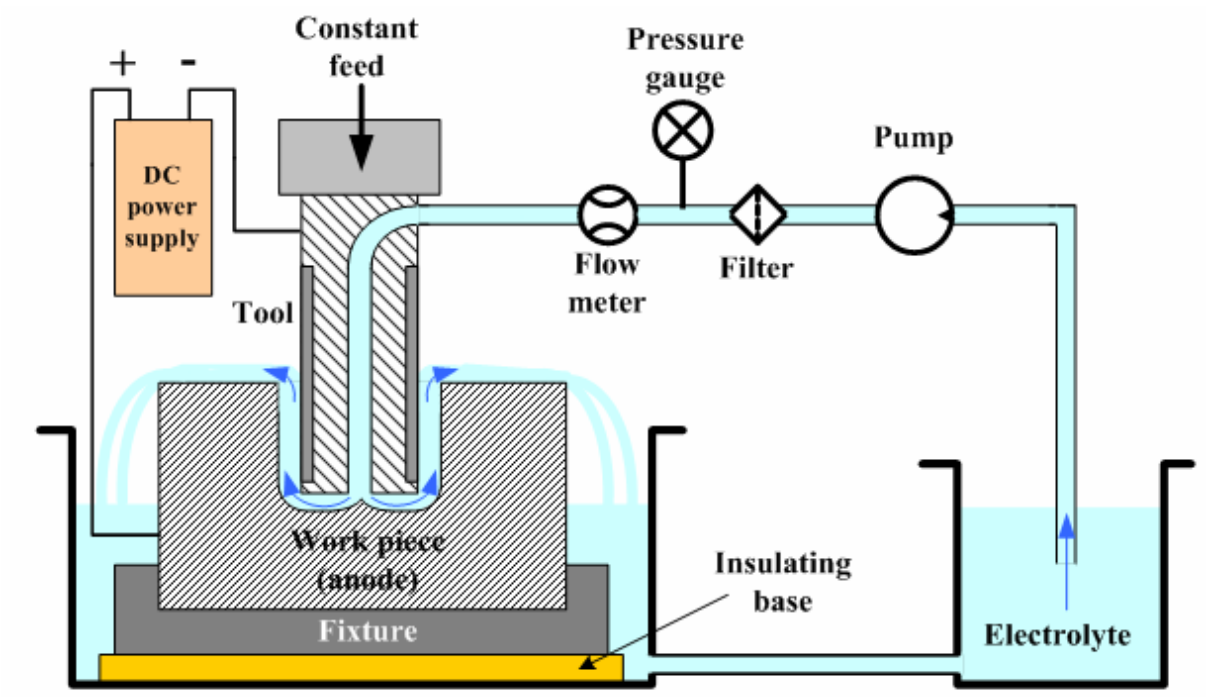

Fig. 1.1 Schematic diagram of ECM

The diagram presented in Figure 1.1 illustrates the essential components and process of electrochemical machining (ECM). The electrolyte is carefully directed from the electrolyte chamber towards the tool-workpiece interface by means of a pump. Subsequently, a specific voltage is applied between the tool and workpiece, initiating the electrochemical machining procedure. The initial inter-electrode gap (IEG) holds significant importance within the ECM process. Maintaining a constant feed of tools from the starting IEG ultimately leads to a consistent gap. It is crucial to establish an appropriate initial inter-electrode gap to prevent the tool from coming into direct contact with the workpiece, which can result in sudden sparking. Such sparks can potentially cause damage to both the workpiece and the tool. During the machining process, any sludge generated is effectively removed through electrolyte filtration. Following this filtration step, the electrolyte is thoroughly cleansed and prepared for reuse.

1.2 Various Advanced Electrochemical Machining Processes

1.2.1 On the basis of the dimension of the final machining zone and tool used

ECM can be classified into three categories as far as the dimension of the final machined zone is concerned – Macro ECM, Micro ECM, Nano ECM

(i) Macro Electrochemical Machining

The mandatory voltage and current requirements for macro-range Electrochemical Machining (ECM) typically fall within the range of 10-30 V and 150-1000 A respectively. The current

density typically ranges from 20-200 A/cm², while the machining rate generally ranges from 0.2-10 mm/min. When the dimensions of the features produced by the electrochemical process on the workpiece exceed 1mm, the process is referred to as macro electrochemical machining. This technique is commonly employed in the production of turbine and compressor blades. In order to achieve the desired range of tolerances, it is sometimes necessary to subject a roughly cut part to an additional ECM process. Large tools are used for this purpose, and complex shape cant be generated, only mirror shapes can be generated from this process. For the purpose of surface polishing and hardening, Electrochemical Polishing (EP) is performed using a water-based solution. Over time, sophisticated servo systems and feedback controllers have been developed, resulting in improved accuracy in macro-ECM processes.

(ii) Electrochemical Micromachining

The voltage recommended for electrochemical micromachining (EMM) is typically below 10V. Although the current density in EMM ranges from 75-100A/cm², the required current is less than 1A due to the minimal surface area of the tool involved. The achievable machining rate in EMM is approximately 5μm/min. Electrochemical micro machining (EMM) refers to the removal of materials through electrochemical dissolution at extremely small dimensions ranging from 1μm to 999μm. The tool used here is on the scale of 50-100 μm .

EMM necessitates an advanced high-frequency pulsed power supply to provide pulse DC power input, as well as X-Y-Z stage controllers for precise movement of the micro tool in relation to the workpiece. The applications of EMM span various industries such as aerospace, automobile, and electronics. It is also widely utilized in the development of sensors, micro electro mechanical systems (MEMS), and biomedical applications.

(iii) Nano Electrochemical Machining

The design and fabrication of features on small objects or products through electrochemical processes within the dimension range of 100 nm to 0.1 nm fall under the category of Nano electrochemical machining (Nano-ECM). Nano products are created by manipulating deposition, dissolution, and modification of electrochemical reactions, which involve both ion transfer and electron transfer reactions. In the Nano range, the significance of molecular motion and quantum effects during the process becomes pronounced, owing to the molecular dimensions involved. To achieve precise nanoscale motions in electrochemical machining in the Nano range, piezo-driven systems are employed instead of mechanical-driven systems like the X-Y-Z stage. The use of piezo-driven systems allows for finer control and manipulation of

nanoscale movements required for the fabrication process. For this process nano scale tools are used, i.e. AFM stylus.

Nano-ECM represents an important field where the understanding and utilization of molecular dynamics and quantum effects play a pivotal role in achieving the desired nanoscale features and properties.

1.2.2 On the basis of different machining processes

Electrochemical machining (ECM) is a non-traditional machining process that uses an electric current to remove material from a workpiece. The workpiece is made the anode of an electrochemical cell, and a tool or electrode is made the cathode. When a voltage is applied to the cell, an electric current flows between the workpiece and the electrode. This current causes the metal at the workpiece surface to dissolve, and the dissolved metal is carried away by the electrolyte.

There are several different types of electrochemical machining processes, each with its own advantages and disadvantages.

(i) Electrochemical turning: This process is used to machine cylindrical parts. The electrode is shaped to the desired profile of the part, and it is rotated as it is fed into the workpiece.

(ii) ECM drilling: This process is used to machine holes in workpieces. The electrode is shaped to the desired diameter of the hole, and it is fed into the workpiece until the hole is complete.

(iii) ECM grinding: This process is used to grind the surface of workpieces. The electrode is shaped to the desired surface profile, and it is fed into the workpiece until the desired surface finish is achieved.

(iv) Wire electrochemical machining (WECM): This process uses a thin wire as the electrode. The wire is fed into the workpiece, and it is eroded away as it cuts the material. WECM is often used to machine complex shapes or to machine materials that are difficult to machine by other methods.

(v) Electrochemical deburring: This process is used to remove burrs from workpieces. The electrode is shaped to the desired profile of the burr, and it is fed into the workpiece until the burr is removed.

(vi) Electrolytic in-process dressing (ELID) grinding: This process is used to dress the grinding wheels in grinding machines. The electrode is shaped to the desired profile of the grinding wheel, and it is fed into the wheel until the desired surface finish is achieved.

EJM is a versatile process that can be used to machine a wide variety of materials. It is often used to machine materials that are difficult to machine by other methods, such as titanium and its alloys, stainless steel, and hardened steel. EJM is also used to machine complex shapes and to machine close tolerances.

1.3 Principle of Electrochemical Jet Machining (EJM) Process

In Electrochemical Jet Machining (EJM), the mechanism of material removal is similar to conventional ECM, where electrochemical dissolution takes place on the anode (workpiece). When a voltage difference is applied between the tool (cathode) and the workpiece (anode), an electrochemical reaction occurs, resulting in the dissolution of material from the workpiece, as discussed in section 1.1.

One of the advantages of the EJM process is that it resolves the complexity of tool shape encountered in ECM. Instead of using a complex-shaped tool, EJM utilizes a simple geometrically shaped tool as the cathode. In this process, the workpiece is connected to the positive terminal, while the tool is connected to the negative terminal of a constant DC power source.

In Figure 1.2, the diagram illustrates the starting position of the machining and the instantaneous position of the tool during the machining process. This demonstrates the movement and positioning of the tool as it carries out the material removal operation in EJM.

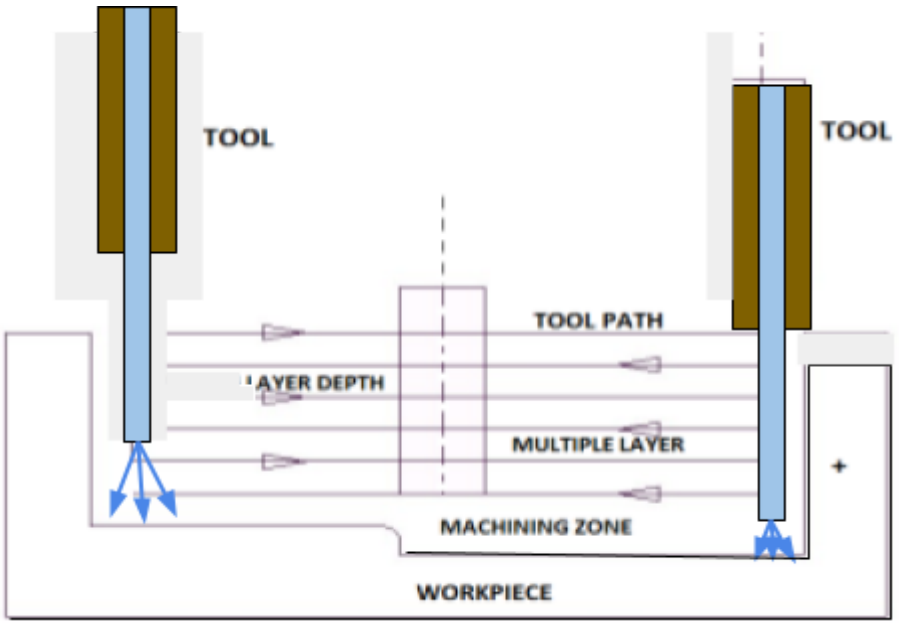

Fig. 1.2 Layer-by-layer method

In Electrochemical Jet Machining (EJM), achieving the desired geometry on the workpiece requires the tool to move at an appropriate speed along a predetermined path. The machining depth in EJM is obtained through multiple downward steps, with the number of layers determined by the amount of material removed in each layer. Similar to other jet machining processes, EJM follows a layer-by-layer approach for material removal.

The tool movement path can be easily modified to alter the shape or profile generated on the workpiece. This flexibility allows for different profiles to be obtained using the same tool. The movement of the tool in the three-axis system can be controlled through a CNC X-Y-Z stage or a control system. For efficient operation, the electrolyte used in EJM should be a highly conductive inorganic salt solution such as sodium chloride (NaCl), sodium bromide (NaBr), or sodium nitrate (NaNO3). The electrolyte is pumped at high pressure through the narrow gap, typically ranging from 0.2 kgf/cm² to 1.1 kgf/cm², while the flow rate typically ranges from 40 to 430 ml/min.

During the machining process, sludge is generated, which is then carried away by the electrolyte in an ultra-granular form. To ensure the electrolyte's cleanliness, it is passed through a filtration unit before being pumped back into the machining zone. This filtration step helps maintain the quality and effectiveness of the electrolyte for subsequent machining operations.

1.4 Difference between EJM with Other Jet Machining Processes

The EJM process is the direct application of electrolysis with the technique of tool movement, the same as water jet machining and Abrasive Jet Machining. The material removal is completely due to electrochemical action. There are many striking similarities between these processes but both the processes can be distinguished easily with the help of the following discussions. A comparison between EJM and other JET MACHINING is shown in Table 1.1 .

Here are the differences between EJM (Electrochemical Jet Machining), AJM (Abrasive Jet Machining), WJM (Water Jet Machining), and PAJM (Plasma Arc Jet Machining):

Table 1.1: Comparison between EJM and other Jet Machining Processes.

Categories	EJM	AJM	WJM	PAJM
Full form Working	Electrochemical Jet Machining	Abrasive Jet Machining	Water Jet Machining	Plasma Arc Jet Machining
Principle Material removal	Electrochemical dissolution using a jet of electrolyte	Material removal by abrasive particles entrained in a high-velocity gas jet	Material removal by a high-velocity jet of water	Material removal by a high-temperature jet of ionized gas
Material removal rate	Low	Medium	Low	High
Surface finish	Good	Poor	Good	Poor
Heat affected zone (HAZ)	None	None	Minimal	Significant
Applicable materials	Conductive materials	Any material	Soft materials	Conductive materials
Equipment cost	High	Medium to low	High to medium	High to medium
Environmental impact	Moderate	High	Low	High
Limitations	Limited to conductive materials and high thickness	Limited to low material removal rates and simple geometries	Limited to soft materials and low material removal rates	Limited to conductive materials , poor surface finish and high equipment cost
Safety	Safe	Safe	Safe	Hazardous
Applications	Medical devices, aerospace, electronics	Prototypes, rapid tooling, jewelry	Stonework, glass, food	Aerospace, defense, medical

1.5 Advantages of EJM

These are additional advantages of the EC JET (EJM) process:

(i) Complex geometries: EC JET allows for the machining of complex geometries without the need for complex tool designs. Unlike conventional ECM, where the tool must mirror the desired profile, EC JET can use a simple-shaped tool to generate any shape of the profile. This simplifies the tooling requirements and expands the possibilities for machining intricate and complex geometries.

(ii) High precision: ECM, including EC JET, can achieve high precision and accuracy in machining. It enables the production of fine features with tight tolerances, making it suitable for applications that require high precision components.

(iii) High material removal rates: ECM, including EC JET, is known for its ability to remove material quickly and efficiently. This leads to higher material removal rates compared to many other machining processes, making it advantageous for applications where productivity is a priority.

(iv) Low surface roughness: ECM processes, including EC JET, can produce very smooth and fine surfaces with low surface roughness. This is beneficial for applications that require high-quality surface finishes, such as aerospace or medical components.

(v) No heat affected zone: Unlike traditional machining processes that generate heat and may introduce a heat-affected zone (HAZ) in the workpiece, ECM, including EC JET, is a non-thermal process. It does not heat the workpiece during machining, eliminating the risk of thermal distortion or undesirable changes in material properties.

(vi) No tool wear: In ECM, the tool electrode does not experience significant wear during the machining process. This allows for extended tool life and the ability to machine a large number of parts without the need for frequent tool replacement.

(vii) Versatility: ECM, including EC JET, is a versatile machining process that can be applied to a wide range of materials, including metals, plastics, and composites. It offers flexibility in material selection for various applications.

(viii) Cost-effectiveness: EC JET can be a cost-effective machining process, especially for the production of complex parts in high volumes. It offers efficient material removal rates and can reduce the need for intricate tooling, resulting in cost savings for manufacturing.

(ix) Formation of oxide layers: During EC JET machining, oxide layers can sometimes be formed on the surface of the workpiece. These oxide layers can provide corrosion resistance and protect the material from environmental degradation. In contrast, in conventional ECM,

the oxide layer can impede further material dissolution. However, in EJM, the oxide layer can be removed at lower voltages.

(x) No residual stress: EJM does not apply mechanical force to remove material, resulting in no residual stress on the workpiece. The mechanical properties of the workpiece remain unaffected after machining, which is advantageous for applications where material integrity is critical.

1.6 Various Challenges in EJM Process

The EJM process offers the capability to generate complex profiles; however, there are certain challenges associated with its implementation. These challenges can be addressed through proper understanding and optimization of the process. The specific difficulties encountered in EJM are outlined below:

(i) Generation of complex shapes: EJM allows for the creation of complex profiles using a simple-shaped electrode. The key requirement is precise control of the tool's movement along a predetermined path. Achieving an accurate profile necessitates the use of highly accurate position or motion controllers, resulting in increased setup costs.

(ii) Development of leak-proof arrangements: EJM operates at high pressure within the tube, making it challenging to establish leak-proof systems, particularly at joint locations that are prone to leakage.

(iii) Electrolyte selection: The choice of electrolyte plays a critical role in the success of the EJM process. The electrolyte must possess electrical conductivity to facilitate the dissolution of the workpiece material. It should also be non-corrosive to both the workpiece and the machine.

(iv) Electrolyte flow rate: Sufficient electrolyte flow rate is necessary to flush away reaction by-products and maintain a stable electrical field during the EJM process.

(v) Tool electrode nozzle design: The design of the nozzle is crucial for achieving effective electrical contact with the workpiece and producing the desired surface finish.

(vi) Process control: EJM is sensitive to various parameters, including electrolyte composition, flow rate, voltage, and current. These parameters must be carefully controlled to ensure the production of high-quality parts.

Despite these challenges, EJM remains a versatile and powerful machining process capable of producing high-quality parts with complex geometries. With proper attention to these difficulties and optimization of the process parameters, EJM can deliver excellent results.

1.7 Different Applications of the EJM Process

The increasing global demand for manufacturing has led to the need for advanced manufacturing processes that can meet the requirements of various industries. EJM, with its versatility and capability to generate complex profiles, finds significant applications in different sectors. Some specific applications of EJM are highlighted below:

Micro-Machining: EJM is often used for micro-machining applications where precision and intricate shapes are required, such as microfluidic devices, microelectronics components, and medical implants.

Aerospace Industry: EJM can be used to shape and finish complex aerospace components like turbine blades, fuel injector nozzles, and other high-precision parts.

Medical Device Manufacturing: EJM is employed in manufacturing medical devices like stents, catheters, and surgical tools, where precision and smooth surface finish are critical.

Tool and Die Making: EJM can be used to create intricate molds, dies, and tooling for industries such as automotive, plastic injection molding, and sheet metal forming.

Electronics Industry: EJM can help in manufacturing electronic components like printed circuit boards (PCBs), semiconductor components, and connectors with high precision and without inducing heat damage.

Automotive Industry: EJM can be applied to shape and finish components like fuel injection nozzles, gears, and transmission parts with high accuracy and reduced wear.

Jewelry Manufacturing: EJM can be used to create intricate and detailed designs on precious metals and gemstones.

Surface Texturing: EJM can be used for creating various surface textures, patterns, and designs on materials for aesthetic or functional purposes.

Rapid Prototyping: EJM can aid in rapid prototyping by producing intricate and precise prototypes of various parts and products.

Fuel Cell Manufacturing: EJM can be employed in shaping and finishing components of fuel cells, which require high precision and intricate designs.

Optical Component Fabrication: EJM can be used to create optical components such as lenses, mirrors, and prisms with precise shapes and smooth surfaces.

Nuclear Industry: EJM can be used for machining radioactive materials, as the process is non-contact and doesn't generate heat, minimizing the risks associated with traditional machining methods.

These applications highlight the versatility of Electrochemical Jet Machining across a wide range of industries that require precision machining and intricate designs.

1.8 EJM of Titanium-Based Alloy

Titanium alloy is highly regarded in the manufacturing industry and finds extensive use in various sectors such as aerospace, chemical processing, medicine, power generation, marine and offshore, sports and leisure, and transportation. It is the fourth most abundant metallic element and the ninth most abundant element in the Earth's crust. The unique properties of titanium and its alloys make them suitable for a wide range of modern applications. One of the major advantages of titanium-based superalloys is their ability to retain their mechanical properties at high temperatures, earning them the designation of high-strength temperature-resistant (HSTR) alloys. These alloys are particularly valued for their usage in gas turbine blades, where they exhibit exceptional strength at temperatures exceeding 400°C. Titanium alloy has a density of approximately 4420 kg/m³, a Young's modulus of 120 GPa, and a tensile strength of 1000 MPa. Conventional machining processes often face limitations due to the challenging nature of tool materials when working with titanium alloys. However, electrochemical machining (ECM) benefits from titanium alloy's high electrical conductivity and electrochemical equivalent, making it an advantageous method for machining this material. While controlling anodic dissolution in ECM of titanium alloys can be a major challenge, the sludge generated during the process is typically electrochemically nonconductive and does not hinder the dissolution process. The material removal in ECM is directly related to the electrochemical equivalence, allowing titanium alloys to be effectively machined through electrochemical dissolution. Consequently, EJM is well-suited for generating complex, three-dimensional contour profiles in titanium alloys.

Titanium alloys possess excellent flexibility due to their low modulus of elasticity, and they are highly biocompatible compared to other materials. These properties have led to their widespread use in various applications. EJM, with its ability to generate three-dimensional surface profiles independent of mechanical properties, proves to be a suitable method for machining titanium alloys. The working principle of EJM on titanium alloys aligns with that

of general EJM, and the subsequent sections will delve into the process and challenges of EJM on titanium alloys in detail.

Properties of Ti6Al4V

For this study, the workpiece selected was titanium alloy grade V, commonly known as Ti6Al4V. The workpiece had a thickness of 5mm and dimensions of 30mm by 50mm. Ti6Al4V is recognized as a high strength temperature resistant alloy and is widely used in various applications. Before conducting the experiments, it is crucial to determine the precise composition of the alloy. The composition of Ti6Al4V is typically specified in terms of weight percentage and atomic percentage for the constituent elements. The actual composition of Ti6Al4V alloy used in this study is presented in Table 1.2, indicating the weight percentage and atomic percentage of titanium, aluminum, and vanadium. These elements contribute to the overall composition of the alloy, with titanium comprising 90% by weight and 84% by atomic weight, aluminum accounting for 6% by weight and 11% by atomic weight, and vanadium constituting 4% by weight and 5% by atomic weight.

Table 1.2: Composition of Ti6Al4V Alloy

Elements of alloy	Weight basis	Atomic weight basis
Ti	90%	84 %
Al	6%	11%
V	4%	5%

Having an accurate understanding of the alloy composition is crucial for ensuring reliable and consistent experimental results throughout the study.

Different mechanical and electrical properties of the Ti6Al4V grade V alloy are shown in Table 1.3.

Table 1.3 Different properties of Ti6Al4V alloy

Property	Value	Units
Atomic volume	0.01	m^3/kmol
Density	4.512	Mg/m^3
Bulk modulus	1250	GPa
Compressive strength	1080	MPa
Ductility	0.18	
Elastic limit	910	MPa
Endurance limit	566	MPa
Fracture toughness	107	$MPa.m^{1/2}$
Hardness	3730	MPa
Modulus of rupture	1080	Mpa
Poisson's ratio	0.37	
Shear modulus	45	GPa
Tensile strength	1200	MPa
Young's modulus	119	GPa
Maximum service temperature	690	K
Melting point	1933	K
Specific heat	570	J/kg.K
Thermal conductivity	7.3	W/m.k

1.8.2 Applications of Titanium Alloy

Titanium is highly resistant to environmental attacks, including pollutants, and can withstand various aggressive environments. This exceptional property has led to its widespread use in different industries:

(i) Aerospace Industry:

Titanium alloys are extensively used in the aerospace industry due to their high temperature performance, strength, creep resistance, and favorable metallurgical structure. Titanium is employed in jet engine components, such as rotating applications and fan blades, to enhance efficiency. It is also utilized in airframes for its high strength-to-density ratio.

(ii) Power Generation:

In power generating plants, titanium's corrosion resistance is utilized in thin-walled condenser tubes that can withstand saline, brackish, or polluted cooling mediums. This eliminates the need for corrosion allowances. High strength temperature resistant (HSTR) titanium alloys are used in thermal power plants for blades subjected to high-temperature vapor.

(iii) Petroleum Industry:

Titanium's lightweight nature makes it suitable for pipelines in petroleum exploration and production. It is also an excellent material for deep-sea production risers. Furthermore, its corrosion resistance in seawater makes it ideal for top-side water management systems.

(iv) Automotive Industry:

Titanium is finding applications in the automotive industry, particularly in aftermarket parts and racing markets. Engine components such as connecting rods, valves, valve retainers and springs, rocker arms, and camshafts are made from titanium alloys due to their durability, strength, lightweight nature, and resistance to heat and corrosion.

(v) Computer Industry:

Titanium is a promising substrate for hard disk drives in the computer industry. Compared to aluminum, titanium offers significant advantages. It is non-magnetic, preventing interference with data storage. Its ability to withstand higher temperatures during the coating process improves manufacturing rates. The purity of titanium allows for closer read/write head tolerances, increasing disk capacity.

(vi) Medical Implants:

Titanium's inertness to human body fluids makes it an ideal material for medical implants, including hip and knee replacements. Titanium implants promote bone growth, increasing their longevity compared to other materials. Titanium plates and mesh are commonly used in reconstructive surgery to support broken bones.

(vii) Armor Applications:

The high strength-to-weight ratio of titanium makes it well-suited for armor applications. It is used in protective armor for personnel carriers, tanks, and personal armor vests and helmets

for law enforcement. Titanium-based armor provides increased mobility and improved comfort compared to alternatives.

These diverse applications highlight the versatility, strength, corrosion resistance, and biocompatibility of titanium in various industries.

1.8.3 Limitations of machining of Titanium and its alloys

Titanium and its alloys have unique properties that make conventional machining methods ineffective for these materials. The high strength temperature resistant alloys used in titanium require harder machine tools than the alloy itself, posing a challenge for conventional machining. Conventional machining processes, which involve the removal of material in the form of chips, encounter difficulties with titanium alloys due to the serrated nature of the generated chips, hampering the machining process. As a result, non-conventional machining processes are more suitable for titanium and its alloys.

Non-conventional machining methods such as conventional electrochemical machining, electrical discharge machining (EDM), and wire EDM have been successfully employed to generate various surface profiles and complex features in titanium and its alloys. Main drawback about Ti and its alloys is hotspot formation. Thermal energy-based non-conventional processes face difficulties due to the high melting point temperature of titanium. Mechanical energy-based non-conventional processes are also ineffective as the hardness of the material exceeds the capabilities of these methods. However, electrochemical energy-based machining processes, taking advantage of the high electrical conductivity and electrochemical equivalent of titanium alloys, can be utilized.

Machining titanium alloys through electrochemical machining differs from the process used for commonly used materials due to the tendency of titanium to form a tenacious passive oxide layer. This passive oxide layer, which contributes to titanium's corrosion resistance, presents challenges in the electrochemical machining of this material. The selection of electrolyte, including the type and concentration, plays a crucial role in electrochemical machining of titanium alloys. Careful consideration of the electrolyte is necessary to ensure successful machining of titanium alloys in an electrochemical environment.

CHAPTER 2

2. OVERVIEW OF EJM

Electrochemical Jet Machining (EJM) is a variant of Electrochemical Machining (ECM) that enables the localized removal of conductive materials through the dissolution process (as shown in figure 2.1). EJM differs from ECM in that it utilizes a jet of electrolyte instead of specialized tooling for material removal. By applying an electrical potential between the nozzle (cathode) supplying the electrolyte and the work-piece (anode), anodic dissolution takes place, resulting in material removal.

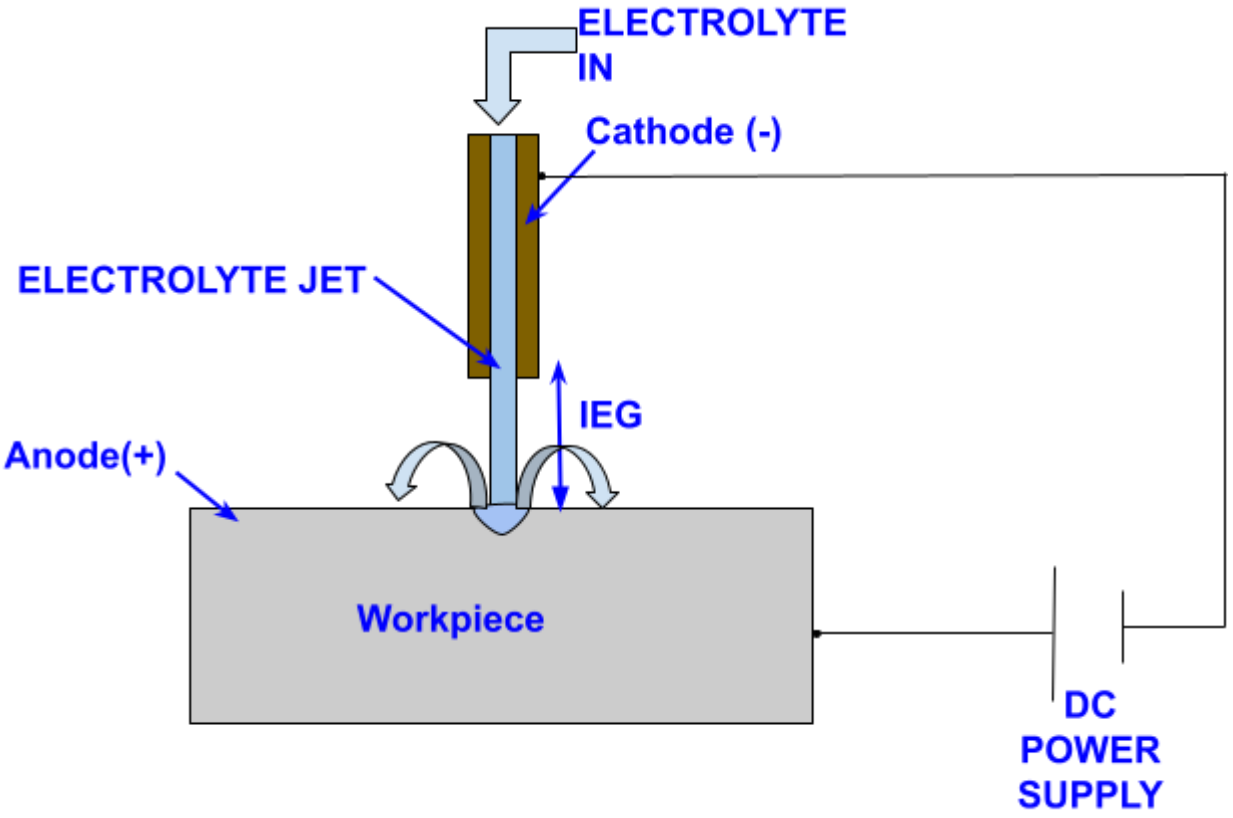

Fig. 2.1:Schematic of Electrochemical Jet Machining

The unique aspect of EJM is that material removal is limited to the area directly below the electrolyte jet, eliminating the need for additional masking. This is achieved by the hydraulic jump phenomenon, where the electrolyte is expelled from the nozzle at a supercritical speed, forming a thin film around the nozzle upon impinging on the work surface. As the film grows shallower due to friction, the hydraulic jump occurs, increasing the thickness of the electrolyte and facilitating localized machining. To further refine the machining process, a compressed air

shroud is directed around the nozzle to constrict the current density field, extending the thin film area and minimizing current stray for more precise machining. The anodic potential of the work-piece plays a crucial role in the performance of EJM, as it enables atomic level dissociation. However, for many Titanium alloys, passivation layers in the form of Titanium dioxides (TiO2) are formed during anodic dissolution, exhibiting high dielectric constant and electrical resistance. These passivating layers hinder material removal, reduce surface finish, and introduce process energy losses known as ohmic overvoltage, caused by the increased resistance of the formed scale. While surface passivating layers can be mechanically removed prior to or after EJM, this adds extra process steps and may be ineffective as oxide layers can reform during processing. In ECM, this issue is addressed through the use of high velocity electrolyte, high initial current, or hybrid processes such as ultrasonic assistance. However, the use of acids in EJM presents safety and waste management concerns, and the application of higher current densities may lead to uncontrolled flashover and arcing between electrodes, damaging the work-piece. Therefore, the exploration of hybrid systems for Titanium machining in EJM is a more favorable option.

2.1 Process Parameters of EJM

EJM, as a modified version of ECM, exhibits several distinct features. To effectively perform EJM, a good understanding of the process fundamentals is necessary. The output of the EJM process is evaluated based on its performance characteristics, and these are influenced by various process parameters. The major process parameters of EJM are as follows:

(i) Applied voltage: The applied voltage is a highly influential parameter in EJM. It helps to overcome the resistance of the electrolyte and facilitates the electrolysis process. A sufficient voltage difference is necessary to overcome the distance between the tool nozzle and work piece. The pre-set voltage determines the rate of electrochemical dissolution, which in turn determines the machining time required to complete the operation.

(ii) Tool scanning rate: The tool scanning rate refers to the speed at which the tool travels over the workpiece. It is the relative speed between the tool and the workpiece. The scanning rate is a critical parameter in EJM. A higher scanning rate results in a lower tool-workpiece interaction time, leading to a lower dissolution rate. Conversely, a lower scanning rate negatively affects machining accuracy, increasing the overcut value. Therefore, the scanning rate should be carefully chosen to balance material removal and machining accuracy.

(iii) Initial inter-electrode gap (IEG): The initial IEG is the distance between the tool and the workpiece before machining begins. The electrochemical reaction starts when the tool reaches the IEG position. Increasing the distance between the tool and the workpiece raises the resistance in the electrolyte. Higher initial IEG values may cause discontinuous dissolution or inhibit dissolution altogether. Conversely, very low initial IEG values prevent the electrolyte from reaching the tool-workpiece interfaces, leading to short circuits. Therefore, the initial IEG is a crucial parameter that requires careful selection.

(iv) Electrolyte pressure and flow rate: The electrolyte needs to reach the interface between the tool and the workpiece to enable the dissolution of the anode material. When machining complex or high aspect ratio jobs, a high electrolyte flow rate is necessary to reach intricate areas. Inadequate removal of sludge in those areas hampers the dissolution process and can lead to short circuits. The use of a rotating tool in EJM enhances electrolyte flow and helps it reach intricate zones.

(v) Type and concentration of electrolyte: Selecting the appropriate electrolyte is essential in EJM. The electrochemical properties of the electrolyte significantly influence the material removal mechanism. The choice of electrolyte depends on the type of workpiece since the reaction occurs between the electrolyte solution and the workpiece. Higher electrolyte concentration accelerates dissolution by providing more ions in the solution, while lower concentration depletes ions, resulting in reduced material removal. Hence, electrolyte concentration should be carefully selected.

(vi) Type of power supply unit: The nature of the power supply unit determines whether it is a constant DC type or a pulse type. With a constant DC power source, continuous dissolution occurs, leading to high average machining current and material removal rate. However, continuous material removal limits the fresh electrolyte's ability to replace sludge, which hampers the dissolution process and can cause short circuits. In the case of a pulse type power supply, voltage is periodically applied in any form. Dissolution occurs during the pulse-on time, while no machining takes place during the pulse-off time. This allows the fresh electrolyte to replace the sludge, enhancing machining quality.

(vii) Frequency of pulse DC power: When using pulse DC voltage, frequency is a significant parameter. The time period of the pulse cycle is inversely proportional to the frequency. Higher frequency leads to lower machining time in a single period.

2.2 Performance Characteristics of EJM

The performance characteristics of EC JET play a crucial role in evaluating the quality and accuracy of the machining process. The key performance characteristics are as follows:

(i) Material removal rate (MRR)

MRR is a significant performance characteristic in any machining process. It represents the amount of material removed during EC JET per unit of time. Factors such as higher current density, machining voltage, duty ratio, feed rate, and lower frequency contribute to an increased MRR. MRR can be calculated by measuring the weight difference of the workpiece before and after machining divided by the machining time. It is typically expressed in grams per minute or cubic centimeters per minute for volumetric MRR.

(ii) Geometrical features

Geometrical features refer to the dimensional variations of the machined zone compared to the desired profile. Some important geometrical performance characteristics include:

(a) Overcut: Overcut is a crucial criterion that determines dimensional accuracy. It is the difference between the dimensions of the obtained machined profile and the desired profile. Different types of overcuts, such as length overcut, width overcut, and depth overcut, can occur in EC JET. Overcut is typically measured in millimeters or as a percentage.

(b) Perpendicularity of sidewall: In ECM, generating a contour or complex 3D structure with perpendicular walls to the base is challenging. Conventional ECM often results in taper walls or round edges between the base and sidewall, which are undesired and should be minimized. EC JET exhibits less divergence of the wall compared to conventional ECM, resulting in improved perpendicularity.

(c) Corner radius: When machining with a simple-shaped tool and changing the tool direction from one axis to another (e.g., generating an 'L' shape), the edge between the two directions should be perpendicular. However, stray current in both ECM and EC JET processes leads to the formation of rounded corners, known as corner radius. Corner radius is an undesirable factor that affects dimensional accuracy and is typically measured in millimeters.

(d) Flatness: Flatness refers to the base profile of the surface obtained after EC JET machining. Inhomogeneous dissolution can cause deterioration of the surface flatness, impacting the overall quality of the machined surface.

(iii) Surface quality

Surface quality indicates the condition of the surface produced by the EC JET process. ECM generally offers better surface quality compared to other non-conventional machining processes. However, EC JET exhibits further improved surface finish compared to ECM. The surface finish of the machined profile depends on the rate of anodic dissolution and the quality of the sludge produced during machining. Surface roughness values, such as Ra, RMS, Rp, and Rz, are used to quantify the surface finish. Typically, the surface roughness value of EC JET for Ti6Al4V is around 1 μm, while for nimonic 263 alloy, it can range from 0.07 to 0.08 μm.

2.3 Electrochemical Reactions during EJM of Ti6Al4V

When NaBr and NaNO3 are dissolved in water, they will dissociate into their constituent ions due to the polarity of the water molecules.

NaBr will dissociate into Na+ and Br- ions:

$NaBr(s) \rightarrow Na^+(aq) + Br^-(aq)$ ……....2(i)

Similarly, NaNO3 will dissociate into Na+ and NO3- ions:

$NaNO_3(s) \rightarrow Na^+(aq) + NO_3^-(aq)$…….2(ii)

The Na+ ions will be attracted to the negative electrode (the cathode) during the electrochemical process, while the Br- and NO3- ions will be attracted to the positive electrode (the anode).

At the anode, the Br- and NO3- ions can be oxidized, depending on the specific conditions of the electrochemical process. The oxidation of these ions can result in the release of electrons to the electrode and the formation of new compounds.

At the cathode, the Na+ ions can be reduced, again depending on the specific conditions of the electrochemical process. The reduction of these ions can result in the uptake of electrons from the electrode and the formation of new compounds.

When Ti6Al4V is used as the anode with NaBr and NaNO3 as electrolytes, the Br- and NO3- ions will be attracted to the anode and may undergo oxidation, depending on the specific conditions of the electrochemical process. The oxidation of Br- and NO3- ions at the anode can result in the formation of new compounds.

For example, the oxidation of Br- ions can lead to the formation of Br2 (diatomic bromine) or other bromine-containing compounds. The oxidation of NO3- ions can lead to the formation of NO2 (nitrogen dioxide) or other nitrogen-containing compounds.

The exact products of the oxidation reactions will depend on factors such as the concentration of the electrolytes, the current density, and the temperature of the electrochemical process.

At the cathode, the Na+ ions may undergo reduction, depending on the specific conditions of the electrochemical process. The reduction of Na+ ions can result in the formation of new compounds, such as sodium hydroxide (NaOH) or other sodium-containing compounds.

Overall, the specific new compounds that may form during the electrochemical process of Ti6Al4V as the anode with NaBr and NaNO3 as electrolytes will depend on the specific conditions of the process and the behavior of the individual ions involved.

The electrochemical equation for the electrochemical process of Ti6Al4V as anode with NaBr and NaNO3 as electrolytes can be written as follows:

At the anode:

$Ti6Al4V(s) \rightarrow Ti6Al4V(4+) + 4e^-$ .....2(iii)

The Ti6Al4V alloy is oxidized, releasing 4 electrons per atom of Ti. These electrons flow through the external circuit towards the cathode.

At the cathode:

$4e^- + 2H2O(l) + O2(g) \rightarrow 4OH^-(aq)$ …….2(iv)

At the cathode, oxygen gas and water molecules react to form hydroxide ions. The electrons flowing from the anode to the cathode reduce the oxygen molecules, forming hydroxide ions.

Overall reaction:

$Ti6Al4V(s) + 2H2O(l) + O2(g) \rightarrow Ti6Al4V(4+) + 4OH^-(aq)$ ……2(v)

This reaction shows the complete electrochemical process of Ti6Al4V as anode with NaBr and NaNO3 as electrolytes. The titanium alloy is oxidized at the anode, while oxygen gas and water molecules are reduced at the cathode, producing hydroxide ions.

2.4 Literature Review

The laws of electrolysis, established by Michael Faraday in the early 19th century, serve as the foundation for the principle of electrochemical dissolution. In 1929, researcher W. Gusseff made significant progress by developing a process for machining materials through electrolysis. Since then, electrochemical machining (ECM) has been continuously developed and refined, with ongoing advancements in the field. ECM has gained industrial significance due to its numerous advantages. It offers unique capabilities for machining complex shapes, hard materials, and heat-sensitive materials, providing high precision and surface quality. The non-contact nature of the process also eliminates the need for mechanical force, minimizing

tool wear and reducing the risk of deformation. Additionally, EJM enables the machining of intricate internal features that are difficult to access using conventional methods. Despite its advantages, EJM poses certain challenges that researchers have been actively addressing to enhance the effectiveness of the process. Some of these challenges include controlling the anodic dissolution, optimizing the electrolyte composition and flow, improving process stability, and enhancing material removal rates. Researchers have dedicated their efforts to overcome these obstacles, and their investigations and findings have been documented in various research works.

The continuous research and development in EJM aims to optimize the process parameters, expand its application range, and improve its overall efficiency. By overcoming the challenges and building upon the advancements made, EJM has the potential to further revolutionize precision machining in various industries.

The work conducted by Huanghai Kong et al. [1] focuses on the investigation of Jet Electrochemical Micromachining (Jet-EJM) of Ti-6Al-4V alloy. The researchers propose a novel model that incorporates multiphysics simulation to simulate the Jet-EJM process and predict the resulting machining profile. The model takes into account the interaction between the electric field, two-phase flow field, and geometry deformation, providing a comprehensive understanding of the process.

One significant aspect considered in the model is the breakdown process of the passivation film that forms on the surface of Ti-6Al-4V alloy. This inclusion allows for more accurate prediction of the machining results. The researchers also perform experimental studies to investigate the passivation film breakdown process of the alloy. To validate the simulation results and explore the influence of travel rate on material dissolution, several experiments on the Jet-EJM of Ti-6Al-4V alloy are conducted. The distribution of current density on the anode surface is examined, providing insights into the machining process. Key parameters used in the experiments include an inner diameter of the tool of 0.8mm, a 20% NaCl solution as the electrolyte, an inter-electrode gap of 500 μm, and a preferred voltage range of 15-50V. The scanning rate employed ranges from 5 to 60 mm/min. Overall, this work contributes to a better understanding of the Jet-EJM process for Ti-6Al-4V alloy, combining multiphysics simulation, experimental investigation, and analysis of key parameters. The proposed model aligns well with the experimental results, and the findings can aid in optimizing the Jet-EJM process for achieving desired machining outcomes.

The research conducted by Hao Zhu et al. [2] focuses on the fabrication of oxide-free dimple structures on germanium (Ge) wafers through the application of electrochemical jet machining

enhanced by opposing laser irradiation. The study aims to improve the efficiency and localization of electrochemical machining (ECM) on Ge wafers by incorporating laser irradiation and addressing the issue of residual oxide particles that typically occur when using a neutral electrolyte. In their approach, a NaNO3 electrolyte jet is generated through a cathodic nozzle and directed perpendicularly onto the bottom surface of the Ge wafer. Simultaneously, nanosecond (ns) laser irradiation is applied from the opposing side to enhance the electrical conductivity of the targeted area. By employing this method, the researchers efficiently fabricate dimple structures on the Ge wafer without any detectable oxidation products. Surface morphology characterization is extensively conducted, revealing the presence of radial lines composed of regular microwaving structures, particularly near the dimple edge. These lines are attributed to the rapid and radial flow of electrolyte along the concave sidewall. In contrast, an irregular corrugated pattern is observed near the dimple center, which is caused by electrolyte turbulence following the impingement. The researchers also perform a parametric experimental study to examine the effects of applied voltage, laser power, and electrolyte concentration on the dimple profile and surface characteristics. The findings provide detailed insights into the influence of these parameters on the resulting dimple structures. Furthermore, a simulation study is conducted to analyze the flow field of the electrolyte, revealing the distribution regularities of velocity and pressure. This simulation contributes to a deeper understanding of the formation mechanism behind the complex surface morphology observed during the fabrication process. Overall, this research successfully demonstrates the fabrication of oxide-free dimple structures on Ge wafers using electrochemical jet machining enhanced by opposing laser irradiation. The comprehensive characterization, parametric experimental study, and simulation analysis contribute to a better understanding of the process and provide valuable insights for further optimization and application of this technique.

The research conducted by Mitchell-Smith et al. [3] focuses on the application of ultrasonic assistance in electrochemical jet machining of titanium (Ti) in order to overcome passivation layers that hinder the machining process. The experiment investigates the use of ultrasonics to partially remove the passivating scale, leading to improved overall machining performance. The results presented in the study demonstrate that ultrasonic assistance has a favorable effect on feature aspect ratio during machining. It increases the depth and minimizes the kerf by 7% when compared to machining without ultrasonic assistance, using identical process parameters. Additionally, surface textures of the machined faces show a reduction in Ra

(average roughness) by 31% along the groove bottom. This reduction is attributed to an increase in low roughness areas caused by an increase in high current density. The findings from this experiment suggest significant advantages in utilizing ultrasonic assistance during electrochemical jet machining of Ti alloys. The use of ultrasonics helps overcome the challenges posed by passivation layers, resulting in improved machining performance, enhanced feature aspect ratio, and reduced surface roughness.

The research conducted by Speidela et al. [4] focuses on electrolyte jet machining of titanium alloys using novel electrolyte solutions. The study aims to establish more stable machining processes and controlled removal of the passivating layer that forms on the surface of titanium alloys. Various electrolytes, including sodium halides (bromide, chloride, and fluoride) and the commonly used sodium nitrate solution, are investigated and compared in terms of surface finish, material removal rate, and pit formations. The concentration of the electrolyte is varied to assess the effectiveness of each solution. The machined features produced using different electrolyte solutions are subjected to typical characterization methods. The research explores the removal mechanism for overcoming the passivating layer and the development of more stable machining regimes. The findings show that machining with sodium chloride electrolyte significantly increases the mass removal rates by over 100% at concentrations below 2.5M compared to the commonly used sodium nitrate electrolyte. Furthermore, the addition of sodium fluoride to sodium chloride electrolytes reduces the overcut effect in machined pits by half compared to the pits formed in chloride, bromide, and nitrate electrolytes. Overall, the study highlights the potential of using novel electrolyte solutions, particularly sodium chloride with or without sodium fluoride doping, for electrolyte jet machining of titanium alloys. These solutions offer improved material removal rates and reduced overcut effects, providing opportunities for more efficient and controlled machining processes.

The research conducted by Dong-Il Seo et al. [5] focuses on the effects of competitive anion adsorption (Br^- or Cl^-) and the semiconducting properties of passive films on the corrosion behavior of additively manufactured Ti–6Al–4V alloys. The study investigates the influence of anions, specifically Br^- and Cl^-, and their interaction with the semiconducting properties on the corrosion resistance of the Ti–6Al–4V alloy produced through additive manufacturing (AM). To understand the relationship between anions and semiconducting properties, the researchers analyze pitting potentials, doping densities, and equilibrium adsorption coefficients. Potentiodynamic polarization curves are used to determine the pitting potentials, Mott–Schottky plots are employed to analyze doping densities, and the Langmuir isotherm simulation model is utilized to study equilibrium adsorption coefficients.

The findings indicate that of the two anions, Br− and Cl−, Br− exhibits a higher equilibrium adsorption coefficient. This higher coefficient is attributed to the more aggressive attack on the passive film of the additively manufactured Ti–6Al–4V alloy. The study provides insights into the corrosion behavior of the alloy in the presence of different anions and highlights the importance of considering the competitive adsorption of anions and the semiconducting properties of passive films in understanding the corrosion resistance of AM Ti–6Al–4V alloys.

The research conducted by Tao Yang et al. [6] focuses on electrochemical cutting with inner-jet electrolyte flushing for titanium alloy (Ti-6Al-4V). The study presents a method for electrochemically cutting Ti-6Al-4V alloy with a 10 mm thickness using a tube electrode with an array of holes and inner-jet electrolyte flushing. The effects of different electrolyte types on the maximum scanning rate (MFR), slit width, and standard deviation are investigated and analyzed. The researchers also explore the use of inner-jet electrolyte flushing assisted by outer-jet electrolyte flushing to address stray corrosion on the slit surface caused by the accumulation of electrolysis products within the slit. best nozzle diameter, flow rate, and electrolyte temperature are determined, and several typical structures are machined on a 10 mm-thick Ti-6Al-4V alloy block using a 5% NaNO3 + 5% NaCl electrolyte and outer-jet electrolyte flushing-assisted machining. The use of the 5% NaNO3 + 5% NaCl electrolyte yields a better balance between machining efficiency and accuracy compared to other electrolytes due to the reduction in Cl−1 ions and increase in NO3−1 ions. However, the accumulation of insoluble electrolysis products in and around the slit poses challenges. It hinders the electrolyte flow, leads to stray corrosion on the upper surface of the slit, and reduces cutting quality. To address this issue, outer-jet electrolyte flushing is employed to quickly remove the slow-flowing waste electrolyte from the slit, reducing the accumulation of electrolysis products and eliminating stray corrosion.

The study concludes that outer-jet electrolyte flushing does not affect machining efficiency but does influence machining accuracy. By selecting appropriate parameters for outer-jet electrolyte flushing, the slit width and standard deviation can be reduced in inner-jet electrolyte flushing electrochemical cutting assisted by outer-jet flushing. Furthermore, selecting an appropriate electrolyte temperature can improve both machining efficiency and accuracy.

The research conducted by Zhuang Liu et al. [7] focuses on electrochemical slurry jet micro-machining (ESJM) of tungsten carbide (WC) using a sodium chloride (NaCl) solution as the jet electrolyte. The objective of the study is to investigate the interaction between

solid-particle impact and anodic dissolution during ESJM with a pH-neutral electrolyte. NaCl solution is chosen as the jet electrolyte due to its safety, affordability, and common usage in industry. It possesses advantages such as rapid material corrosion and the absence of a passivation film on the machining surface for ferrous materials. However, when using a NaCl solution in the electrochemical processing of WC alloys, a surface oxide layer is generated because tungsten readily oxidizes in a pH-neutral aqueous solution. During ESJM, the high kinetic energy particles impact the surface and damage the oxide layer, enabling continuous anode dissolution by exposing the target surface to the corrosive environment. The study investigates the effects of working voltage, abrasive concentration, slurry jet velocity, and solution concentration on the ESJM of WC specimens. These factors are compared to abrasive slurry jet machining (ASJM) and electrochemical jet machining (EJM), which represent erosion alone and corrosion alone, respectively. Furthermore, the research aims to determine and discuss the material removal mechanisms and machining localization in ESJM. The study provides insights into the best parameters for achieving effective and controlled material removal in WC using ESJM with a NaCl solution.

In the research conducted by A.T. Clare et al. [8], the manipulation of the angle of address in electrochemical jet machining (ECJM) was investigated. This study explored the viability and effects of articulating the nozzle relative to the workpiece, which had not been previously investigated. Two machining conventions were defined: normal convention, where the jet is maintained perpendicular to the transverse direction, and push/pull convention, where the nozzle is rotated with respect to the direction of travel. With the normal convention, it was discovered that different surface geometries could be created, resulting in unique profiles. By rotating the head, the slopes of the cut walls could be varied, with up to an 80% difference in slope observed between the cut walls. The adjacent wall to the nozzle exhibited a decrease in slope as the jet angle approaches 90°, while the opposite side wall slope increased. The researchers were able to define predictable ratios of the differing slopes of the striation side walls. The push/pull convention demonstrated that deeper and sharper cuts could be achieved by inclining the nozzle, leveraging the highly localizing current density effect. This approach resulted in a 35% increase in depth without requiring additional energy. Additionally, the surface finish was greatly improved, with the profile roughness (Ra) reduced from 0.2 μm in the pull mode to 0.04 μm in the push mode, achieving a mirror-like finish. The mechanics of these phenomena were investigated and defined.

The study also examined the influence of nozzle jet speed variation combined with inclining the jet. It was found that the variation in jet velocity had no noticeable impact on the resultant

profile when the nozzle was inclined. However, when the nozzle was in the normal position, jet velocity had a direct influence due to polarization effects related to poor clearance of machining debris and the formation of oxides.

Overall, the research demonstrated that by manipulating the angle of jet address, an additional level of flexibility and performance could be achieved in electrochemical jet machining processes.

In the study conducted by Jae-Bong Lee et al. [9], the corrosion behavior of additively manufactured (AM) Ti-6Al-4V alloys was investigated, focusing on the effects of competitive anion adsorption (Br− or Cl−) and the semiconducting properties of the passive films. The researchers examined the relation between the pitting potentials and equilibrium adsorption of Br− and Cl− anions using potentio-dynamic polarization curves, Mott–Schottky plots, and the Langmuir isotherm model. The Mott–Schottky plots were measured using the microdroplet cell technique, which is based on the capacitance of the passive films on both dark and bright grains of the AM Ti-6Al-4V alloy. The pitting potential, which is an indicator of pitting corrosion resistance, was found to be influenced by the doping densities, α′ phase distribution, and equilibrium adsorption coefficients of Br− and Cl−. The equilibrium adsorption coefficients were predicted using the Langmuir isotherm simulation. The results of the study showed that the pitting corrosion of the AM Ti-6Al-4V alloy could be determined based on the equilibrium adsorption coefficient, the donor density obtained from the Mott–Schottky plots, and the α′ phase distribution determined by the micro-Vickers hardness test. The pitting potentials of the bright and dark grain areas were measured using the microdroplet cell technique. By considering the competitive adsorption model between Br− and Cl−, it was observed that the higher equilibrium adsorption coefficient of Br− contributed to a more aggressive attack on the passive film of the AM Ti-6Al-4V alloy. The presence of a higher α′ phase distribution in the alloy indicated the presence of more defects, which correlated with a higher donor density on the passive film as observed in the Mott–Schottky plots. Overall, the study provided insights into the corrosion behavior of AM Ti-6Al-4V alloys and highlighted the significance of competitive anion adsorption and the semiconducting properties of passive films in determining the pitting corrosion resistance.

Hackert-Oschätzchena et al. [10], presented a study on the dynamic generation of the jet shape in Jet Electrochemical Machining (Jet-ECM). This technology enables the rapid creation of microstructures in metallic parts, independent of material hardness, without any thermal or mechanical impact. Jet-ECM ensures a smooth processed surface and eliminates tool wear. However, the shape of the jet, which significantly influences the Jet-ECM process, remains

challenging to predict accurately. In a previous study by Hackert (2010), a numerical model based on a predefined jet shape was developed using COMSOL Multiphysics. In this present study, the authors introduced a new model that integrates fluid dynamics using the level set method for two-phase flow. The simulation was divided into two steps: jet formation and anodic dissolution. The dynamic behavior of the electrolyte jet during the dissolution process was accurately simulated, revealing effects that impact the machining results.

The findings of this study contribute to a better understanding of electrochemical machining through the electrolytic free jet. Notably, the study verified the occurrence of secondary electric contacting of the nozzle by electrolyte reflected from the workpiece. The insights gained from this research enhance the knowledge of the Jet-ECM process and its underlying mechanisms, thereby facilitating improvements in machining precision and efficiency.

Alistair Speidel et al. [11] , investigated the use of electrolyte jet machining (EJM) for the machining of titanium alloys. EJM is a non-contact machining process that uses a high-pressure jet of electrolyte to remove material from a workpiece. The authors found that the use of novel electrolyte solutions, such as those containing sodium chloride or sodium fluoride, can improve the machining performance of EJM for titanium alloys. In particular, the use of these electrolytes can lead to increased material removal rates, improved surface finish, and reduced overcut. The authors' findings are significant because researchers demonstrate the potential of EJM for the machining of titanium alloys. Titanium alloys are difficult to machine using traditional methods, such as milling or turning, due to their high strength and toughness. EJM is a promising alternative to these traditional methods because it can provide a high level of accuracy and precision, even for difficult-to-machine materials.

Hackert-Oschätzchena et al. [12] Inverse jet electrochemical machining (Jet-ECM) is a novel process for machining micro-scale features in conductive materials. In Jet-ECM, a high-velocity electrolyte jet is used to erode the workpiece, while a counter-electrode is used to complete the electrical circuit. The process is characterized by high precision, good surface finish, and no tool wear. In this paper, the authors present a new method for using Jet-ECM to create functional edge shapes in micro bores. The method is based on the principle of inverse machining, in which the desired edge shape is used to generate the tool path. The authors demonstrate the feasibility of the method by machining a variety of micro bores with complex edge shapes. The results of this study show that Jet-ECM is a promising process for the functional edge shaping of micro bores. The process is capable of producing high-precision, smooth-surfaced features with complex edge shapes. The method presented in this paper provides a simple and effective way to use Jet-ECM for this purpose.

Investigation on parametric effects on groove profile generated on Ti1023 titanium alloy by jet electrochemical machining" by Wang et al. [13] investigates the effects of process parameters on the groove profile generated by jet electrochemical machining (JECM) of Ti1023 titanium alloy. The authors used a numerical model to simulate the JECM process and experimental results to validate the model. The results showed that the groove profile is affected by the applied voltage, inter-electrode gap, electrolyte flow rate, and nozzle traveling rate. The authors concluded that the best process parameters for JECM of Ti1023 titanium alloy are 24 V of applied voltage, 0.6 mm of inter-electrode gap, 2.1 L/min of electrolyte flow rate, and 25 μm/s of nozzle traveling rate.

The paper by D. Baehre et al. [14] investigates the electrochemical dissolution behavior of titanium and titanium-based alloys in different electrolytes. The authors used a modified micro-flow cell to perform cyclic voltammetry, linear sweep voltammetry, and chronoamperometry on three types of titanium materials: commercially pure titanium (cp Ti), Ti90Al6V4 (Ti grade 5), and Ti60Al40 (γ-TiAl).

The results showed that the electrochemical dissolution behavior of titanium and its alloys is strongly influenced by the type of electrolyte. In aqueous NaNO3 and NaCl solutions, the cp Ti and Ti90Al6V4 alloys showed a passive behavior, while the Ti60Al40 alloy showed a transpassive behavior. In a KBr solution, all three alloys showed a transpassive behavior.

The authors concluded that the type of electrolyte plays a decisive role in the electrochemical dissolution behavior of titanium and its alloys. Researchers also suggested that the transpassive behavior of Ti60Al40 in KBr solution could be used for electrochemical machining of this alloy.

In their study, "Improving material removal rate in macro electrolyte jet machining of TC4 titanium alloy through back-migrating jet channel," Minglu Wang et al [15] investigate an innovative approach to enhance the material removal rate (MRR) in macro electrolyte jet machining of TC4 titanium alloy. The authors start by addressing the significance of efficient material removal techniques for titanium alloys, considering their extensive applications in aerospace, automotive, and biomedical industries. Researchers highlight the challenges associated with traditional methods and introduce the concept of macro electrolyte jet machining as a promising alternative. Wang et al propose a novel technique involving a back-migrating jet channel, aiming to optimize the material removal process. Researchers present a detailed experimental setup and methodology to evaluate the effectiveness of this approach. The study involves systematic investigations of various process parameters, such as jet pressure, voltage, and electrolyte concentration, to assess their influence on MRR. The

experimental results obtained by Wang et al demonstrate significant improvements in MRR using the back-migrating jet channel technique compared to conventional approaches. Researchers provide quantitative data and graphical representations to support their findings, validating the enhanced material removal efficiency achieved with this method. The researchers discuss the underlying mechanisms responsible for the improved MRR, including enhanced jet velocity and increased current density at the machining interface. Researchers provide a comprehensive analysis of the electrochemical reactions and fluid dynamics involved in the process. The findings presented in this study by Minglu Wang et al offer valuable insights for researchers and practitioners working with titanium alloys. The introduction of the back-migrating jet channel technique provides a novel and effective means to enhance material removal rates, contributing to the optimization of machining processes. Overall, the experiment conducted by Wang et al demonstrates the potential of the back-migrating jet channel technique for improving the material removal rate in macro electrolyte jet machining of TC4 titanium alloy. Their comprehensive analysis, supported by experimental data, strengthens our understanding of the process and its underlying mechanisms.

In their experiment titled "Study on surface roughness of large size TiAl intermetallic blade in electrochemical machining," Yudi Wang et al [16] investigate the surface roughness characteristics of large-sized TiAl intermetallic blades using electrochemical machining (ECM) techniques. The authors begin by highlighting the importance of TiAl intermetallic blades in the aerospace industry due to their desirable properties such as high strength and low density. However, achieving high-quality surface finishes on these blades poses challenges due to their complex geometry and material characteristics. Wang et al present a comprehensive experimental setup and methodology for their study. Researchers systematically vary ECM process parameters, including current density, electrolyte concentration, and machining time, to assess their impact on the resulting surface roughness. The experimental results obtained by Wang et al provide valuable insights into the surface roughness characteristics of TiAl intermetallic blades in ECM. Researchers present quantitative data, supported by statistical analysis and graphical representations, to demonstrate the effects of the process parameters on the surface roughness values. The researchers discuss the mechanisms underlying the observed surface roughness variations, considering factors such as material removal rate, passivation, and dissolution behavior. Researchers provide a detailed analysis of the ECM process and its influence on the resulting surface finish.

The findings presented in this study by Yudi Wang et al contribute to our understanding of surface roughness in large-sized TiAl intermetallic blades manufactured using ECM. The study provides valuable guidance for optimizing ECM parameters to achieve the desired surface quality required for aerospace applications. In conclusion, the experiment conducted by Yudi Wang et al on the surface roughness of large size TiAl intermetallic blades in electrochemical machining offers valuable insights into the influence of process parameters on the surface finish. Their comprehensive analysis, supported by experimental data, enhances our understanding of ECM techniques for manufacturing TiAl intermetallic blades.

2.5 Objectives of the Present Research Work

The importance of surface finish is evident in various industries. In aerospace applications, such as jet engines, aircraft structures, and spacecraft, the surface finish plays a crucial role. It reduces drag in the aerospace industry, thereby improving efficiency and ensuring optimal performance. In medical applications, like implants, surgical instruments, and dental restorations, Ti6Al4V biocompatibility is valuable. A high surface finish minimizes the risk of infection and enhances performance within the human body. Sporting goods, such as golf clubs, tennis rackets, and bicycles, benefit from Titanium's strength and lightweight properties. The high surface finish enhances performance, durability, and aesthetics. For turbine blades, surface finish directly impacts performance and efficiency. A smooth surface reduces drag, turbulence, and allows for efficient airflow. It improves heat transfer, corrosion resistance, and minimizes erosion damage. A high-quality blade has a surface finish of less than 0.2 µm, which increases fatigue strength, durability, efficiency, and lifespan.

In the context of the literature review and the challenges posed by the Electrochemical Jet Machining (EJM) process, the present research work aims to determine the most influential process parameters and their impact on various performance characteristics, particularly the surface finish criteria. The focus is on achieving complex profiles with good surface finish on High-Strength Temperature Resistance (HSTR), specifically titanium alloy. The objective is to fill the existing knowledge gap and provide a comprehensive understanding of the EJM process. By elucidating the influential parameters, the study can offer insights into optimizing the process and overcoming the challenges associated with achieving complex profiles and

high-quality surface finish on HSTR titanium alloy. Ultimately, the goal is to contribute to the advancement of EJM technology by providing valuable information and recommendations for enhancing the process parameters that have the greatest impact on surface finish criteria. This research work seeks to address the limitations identified in the literature review and pave the way for improved EJM capabilities on challenging materials like titanium alloy. Hence, the main objectives of this research work are as follows:

(i) To design and modify the existing set up which is likely to consist of different subunits such as mechanical unit, electrolytic supply unit, power supply unit and control unit etc. The developed EJM setup should be capable of performing EJM experimentation for investigating the surface finish of machined workpieces of titanium alloy e.g. Ti6Al4V.

(ii) To investigate the effect of different types of nozzles on surface roughness, percentage overcut and depth of penetration.

(iii) To evaluate the most influence process parameters by using Taguchi method, and furthermore to use them according to their ranking order to further determine the best parametric combination to be used for achieving the optimum surface finish.

(iv) To investigate the most influencing EJM process parameters such as scanning rate, voltage etc. and explore their influence on various major performance criteria e.g., surface finish, percentage overcut and Depth of penetration through extensive experimentation during machining of Ti6Al4V.

(v) Applying the best process parameter condition to achieve the optimum surface finish.

CHAPTER 3

3. EJM SET-UP DEVELOPMENT

The setup for EJM requires specialized attachments and components to facilitate the intended motion of the tool and generate predefined profiles or contours on the workpiece. It consists of several subcomponents, including a mechanical unit, power supply unit, electrolyte supply unit, and control unit. A schematic diagram of the developed EC JET setup is shown in Figure 3.1.

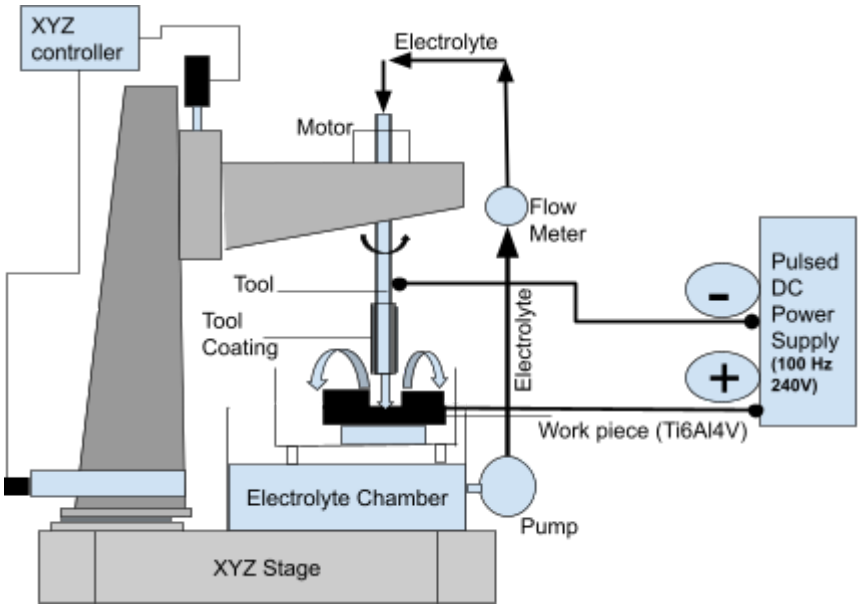

Fig 3.1 Developed EJM Setup.

The diagram illustrates the overall setup, which includes an x-y-z system, power supply, electrolyte flow system, motion control system, machining chamber, and tool holding setup. Bypass pressure valves are employed to regulate the electrolyte flow according to the requirements. The power source is connected to the pump, computer, and x-y-z control system. Further details regarding the individual parts of this setup are discussed in Figure 3.1. Some modifications have been made to the holding unit to enhance rigidity and simplify the electric connection. Additionally, tool development has played a crucial role in the successful implementation of the experiment.

3.1 Detailed Description of the EJM Setup

The characterization of the machined titanium alloy was conducted using a custom-developed setup comprising mechanical units, electrolytic supply units, power supply units, and control units, among others. Figure 3.2 presents an overview of all the essential units required to carry out the machining process. The mechanical unit serves as the fundamental structure of the electrochemical machining setup, facilitating workpiece mounting, tool holding, and tool movement.

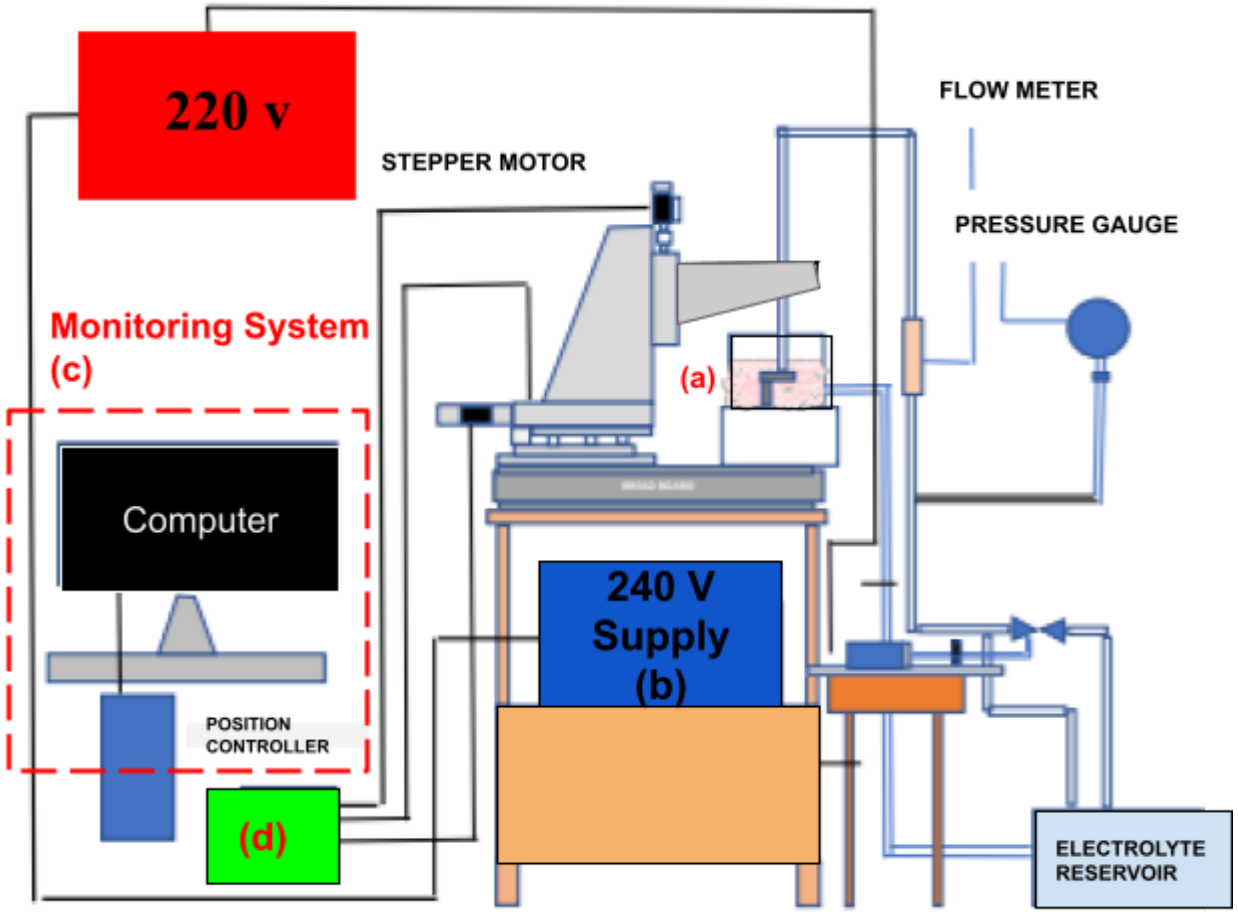

Fig. 3.2 Schematic of the Full Set Up

In electrochemical jet machining, precise control of tool movement is crucial. The mechanical machining unit of the electrochemical jet setup includes the machining chamber, CNC stage, tool holding arrangement, tool, and nozzle. These components work together to facilitate accurate and controlled tool movement during the machining process. All the major parts of the set-up are described as follows:

(i) Machining chamber

The machining chamber in the electrochemical jet setup is constructed using Perspex material as shown in fig 3.2(a) . It has dimensions of 350mm × 250mm × 200mm with a wall thickness of 10mm. The machining chamber serves two main purposes: it allows the electrolyte to be supplied from the reservoir, and it houses the work holding arrangement. Perspex is chosen for the machining chamber due to its non-conductive, chemically inert, and transparent properties.

The machining chamber is positioned above a platform, also made of Perspex, with dimensions of 432mm × 300mm × 130mm. The platform is securely fastened to the breadboard of the base of the XYZ stage using nut and bolt connections. Two outlets with regulating valves are located at the bottom of the machining chamber, and flexible pipes are used to carry the electrolyte from the chamber back to the reservoir.

The work holding device, also made of Perspex, is designed with clear slots and gaps matching those on the work table. This allows for the clamping of workpieces of different sizes on the same work table. The dimensions of the work holding device are 220mm × 40mm × 200mm, with 6mm clear slots and a 50mm gap.

(ii) Power supply unit

For the experimentations, a pulse DC power supply has been used as shown in fig 3.2 (b); this power supply has a maximum voltage rating of 240V. The frequency range is 100 Hz. The three-phase AC 440V input is connected to the primary winding of the step-down transformer. The secondary winding of the transformer is connected to a rectification circuit consisting of diodes configured in a full-wave bridge rectifier configuration. This rectified output is then passed through a filtering circuit to reduce ripple. Finally, the variac is connected to regulate the output voltage to the desired level of DC 240V. By adjusting the variac the voltage has been controlled. The power supply has one analog ammeter to check the current for the experiment. The power supply is protected against surge current caused by short circuit by HSBC fuse of 10 amp .

(iii) Motion control system

For motion control in the EC JET operations, an X-Y-Z linear stage manufactured by Holmark has been utilized. The XYZ stage is designed in a cantilever-type configuration, with a cantilever unit attached at the front where the tool is also mounted. The X and Y movements occur in two perpendicular axes parallel to the base of the stage, while the Z movement is limited to the vertical axis. These movements are crucial for positioning the tool accurately over the workpiece to generate different profiles.

The X-Y-Z linear stage used in this research work features three axes (X, Y, and Z), each driven by a stepper motor. The movements of these axes are controlled by an APT (Advanced Positioning Technology) controller, offering a resolution of 0.1 μms. The stage has a maximum travel capacity of 100 mm for each axis (X, Y, and Z). The overall maximum travel of the stage is 300 × 300 × 300 mm, and the Z-axis slide can bear a maximum load of 25 kg. The stage is equipped with a CNC controller that enables movement along the desired path while synchronizing the stepper motors.

In this research work, the workpiece remains stationary while the X-Y-Z linear stage precisely positions the tool for performing the machining operations.

(iv) Monitoring system set up

Various monitoring devices are employed during the machining process, including a multimeter, and stopwatch. Computer monitor acts as a monitoring device by tracking the tool path movement. Multimeter is employed to monitor the machining current and voltage. These devices play a crucial role in ensuring the accurate measurement and control of the machining parameters. A digital oscilloscope is used to monitor the nature of the pulse.

(v) Electrolyte flow system

The electrolyte flow system is an essential component of the EC JET setup, responsible for transferring the electrolyte from the reservoir to the system. To monitor the flow parameters, various measurements are taken, including the electrolyte flow rate and flow pressure. A gear pump made of stainless-steel to protect from corrosion is utilized to circulate the electrolyte from the reservoir through the flow line. The pump has a capacity of 0-430 ml/m and can generate a maximum pressure of 10 kgf/cm2. Its motor is rated at 0.5hp, and both the suction and discharge are 0.5 inch. The pump has a maximum capacity of 20 lpm and operates at a maximum speed of 1440 RPM.

To address the resistance in flow caused by the tool's hole pattern, an analog pressure gauge is employed to measure the pressure in the line, with a range of up to 10 kgf/cm2. Additionally, a rotameter is used in the flow line to measure the electrolyte flow rate. The rotameter functions by positioning a float on a scale and can measure up to 10 lpm. Proper cleaning of the line is necessary after the machining operation to maintain the devices in best working condition due to the corrosive nature of the flowing electrolyte. Flexible nylon pipes and PVC pipes with a diameter of 0.5 inches are employed to supply the electrolyte up to the internal flushing arrangement. The electrolyte reservoir serves as a container for storing the electrolyte. The electrolyte is drawn from the reservoir by the pump and circulated through the system. The electrolyte mixed with sludge returns to the reservoir from the output port of the machining chamber. A filtering provision is incorporated by attaching a filter with the suction valve. This continuous circulation of fresh electrolyte ensures best machining conditions.

(vi) Position control unit

The position controller plays a crucial role in precisely controlling the tool motion and position in electrochemical JET machining fig 3.2 (d) . The accuracy of the generated profile heavily relies on the tool's motion. The position control unit of the CNC stage is responsible for controlling three stepper motors, corresponding to the three axes, which are connected to a computer. The movements of the three axes can be achieved through software and controller-generated electrical signals, facilitated by computer programming. The controller is connected to the machine and computer through parallel ports.

To achieve the maximum speed, direction reversal, and rapid speed changes, it is essential to run the motor or the drive electronics components at their maximum permitted voltage. Likewise, obtaining the maximum torque relies on running the motor at its maximum permitted current.

In this electrochemical JET machining setup, Mach 3 software is utilized as a highly flexible program window designed specifically for controlling machines like JET machines and lathes, as depicted in Figure 3.3. The position controller incorporates an emergency stop feature, allowing the motor to be halted instantly in case of emergencies. The programming is performed using G and M codes, similar to a CNC controller. The programs are designed in such a way that any required changes in rotational steps, direction of rotation, or delays can be easily incorporated.

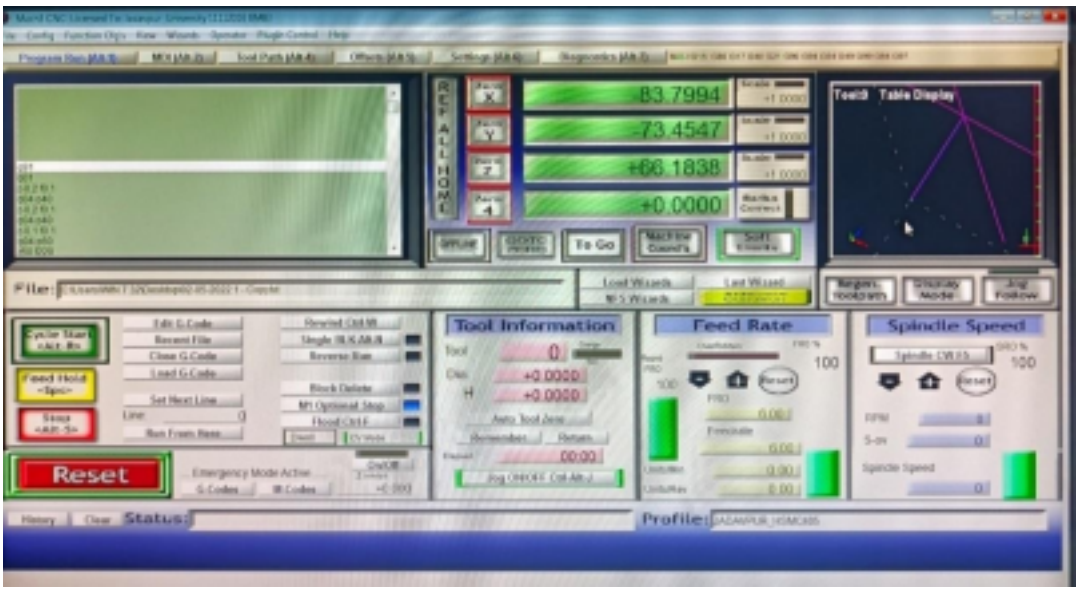

Fig. 3.3 Photographic view of control unit Mach 3 loader.

3.2 Development of Tool Holding Attachment of the EJM Setup

The tool holding arrangement is a crucial component of the mechanical machine unit in the electrochemical JET process. It plays a vital role in the movement of the tool, which is responsible for generating various complex profiles or contours on the workpiece. The tool, along with its holding arrangement, is mounted in the Z-axis slide and can move accordingly. To ensure the safety of the operator and prevent any electrical issues, the tool holding arrangement must be electrically non-conductive. This protects the entire setup body from the flow of current. Additionally, the tool holding arrangement needs to be rigid to minimize vibrations during machining operations.

3.2.1 Various challenges faced on tool holding attachment

The tool holding attachment in the EC JET machining setup consists of various components such as a copper shaft for holding the tool, a base for tool rotation, bearings, and bearing holding units. This attachment serves two main purposes: holding the tool and supporting the tool rotation unit.

However, there are certain challenges associated with the tool holding attachment. One issue is the potential leakage of electrolyte while flowing through the shaft, which can reduce the

current flow and potentially damage the CNC XYZ stage. Another problem is the occurrence of unwanted vibrations in the tool holding attachment.

To address these challenges, modifications are required. One modification involves using a stainless-steel box to cover the tool rotation unit and provide support to the tool holder. This helps to minimize vibrations compared to the previous lightweight bakelite material. Additionally, the height of the shaft needs to be adjusted to reduce eccentricity and improve stability.

By making these modifications to the tool holding attachment, the issues of electrolyte leakage, vibration, and eccentricity can be minimized, enhancing the overall performance of the EC JET machining setup.

3.2.2 Tool holding unit

To provide additional support to the tool holding shaft, a roller ball bearing is incorporated between the tool and the holding unit. Specifically, an SKF 6202 bearing is utilized for this purpose. To prevent the shaft from tilting like a cantilever, a square box made of bakelite material is employed.

The bakelite square box serves as a holder for the bearing and ensures stability. It consists of three square plates, each measuring 50mm × 50mm × 10mm. Two plates are positioned vertically on the slab using a screw system, while the third plate is designed to accommodate the bearing. This plate is attached horizontally to the other square plates using a screw thread system.

The shaft is press-fitted between the hole of the bearing and the cuboid to create a leak-proof system. This press fit mechanism ensures that the components are securely connected. The front view and side view of the tool holding unit can be seen in Fig 3.4 and Fig 3.5, respectively. By incorporating the roller ball bearing and the bakelite square box, the tool holding unit provides additional support and stability to the shaft, contributing to the overall effectiveness and reliability of the EC JET machining setup.

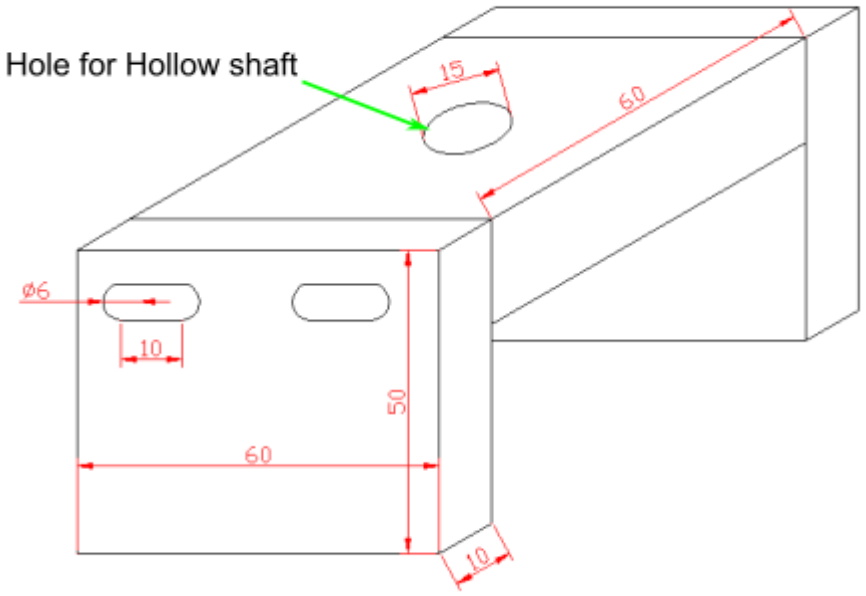

Fig. 3.4 Tool Holding Attachment.

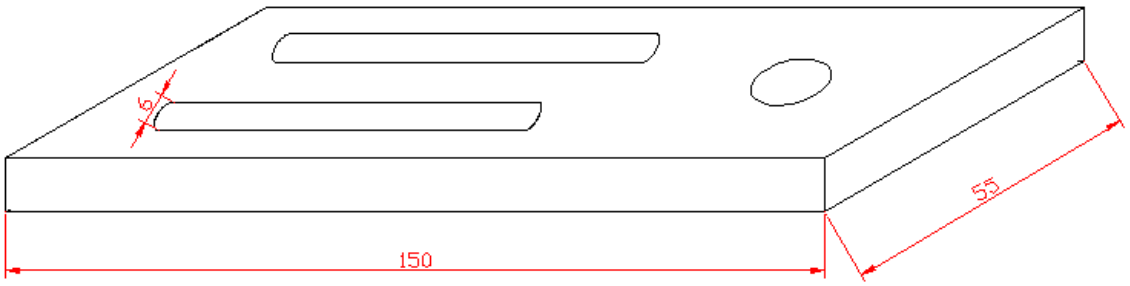

Fig. 3.5 Tool Holding Attachment.

3.3 Development of Nozzle

The process involves the use of a conductive electrolyte solution and a nozzle that directs a high-velocity stream of the solution onto the workpiece. The jet is typically produced using a gear pump, which creates a high-pressure flow of the electrolyte solution.

The development of the nozzle is a critical aspect of the EJM process. The nozzle's design and construction have a significant impact on the machining performance, efficiency, and precision. Here are some reasons why the development of the nozzle is important in EJM:

(i) Control of jet properties

The nozzle's design determines the size, shape, and velocity of the jet. These properties play a crucial role in the machining performance and precision. The nozzle must be designed to produce a stable and consistent jet to achieve accurate machining. A well-designed nozzle ensures the correct jet size and shape, which leads to precise material removal.

(ii) Optimization of machining parameters

The nozzle's design also affects the machining parameters, such as the voltage, current, and feed rate. The machining parameters, in turn, impact the material removal rate, surface finish, and tool life. With an optimized nozzle design, the machining parameters can be adjusted for maximum efficiency and effectiveness. The nozzle used by previous researchers was a normal cone nozzle as shown in figure 3.8

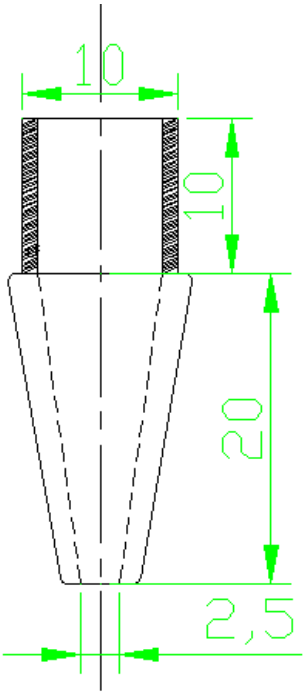

Fig. 3.8: Schematic of Nozzle Used previously.

But modifications have been done here after investigation on different nozzles, a straight hollow portion of inner dia 1 mm has been added fig 3.9 below.

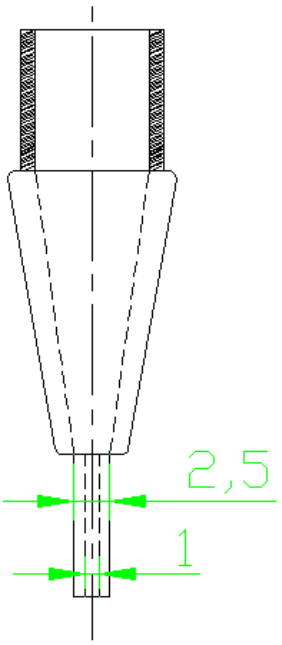

Fig. 3.9 Schematic of Nozzle Newly Developed.

Keeping in mind about more flexibility one new nozzle has been developed as shown in fig 3.10, so that the jet diameter can be varied according to experiments. In this modification by changing only the tip of the Nozzle head can vary the jet diameter, according to our choice. Benefits of using this flexible set up are.

(i) More flexibility of jet dia, varying from 0.2 μm to 2 mm. This much range variation can be possible.

(ii) As the jet tip is prone to huge pressure there is a possibility of damage of the jet tip, but now even if it damages it can be brought from the local market, which is even better in strength and accuracy than the workshop made.

(iii) To change the nozzle we don't need to work too hard or spend time assembling the set up again and again.

(iv) As fewer assemblies are done so the chances of leakage reduces, because the more we assemble and reassemble the part the chances of leakage increases, but in this case the chances are less.

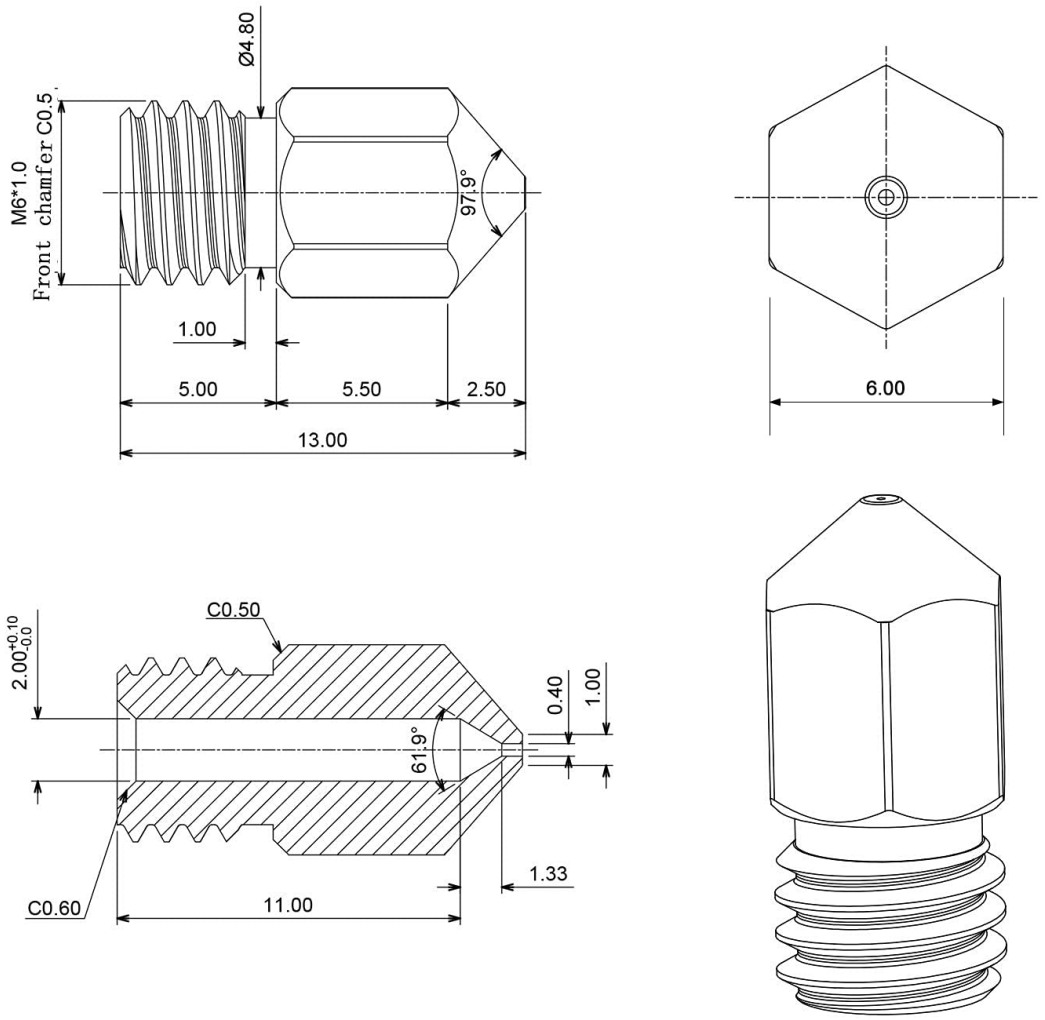

Fig. 3.10 Schematic of flexible Nozzle attachment .

3.3.1 Advantages of cone-straight nozzle over normal nozzle

Straight cone nozzles are specialized nozzles used in various applications such as fluid spraying, powder dispersion, and fuel injection. Compared to a normal nozzle, straight cone nozzles offer several advantages. Here are some of them:

(i) Higher Efficiency: The straight cone nozzle is designed in such a way that it creates a fine, even spray pattern. This leads to higher efficiency in fluid delivery, making it an ideal choice for coating, painting, or lubricating applications.

(ii) Consistent Flow: Unlike normal nozzles, which can produce an inconsistent flow pattern due to the varying angles of the spray, straight cone nozzles maintain a consistent flow rate. This allows for precise application and reduces the need for rework.

(iii). Reduced Downtime: Straight cone nozzles are less prone to clogging, which reduces the downtime for maintenance and cleaning. This makes them a cost-effective choice for industrial application

3.4 Photographic View of Final Developed EJM Set-up

The final developed set-up as shown in fig 3.11, consists of several units i.e. XYZ stage , stage controller, power supply, program generator software , tool holding unit, pump, pressure gauge, machining chamber, rotameter. The developed set-up is fully able to carry out machining operations.

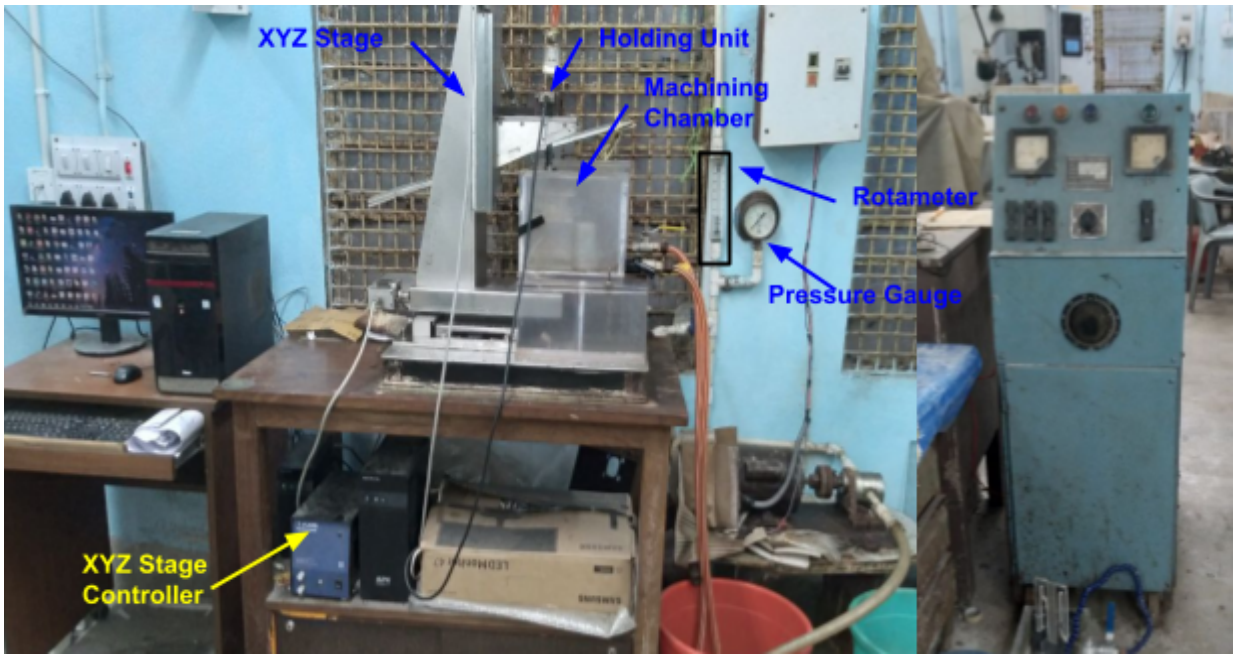

Fig 3.11 Photographic View of EJM Set-Up.

CHAPTER 4

4. EXPERIMENTAL ANALYSIS BASED ON TAGUCHI METHODOLOGY

The primary objective of the electrochemical jet (EC JET) process is to generate complex 3D shapes, surface profiles, cutting grooves, and slots using a simple-shaped tool. Unlike conventional electrochemical machining, which produces a shape that is a mirror image of the tool and requires complex tool designs, the EC JET process offers a more efficient and versatile approach. This study focuses on the experimental results obtained from the Taguchi methodology of the electrochemical jet process applied to Ti6Al4V material. The experiments were conducted using a setup that was developed internally and described in detail in Chapter 3. The purpose of this research is to analyze and discuss the outcomes of utilizing the indigenously developed EC JET setup for machining Ti6Al4V.

4.1 Experimental Planning

In order to explore the effects of different process parameters on the performance characteristics of electrochemical jet (EC JET) machining, preliminary experiments were conducted on titanium alloy. These initial experiments aimed to identify the appropriate range of process parameters for further investigation. The experiments were performed on the experimental setup that was previously described in Chapter 3. This setup was specifically developed for EC JET machining and provided the necessary infrastructure for conducting the experiments. By systematically varying the process parameters during these preliminary experiments, the researchers aimed to understand how each parameter affected the performance of the EC JET process. The results obtained from these experiments would serve as a foundation for further analysis and optimization of the process parameters to achieve desired machining outcomes.

Selection of tool

Experimental trials were conducted on a titanium-based superalloy plate to investigate the impact of machining parameters on various performance characteristics in electrochemical jet (EC JET) machining. To ensure best conductivity, a cylindrical hollow tool made of pure copper (Cu) was selected as the tool connector. Additionally, a stainless steel SS304 nozzle was employed due to its strength and corrosion resistance properties. To mitigate overcut

caused by stray current, the sidewall of the tool was carefully protected using Teflon tape. Insulating the tool wall was crucial to prevent tapering and increased width of the sidewall caused by the tool sinking into the machining zone without insulation. The nozzle used in the experiments had an outer diameter of 3 mm and an inner diameter of 1 mm. Effective removal of sludge played a vital role in achieving machining accuracy and a high material removal rate. The smaller inner hole diameter of the nozzle contributed to higher surface roughness, and the uniformity of the machining zone was primarily influenced by this dimension. It was observed that using a normal nozzle as a tool presented challenges in sludge removal, resulting in irregular edges, rough impressions, and inhomogeneous material removal. The availability of excess electrolyte near the machining zone combined with stray current effects compromised the flatness of the machined surface and led to higher overcut values. To address these issues and improve machining accuracy, a cone-straight nozzle was chosen instead. The electrolyte flow through the inner hole of the cone-straight nozzle provided a concise and precise entry into the machining zone. This nozzle design offered higher flushing pressure, facilitating efficient sludge removal without the formation of sludge layers. The smaller and uniform jet diameter of the cone-straight nozzle further enhanced machining accuracy and reduced overcut. Therefore, in this study, the cone-straight nozzle was selected as the preferred tool configuration over the normal nozzle to improve machining zone accuracy and overall performance.

Selection of Electrolyte

The selection of the electrolyte is a critical aspect in electrochemical jet (EC JET) machining. Different electrolytes are utilized based on the material being machined. For instance, sodium chloride (NaCl) with a high concentration is commonly used for machining stainless steel in conventional electrochemical machining. Sodium chlorate (NaClO3) and sodium nitrate (NaNO3) are used for mild steel. In the case of Ti6Al4V, sodium chloride (NaCl), sodium bromide (NaBr), and sodium nitrate (NaNO3) can be effectively used as electrolytes. Researchers have conducted experiments using these electrolytes at various concentrations to determine the suitable electrolyte and best concentration for accurate machining of Ti6Al4V. The concentration of the electrolyte is crucial in electrochemical machining, as a low concentration leads to non-uniform dissolution and unstable machining due to ion depletion. Conversely, a high concentration of electrolyte negatively affects the accuracy of the machined profile due to an excessive concentration of ions. Machining titanium presents unique challenges compared to commonly used materials due to its tendency to form a passive

oxide layer. This oxide layer impedes the electrochemical machining process. Breaking down this passivating layer and making it transpassive is essential for electrochemical dissolution. There are two main types of electrolytes: passive and non-passive. Passive electrolytes, such as NaNO3, contain oxidizing anions and offer better precision and control by forming a protective oxide film. On the other hand, non-passive electrolytes, like NaBr, are non-passivating and contain more aggressive anions that help break down the passive oxide layer at moderate voltages and facilitate material removal. A mixture of NaBr and NaNO3 electrolytes was employed in this study. NaNO3 was included in the mixed electrolyte to overcome the limitations of NaBr electrolyte. The use of NaBr in the mixed electrolyte increased the generation of hydrogen bubbles at the anode surface, resulting in the complete removal of the passive layer. Basic experiments were conducted using aqueous solutions of 0.5 M, 1 M, and 1.5 M concentrations. Researchers successfully conducted EC JET of Ti6Al4V using 1 M electrolyte of NaBr and 1 M concentration of NaNO3 separately. Increasing the concentration primarily improves the material removal rate (MRR), but after a certain level, the accuracy of the machined zone deteriorates due to excess NaCl. From the basic experiments, it was observed that the machined zone maintained surface finish and overcut accuracy with the 1 M mix electrolyte. Thus, a 1 M solution was chosen for further parametric studies.

4.1.1 Selection of Major Electrochemical JET Process Parameters

In this study, the aim was to identify the most influential process parameters and their suitable ranges in EC JET by initially machining simple slots on the workpiece based on Taguchi method. The electrical process parameters considered were voltage, input current, pulse type, pulse frequency, and duty ratio. Non-electrical parameters included feed rate, JET layer depth, initial inter-electrode gap, electrolyte type and concentration, electrolyte pressure and flow rate, and tool rotation with rotational speed. Among these parameters, feed rate, JET layer depth, and tool rotation were found to have the most significant impact on EC JET performance, according to the researchers. Flushing pressure was also observed to greatly influence the performance characteristics of EC JET. Effective sludge removal and the supply of fresh electrolyte to the machining zone were achieved through proper flushing. Various process parameters were considered to optimize the EC JET performance. The selected voltage range was 40V-140V, taking into account the desired responses. Input current was determined based on the inter-electrode gap (IEG) and electrolyte conductivity. The flow rate

of the electrolyte was set between 230 ml/min and 430 ml/min. For macro-EC JET, a voltage of around 20V was sufficient to overcome the passivation nature of the workpiece surface and initiate material removal.

4.1.2 Taguchi Based Planning for Experimentation

There are several reasons to use the Taguchi method over other optimization methods some of them are as follows:

(i) The Taguchi method is designed to minimize variation. This is important because variation can lead to defects, which can cost businesses money in terms of rework, scrap, and warranty claims. The Taguchi method helps to identify and minimize the sources of variation, which can lead to improved product quality and reduced costs.

(ii) The Taguchi method is relatively easy to use. It does not require a lot of statistical expertise, and it can be used by engineers and technicians with a basic understanding of statistics. This makes it a good option for businesses that do not have a lot of resources to invest in statistical training.

(iii) The Taguchi method can be used to optimize a wide variety of products and processes. It has been used successfully in a wide range of industries, including manufacturing, electronics, and healthcare. This makes it a versatile tool that can be used to improve the quality of a wide range of products and services.

The Taguchi method is a statistical technique that is commonly used in the field of engineering to optimize the design of products and processes. It was developed by Genichi Taguchi, a Japanese engineer, in the 1950s and 1960s. The Taguchi method emphasizes on improving product quality and reducing costs through the systematic identification and optimization of controllable factors that impact product performance.Taguchi method is a powerful statistical technique that can be used to optimize product and process design. By systematically identifying and optimizing the controllable variables that impact product performance, the Taguchi method can improve product quality, reduce costs, and increase productivity. The Taguchi method is widely used in industries such as manufacturing, engineering, and healthcare, and has been shown to be effective in a wide range of applications.

The method uses a structured approach to conduct experiments that aims to identify the best set of conditions for a given product or process. The Taguchi method is particularly useful

when the goal is to optimize a process or product with multiple input variables that may interact with each other in complex ways.

The Taguchi method involves several steps, which are as follows:

Step 1: Define the problem and the objective: The first step is to define the problem that needs to be solved and the objective that needs to be achieved. This could be improving product quality, reducing costs, or increasing productivity.

Step 2: Identify the variables: The second step is to identify the variables that may impact the objective. These variables are divided into two types: control variables and noise variables. Control variables are the variables that can be manipulated to achieve the desired objective, while noise variables are the variables that cannot be controlled but can impact the objective.

Step 3: Design the experiment: The third step is to design the experiment that will be used to optimize the process or product. This involves selecting the appropriate experimental design, such as the Taguchi L9 or L12 design, and determining the levels of each variable that will be tested.

Step 4: Conduct the experiment: The fourth step is to conduct the experiment by varying the levels of the control variables and measuring the response of the process or product.

Step 5: Analyze the data: The fifth step is to analyze the data using statistical techniques such as ANOVA (analysis of variance) to determine the impact of each variable on the objective.

Step 6: Optimize the process or product: The sixth step is to use the results of the analysis to optimize the process or product. This may involve adjusting the levels of the control variables or making other changes to the process or product.

Step 7: Verify the results: The final step is to verify the results by conducting additional experiments or testing the optimized process or product under different conditions.

Some important terms used here are as follows.

1. Levels: Levels refer to the different settings or values of a factor that can be tested in an experiment. For example, if the effect of temperature on a process is tested, different levels of temperature could be 50°C, 60°C, and 70°C.

2. Signal to Noise Ratio (SNR): SNR is a measure of the variation in the response variable that is due to the factors being studied. A high SNR indicates that the factors have a large impact on the response variable and are important to consider in the experiment.

3. Analysis of Variance (ANOVA): ANOVA is a statistical technique used to analyze the results of an experiment and determine the significance of the different factors and their interactions. This can help identify the most important factors to consider in optimizing the system.

4. Residual Plots: Residual plots are graphical tools used to evaluate the fit of a model to the data. Percent vs residual, frequency vs residual, residual vs fitted value, and residual vs observation plots are all common types of residual plots used in Taguchi method to assess the quality of the model fit.

Here are some of the advantages of the Taguchi method over other optimization methods:

(i) The Taguchi method is more efficient. It can identify the most important factors that affect product quality with fewer experiments than other methods.

(ii) The Taguchi method is more effective. It can reduce variation and improve product quality more than other methods.

(iii) The Taguchi method is more robust. It can be used to optimize a wider range of products and processes than other methods.

Calculation of S/N Ratio

The signal-to-noise ratio (SNR) is a measure of the quality of a signal. It is calculated as the ratio of the power of the signal to the power of the noise. The SNR can be expressed in decibels (dB) using the following equation:

SNR (dB) = 10 log10 (signal power / noise power).....4.1

The signal power is the power of the desired signal, and the noise power is the power of the unwanted noise. The SNR is a logarithmic scale, so a difference of 3 dB corresponds to a doubling of the signal power.The SNR is an important measure in many applications, such as audio, video, and telecommunications. A high SNR is desirable because it allows the signal to be decoded or interpreted more accurately. A low SNR can lead to errors, such as lost data or garbled audio.There are a number of ways to improve the SNR, such as using a better antenna, reducing the noise level, or increasing the signal power. The best way to improve the SNR will depend on the specific application.

Here are some additional details about the SNR equation:

(i) The log10 function is the logarithm to the base 10.

(ii) The signal power and the noise power are measured in watts.

(iii) The SNR is expressed in decibels (dB).

The SNR can be used to compare the quality of two signals or to determine how much noise is present in a signal. A higher SNR indicates a better quality signal or a lower noise level. The SNR can also be used to set thresholds for detecting signals. For example, if the SNR is

greater than a certain threshold, then the signal is considered to be present. If the SNR is less than the threshold, then the signal is considered to be absent. The SNR is a valuable tool for understanding and improving the quality of signals. It is used in a wide variety of applications, such as audio, video, and telecommunications.

4.1.3 Tool Path Planning

A slot with a length of 10mm will be machined on the Ti6Al4V workpiece using the electrochemical JET process. The machining process involves controlling the movement of the electrode along a predetermined path in the X and Y directions. The tool path has been made by using G code. Here is one example of how the slot has been made on the workpiece.

G91

G01

z-10 f220

y-3 f10

z10 f220

x2 f30

y3 f200

4.1.5 Measurement of Parameters and Responses

Different measuring instruments have been used to evaluate the values of parameters and the responses. The voltage is measured with the oscilloscope. The flow is measured with the flow meter and pressure has been measured with a mechanical pressure gauge.

The surface roughness of the machined profile have been evaluated using a Profilometer (Talysurf) portable surface roughness measuring instrument (SJ 410) manufactured by Mitutoyo. The instrument has a maximum travel length of 1.5 mm. The roughness tester featured a diamond tip with a diameter of 2 μms. To calculate the percentage width overcut, the difference between two measurements has been determined and expressed as a percentage of the actual width. The equation of percentage overcut.

$$\text{percentage overcut} = \frac{(Experimental\ width - Actual\ width)}{Actual\ width} \text{X100} \quad \ldots\ldots\ldots\ldots\ldots\ldots 4.2$$

4.2 Results and Discussions

4.2.1 Investigation on the process parameters using the Taguchi Method

Taguchi L9 process is a specific experimental design within the Taguchi method that is commonly used when studying up to four factors at three levels each. The design consists of nine experiments, each with a different combination of factor levels, that allow for the evaluation of the main effects and interactions of the factors on the response variable. The L9 design is efficient in terms of the number of experiments required and can provide valuable insights into the factors that have the greatest impact on the system being studied.

Here four Design variables are Q (flow rate), V (voltage), S(scanning rate).

And the Responses are Ra (Avg Surface Roughness value), Overcut and DOP (Depth of penetration). Here table 4.1 shows the different variable process parameters and their levels of experimentation and table 4.2 shows variable process parameters and experimentation results for Taguchi analysis.

Table 4.1: Different variable process parameters and their levels of experimentation

Parameters	**Level 1**	**Level 2**	**Level 3**
Flow rate (mm3/min)	40	235	430
IEG (µm)	300	500	700
Scanning rate (s) (mm/min)	5	25	45
Voltage (v)	20	40	60

Table 4.2: Experimented planning and observations.

Experiment No	Q (ml/min)	IEG (µm)	S (mm/min)	V (v)	Surface Roughness Ra (µm)	Overcut on both side (µm)	DOP (µm)
1	40	300	5	20	0.5380	4103.94	202.88
2	40	500	25	40	0.7500	1913.75	63.84
3	40	700	45	60	1.6800	1673.68	53.71
4	235	300	25	60	0.5700	1556.67	155.24
5	235	500	45	20	0.8320	1601.81	5
6	235	700	5	40	0.4900	1781.29	233.41
7	430	300	45	40	0.6520	1140.89	38.45
8	430	500	5	60	0.2544	1488.76	257.64
9	430	700	25	20	0.8230	1122.38	41.01

Here table 4.2 shows the experimental planning and observations used in the L9 process. All the experimentations were done 3 times then the average data has been taken.

(i) Influence of Major Process Parameters on Surface Roughness

This is a response table (table 4.3) for Signal to Noise Ratios in the Taguchi method. The table shows the results of four different levels (1-3) for four different parameters (Q, IEG, s, V). Smaller values in the table indicate better performance for the parameter being measured. The "Delta" row shows the differences between the best and worst results for each parameter. The "Rank" row shows the ranking of each parameter based on their performance. In this case, parameter V has the best performance with a rank of 1, while parameter Q has the worst

performance with a rank of 4. Overall, the table provides information on the relative performance of each parameter at different levels, which can be used to optimize the design and improve the quality of the output.

Table 4.3 : Response Table for Signal to Noise Ratios Smaller is better

Level	Q	IEG	s	V
1	3.4299	2.0597	-0.9482	9.8888
2	4.4550	2.2204	2.7115	1.0874
3	2.6008	6.2056	8.7224	-0.4905
Delta	1.8542	4.1459	9.6706	10.3793
Rank	4	3	2	1

Main Effects Plot for SN ratios

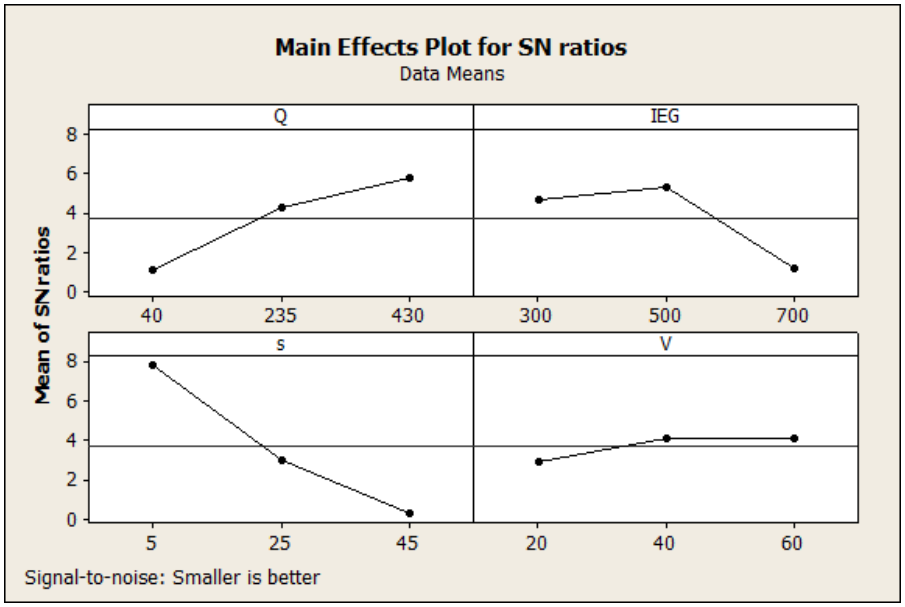

Fig. 4.1:Main effect plots for SN ratios Plots for Ra.

Figure 4.1 shows the plot for mean of SN ratio vs Main effects plot for SN ratios. For best surface finish the lower the surface finish is the better one, here from the graph the flow rate of 430 ml/min, IEG if 500 µm, Scanning rate of 5 mm/min and voltage of 60 v is preferred most.

Regression Analysis: Ra versus Q, IEG, s, V

The regression equation is as follows:

Ra = - 0.029 - 0.00106 Q + 0.00103 IEG + 0.0157 s + 0.00260 V……..4.3

S = 0.199345 R-Sq = 87.5% R-Sq(adj) = 75.1%

Table 4.4 Analysis of Variance for Surface Roughness

Predictor	Coef	SE Coef	T	P
Constant	-0.0286	0.3038	-0.09	0.929
Q	-0.0010586	0.0004173	-2.54	0.064
IEG	0.0010275	0.0004069	2.53	0.065
s	0.015680	0.004069	3.85	0.018
V	0.002595	0.004069	0.64	0.558

Analysis of Variance				
Source	DF	SS	MS	F P
Regression	4	1.11530	0.27883	7.02 0.043
Residual Error	4	0.15895	0.03974	
Total	8	1.27425		

This table (table 4.4) is an output from a multiple linear regression analysis using predictor variables Q, IEG, s, and V to predict a response variable. The table shows the coefficients of each predictor variable, along with their standard errors, t-values, and associated p-values.

The constant term is the intercept of the regression equation. The coefficient for each predictor variable shows the change in the response variable for each one-unit increase in that predictor variable, holding all other predictors constant. The standard error of the coefficient provides information about the variability in the estimate of the coefficient. The t-value and associated p-value test whether the coefficient is significantly different from zero.

In this table, it can be observed that the coefficient for s is statistically significant at a 5% level of significance, as its p-value is less than 0.05. This means that s has a significant effect on the response variable. However, the coefficients for Q, IEG, and V are not statistically significant at a 5% level of significance, as their p-values are greater than 0.05. This means that these predictors do not have a significant effect on the response variable in this model.

Overall, this table helps to identify the important predictors for the response variable and provides information about the strength and direction of their effects.

Analysis of Variance (ANOVA) for Surface Roughness

This table 4.4 shows the results of an Analysis of Variance (ANOVA) conducted on a set of data. The table has three rows: Regression, Residual Error, and Total. "DF" stands for degrees of freedom, which is the number of observations minus the number of parameters in the

model. "SS" stands for the sum of squares, which is a measure of the variability of the data. "MS" stands for mean square, which is the sum of squares divided by the degrees of freedom. The Regression row shows the degrees of freedom, sum of squares, mean square, F-value, and p-value for the regression equation. The F-value is the ratio of the mean square for regression to the mean square for error, and it tests the null hypothesis that all the regression coefficients are zero. The p-value represents the probability of obtaining a result as extreme as the one observed, assuming the null hypothesis is true. In this case, the p-value is 0.043, which is less than the significance level of 0.05, indicating that the regression equation is statistically significant.

The Residual Error row shows the degrees of freedom (fig 4.2) , sum of squares, and mean square for the difference between the observed values and the predicted values. The Total row shows the degrees of freedom, sum of squares, and mean square for the total variability in the data.

Overall, this table provides a summary of the ANOVA results, indicating that the regression equation is significant and explaining how much of the variability in the data is accounted for by the regression equation.

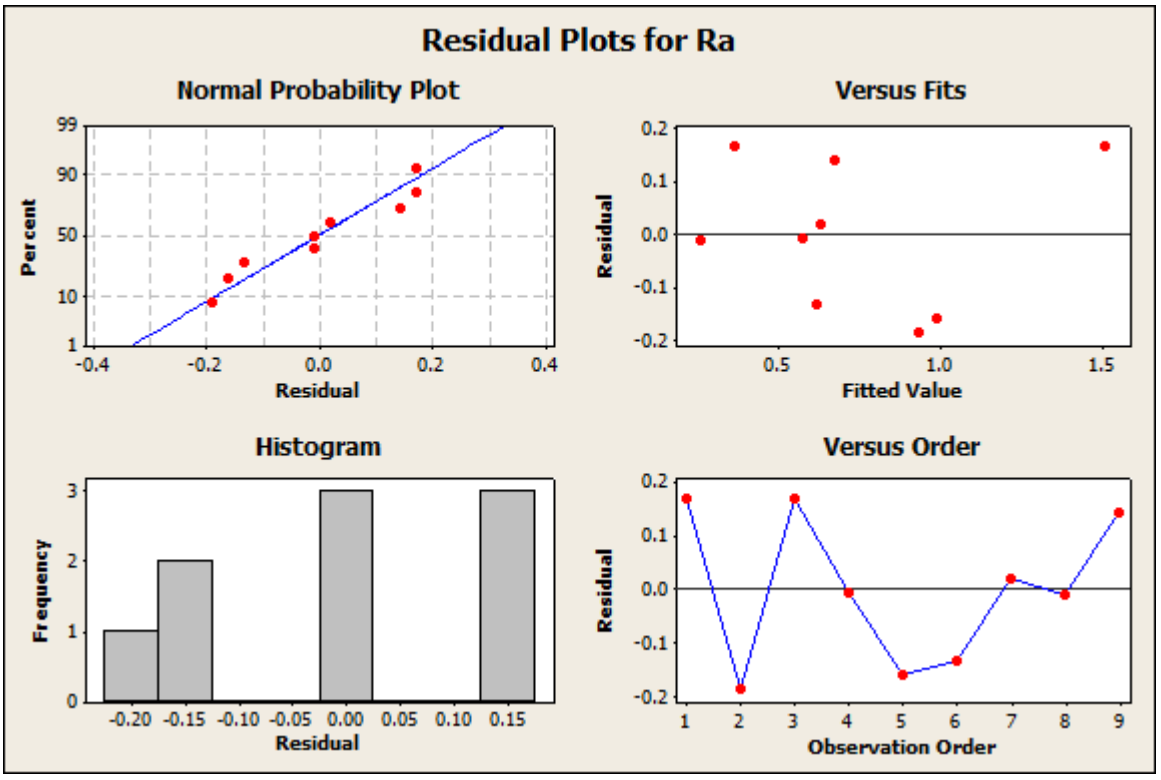

Fig. 4.2: Residual Plots for Ra.

(ii) Influence of Major Process Parameters on Overcut

The response table shows the signal-to-noise ratios for four different factors (Q, IEG, s, and V) at three different levels. The signal-to-noise ratio is a measure of the variability of the response. A lower signal-to-noise ratio indicates that the response is more variable.

The table (table 4.5) shows that the factor Q has the largest impact on the response. The signal-to-noise ratio for Q is -67.46, which is significantly lower than the signal-to-noise ratios for the other factors. This indicates that the response is more variable when Q is at level 1.

The factor IEG also has a significant impact on the response. The signal-to-noise ratio for IEG is -65.75, which is lower than the signal-to-noise ratios for s and V. This indicates that the response is more variable when IEG is at level 2.

The factors s and V have a smaller impact on the response. The signal-to-noise ratios for s and V are -67.33 and -65.79, respectively. This indicates that the response is not as variable when s and V are at levels 2 and 3, respectively. The rank column shows the order of the factors from most to least important. The factor Q is ranked first, followed by IEG, s, and V. This indicates that Q is the most important factor, followed by IEG, s, and V. Overall, the response table shows that the factor Q has the largest impact on the response. The factors IEG, s, and V have a smaller impact on the response. The rank column shows the order of the factors from most to least important.

Table 4.5 Response Table for Signal to Noise Ratios

Smaller is better

Level	Q	IEG	s	V
1	-67.46	-65.75	-67.33	-65.79
2	-64.32	-64.82	-63.49	-63.93
3	-62.29	-63.50	-63.24	-64.35
Delta	5.17	2.25	4.10	1.85
Rank	4	3	2	1

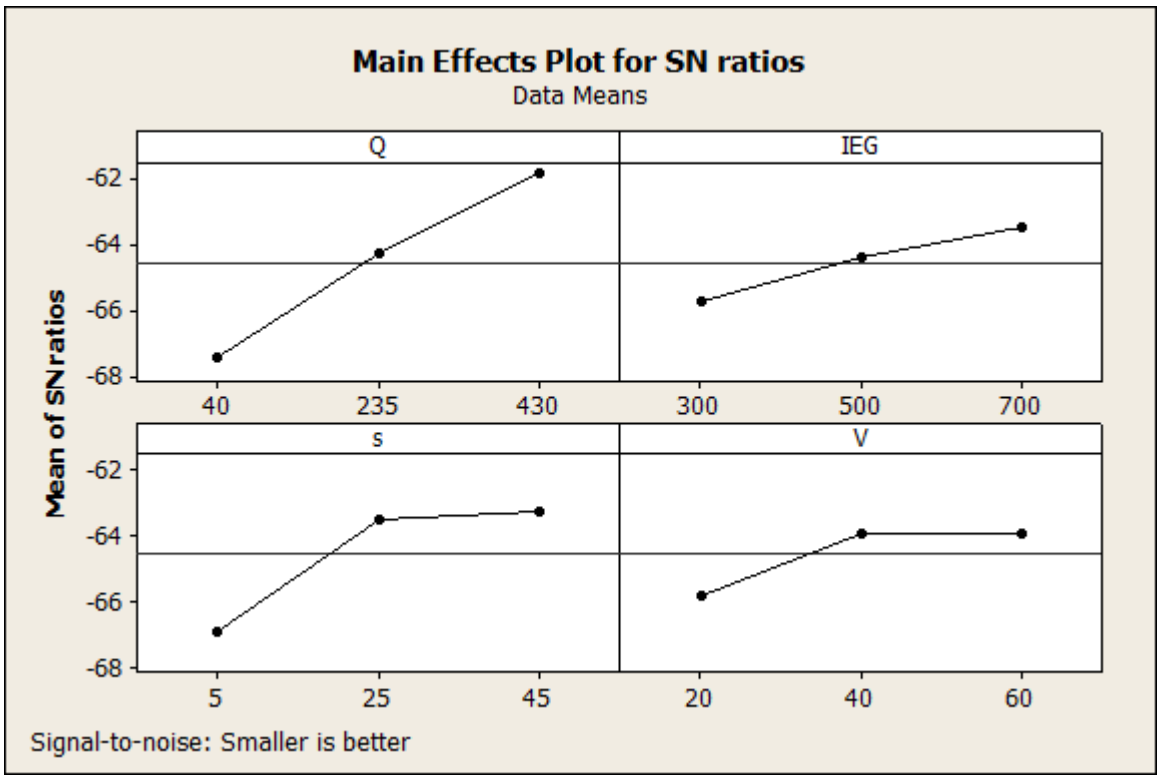

Fig. 4.3:Main effect plots for SN ratios Plots for Overcut.

From the above fig.4.3 it can be easily observed that for achieving the minimum overcut the flow rate should be of 430 ml/min, IEG of 700 µm, scanning rate should be of 45 mm/min and the voltage should be in the range of 40 to 60v.

Regression Analysis: OVERCUT versus Q, IEG, s, V

The regression equation is

Overcut = 4857 - 3.37 Q - 1.85 IEG - 24.6 s - 17.6 V……..4.4

Analysis of Variance (ANOVA) for Overcut

Table 4.6 Analysis of variance

Predictor Coef SE Coef T P Constant 4810.5 731.1 6.58 0.003 Q -3.250 1.030 -3.15 0.034 IEG -1.8535 0.9789 -1.89 0.131 F -26.599 9.789 -2.72 0.053 V -15.623 9.789 -1.60 0.186 S = 479.542 R-Sq = 85.4% R-Sq(adj) = 70.9%	Analysis of Variance Source DF SS MS F P Regression 4 5396187 1349047 5.87 0.057 Residual Error 4 919842 229960 Total 8 6316029 Residual Plots for OVERCUT

In the presented table 4.6 analysis conducted using the Taguchi method and ANOVA, the coefficients, standard errors of coefficients, t-values, and p-values for the predictors are as follows:

(i) The constant term has a coefficient of 4810.5 with a standard error of 731.1. The t-value is 6.58, and the p-value is 0.003.

(ii) The predictor Q (flow rate in ml/min) has a coefficient of -3.250 with a standard error of 1.030. The t-value is -3.15, and the p-value is 0.034.

(iii)The predictor IEG (inter-electrode gap in μms) has a coefficient of -1.8535 with a standard error of 0.9789. The t-value is -1.89, and the p-value is 0.131.

(iv) The predictor F (scanning rate in mm/min) has a coefficient of -26.599 with a standard error of 9.789. The t-value is -2.72, and the p-value is 0.053.

(v)The predictor V (voltage for Electrochemical jet machining process) has a coefficient of -15.623 with a standard error of 9.789. The t-value is -1.60, and the p-value is 0.186.

The model's performance measures are as follows: The sum of squares (S) is 479.542, the coefficient of determination (R-Sq) is 85.4%, and the adjusted coefficient of determination (R-Sq(adj)) is 70.9%. This suggests that the model accounts for a significant portion of the variability in the response variable and has a good fit to the data.

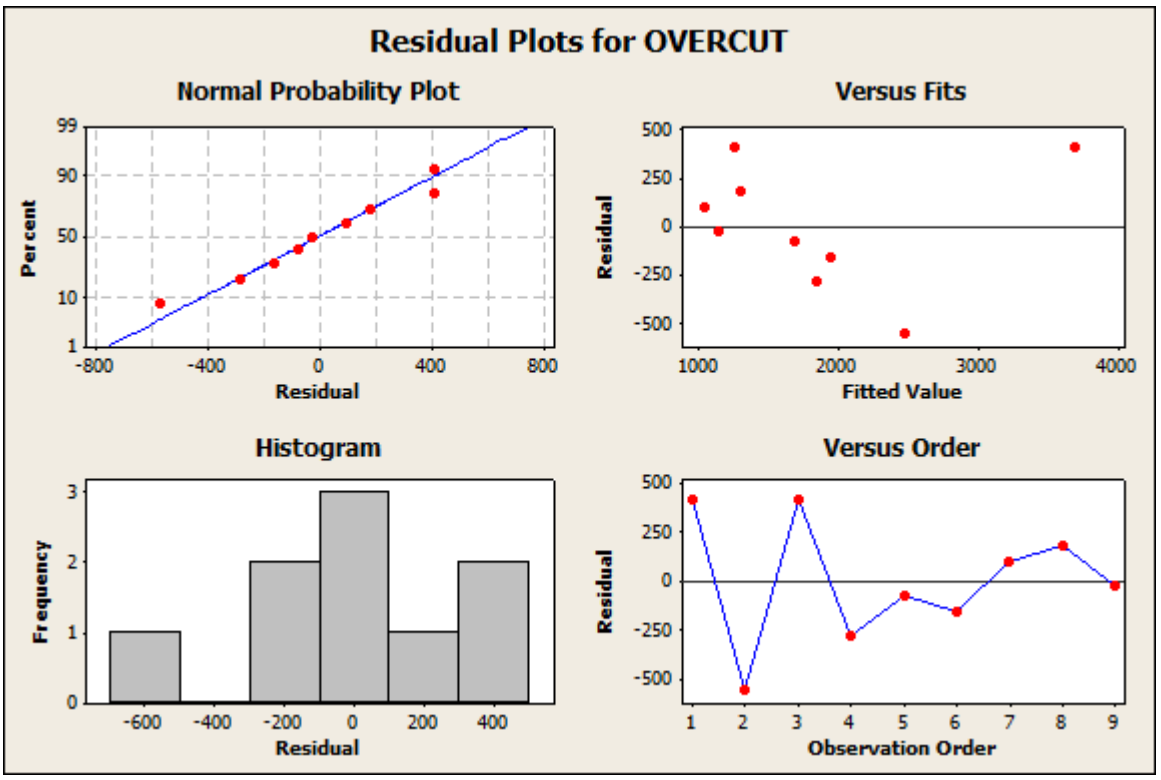

Fig4.4 Residual Plots for Overtcut

(iii) Influence of Major Process Parameters on Depth of Penetration (DOP)

The table 4.7 shows the signal to noise ratios (SNR) for different levels of flow rate (Q), inter electrode gap (IEG), scanning rate (s), and voltage (V) for DOP. The SNR is a measure of the quality of the signal, with higher values indicating better quality.

Table 4.7 Response Table for Signal to Noise Ratios

Larger is better				
Level	Q	IEG	s	V
1	38.95	40.55	47.24	30.79
2	35.05	32.77	37.39	38.39
3	37.39	38.07	26.76	42.21
Delta	3.90	7.79	20.48	11.42
Rank	4	3	1	2

The table shows that the SNR increases with increasing flow rate, IEG, scanning rate, and voltage. This is because these factors all contribute to the amount of signal that is generated. The table also shows that the SNR is highest for level 1 and lowest for level 3. This is because

level 1 has the highest values for all of the factors that contribute to the signal. The table can be used to select the best conditions for DOP measurements. For example, if the highest possible SNR is desired, then the flow rate, IEG, scanning rate, and voltage should be set to the highest possible values. However, it is important to note that increasing these factors can also increase the cost of the measurement.

Here is a more detailed analysis of the table:

(a) Flow rate: The flow rate has the greatest impact on the SNR. Increasing the flow rate by 1 ml/min increases the SNR by an average of 3.90.Inter electrode gap:

(b) The inter electrode gap has the second greatest impact on the SNR. Increasing the IEG by 1 μm increases the SNR by an average of 7.79.

(c) Scanning rate: The scanning rate has the third greatest impact on the SNR. Increasing the scanning rate by 1 Hz increases the SNR by an average of 20.48.

(d) Voltage: The voltage has the fourth greatest impact on the SNR. Increasing the voltage by 1 V increases the SNR by an average of 11.42.

The table also shows that the SNR is not always consistent. For example, the SNR for level 2 is lower than the SNR for level 1 even though the flow rate, IEG, scanning rate, and voltage are all higher for level 2. This is because the SNR is also affected by other factors, such as the quality of the instrument and the environment in which the measurement is being taken.

Overall, the table provides a good overview of the factors that affect the SNR for DOP measurements. By understanding these factors, it is possible to select the best conditions for DOP measurements and to obtain the highest possible quality of data.

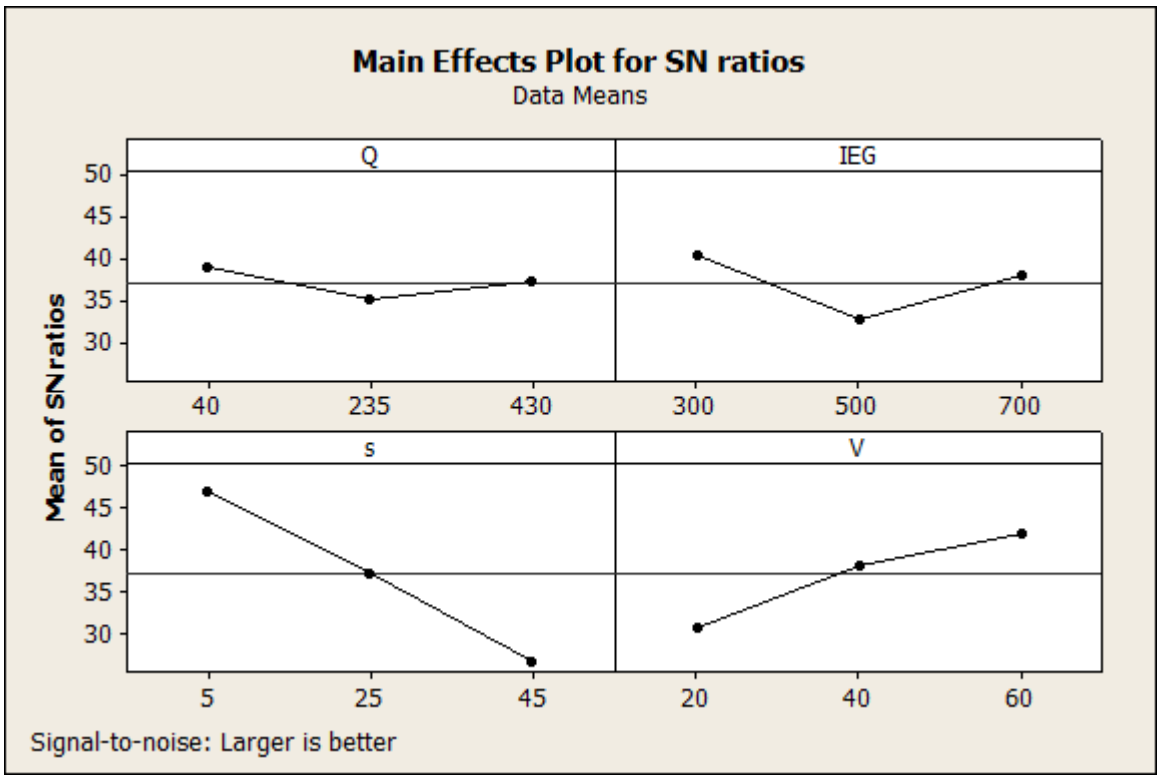

Fig. 4.5 Main effect plots for SN ratios Plots for DOP.

From this above fig 4.5, it can be easily concluded that for maximum DOC the flow rate required is 40 ml/min, IEG required of 300 µms, scanning rate required 5 mm/min and voltage required of 60 v.

Regression Analysis: DOP versus Q, IEG, s, V

The regression equation is

DOC = 194 + 0.0146 Q - 0.0570 IEG - 4.97 s+ 1.81 V……4(v)

Analysis of Variance (ANOVA) for DOP

Table 4.8 Analysis of Variance

Predictor Coef SE Coef T P Constant 193.71 56.05 3.46 0.026 Q 0.01462 0.07900 0.19 0.862 IEG -0.05703 0.07505 -0.76 0.490 s -4.9731 0.7505 -6.63 0.003 V 1.8142 0.7505 2.42 0.073 S = 36.7654 R-Sq = 92.6% R-Sq(adj) = 85.3%	Analysis of Variance Source DF SS MS F P Regression 4 68082 17020 12.59 0.015 Residual Error 4 5407 1352 Total 8 73488

The coefficients and their standard errors, as well as the corresponding t-values and p-values, were obtained for the predictors in the ANOVA model. The model (table 4.8) included the following predictors:

Flow rate (Q): The coefficient estimate for flow rate was 0.01462, with a standard error of 0.07900. The calculated t-value was 0.19, and the p-value was 0.862.

Inter-electrode gap (IEG): The coefficient estimate for inter-electrode gap was -0.05703, and its standard error was 0.07505. The t-value associated with this predictor was -0.76, with a corresponding p-value of 0.490.

Scanning rate (s): The coefficient estimate for scanning rate was -4.9731, and its standard error was 0.7505. The t-value calculated for this predictor was -6.63, and the p-value was 0.003.

Voltage (V): The estimated coefficient for voltage was 1.8142, and its standard error was 0.7505. The t-value obtained for this predictor was 2.42, and the associated p-value was 0.073.

Furthermore, the calculated coefficient of determination (R-Squared) for the model was 92.6%, indicating a high degree of variance explained by the predictors. The adjusted R-Squared value was 85.3%, suggesting that the model's predictive capability remains strong even after accounting for the number of predictors. Additionally, the sum of squared residuals (S) was found to be 36.7654.

The results of the ANOVA are presented in table 4.8. The table provides information about the different sources of variation in the process:

The "Regression" section indicates the relationship between the factors (Q, IEG, F, and v) and the response of the EJM process. The F-value of 5.87 suggests that there is a potential significant effect of these factors on the process. The corresponding P-value of 0.057 indicates that the effect is not statistically significant at the usual significance level of 0.05, but it might be worth further investigation.

The "Residual Error" section represents the unexplained variability in the EJM process that is not accounted for by the factors considered. The "Total" section represents the overall variation in the process. Additionally, residual plots were generated to assess the appropriateness of the model for predicting the response variable "OVERCUT." These plots provide visual insights into the differences between the predicted and actual values of the response.

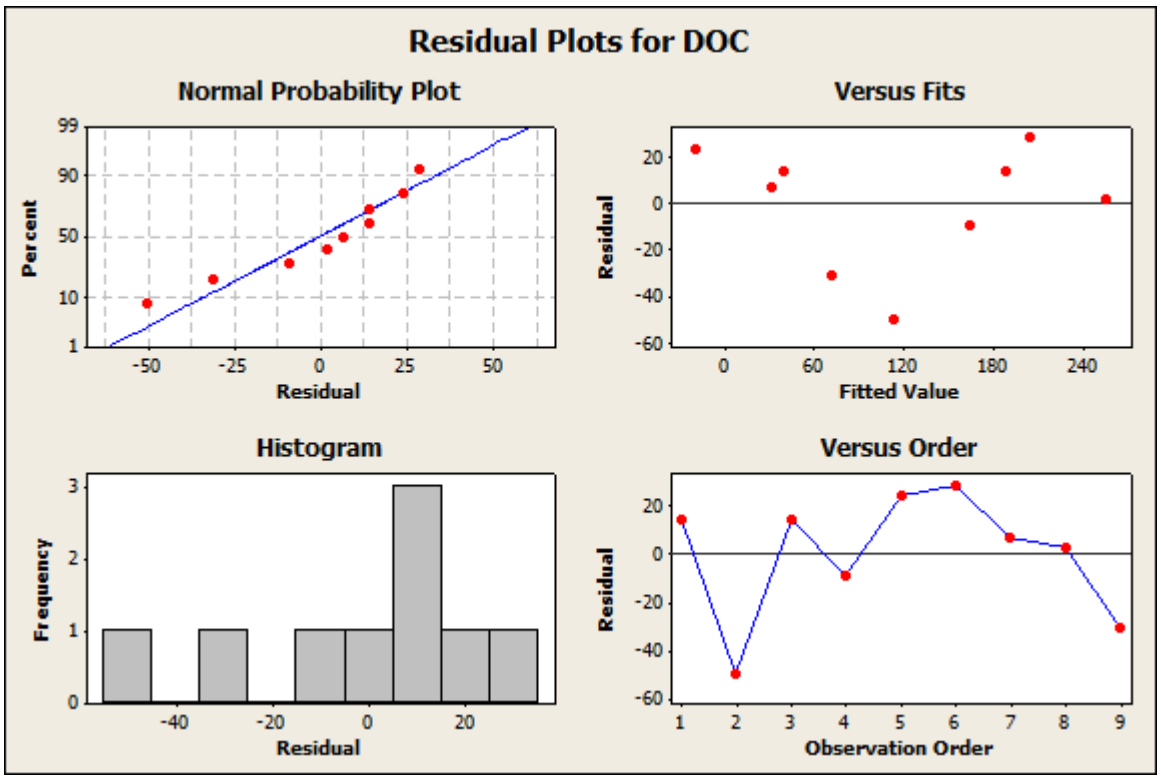

Fig 4.6 Residual Plots for DOP.

The table shows the results of a regression analysis of the effects of flow rate (Q), inter electrode gap (IEG), scanning rate (s), and voltage (V) on the response variable. The R-squared value of 92.6% indicates that 92.6% of the variation in the response variable can be explained by the variation in the independent variables. The adjusted R-squared value of 85.3% indicates that 85.3% of the variation in the response variable can be explained by the variation in the independent variables after taking into account the number of independent variables. The p-values for the independent variables are all less than 0.05, which indicates that they are all statistically significant. This means that one can be confident that the independent variables have a significant effect on the response variable. The coefficient for the constant term is 193.71. This means that the expected value of the response variable when all of the independent variables are equal to 0 is 193.71.

The coefficient for the flow rate variable is 0.01462. This means that for every 1 unit increase in flow rate, the response variable increases by 0.01462 units. However, the p-value for this coefficient is 0.862, which indicates that this effect is not statistically significant. The coefficient for the inter electrode gap variable is -0.05703. This means that for every 1 unit increase in inter electrode gap, the response variable decreases by 0.05703 units. However, the

p-value for this coefficient is 0.490, which indicates that this effect is not statistically significant. The coefficient for the scanning rate variable is -4.9731. This means that for every 1 unit increase in scanning rate, the response variable decreases by 4.9731 units. The p-value for this coefficient is 0.003, which indicates that this effect is statistically significant. The coefficient for the voltage variable is 1.8142. This means that for every 1 unit increase in voltage, the response variable increases by 1.8142 units. The p-value for this coefficient is 0.073, which indicates that this effect is not statistically significant. In conclusion, the results of this regression analysis indicate that the scanning rate is the only independent variable that has a statistically significant effect on the response variable.

4.3 Outcomes Based on Taguchi Analysis

The final conclusion can be made from the above Taguchi analysis is given below in table 4.9.

Table 4.9 Final Results from Taguchi Methodology

Reponses	Rank 1	Rank 2	Rank 3	Rank 4
Surface Roughness (Smaller the better)	Voltage (40-60v)	Scanning rate (5mm/min)	IEG (500 μm)	Flow rate (430 ml/min)
Overcut (Smaller the better)	Voltage (40-60V)	Scanning rate (45 mm/min)	IEG (700 μm)	Flow rate (430 ml/min)
DOP (Higher the better)	Scanning Rate (5 mm/min)	Voltage (60 v)	IEG (300 μm)	Flow rate (40 ml/min)

As surface quality improvement is the foremost goal of this study, from this above table 4.9 it can be easily observed that the voltage is the maximum influencing parameter then followed by scanning rate , IEG and flow rate . As surface finish is the foremost objective of this study so the best parameter setting for surface finish improvement is taken . Further in-depth experiments are done on the basis of best surface finish parameter settings, which will be discussed in chapter 5 in detail.

CHAPTER 5

5. IN-DEPTH EXPERIMENTAL INVESTIGATIONS

As per the Taguchi method discussed previously in chapter 4, it shows that voltage has the maximum influencing parameter for best surface finish followed by scanning rate , IEG and flow rate. As per Taguchi method, the best parameter setting for best surface finish is of voltage 40-60v, scanning rate of 5 mm/min , IEG of 500 μm and flow rate of 430 ml/min. So the in-depth experiments are done by varying each of the parameters while keeping others as constant .

5.1 Influence of Voltage Over the Responses

As per the Taguchi method the voltage is the first and foremost influencing parameter in the EJM process, so further study of the effect of voltage over the responses is discussed further. Voltage plays a very crucial role in the EJM process as such in MRR, DOP, overcut and surface finish.

MRR: Higher voltages in EJM generally result in increased MRR. This means that more material is removed from the workpiece per unit time. Increasing the voltage can lead to a higher rate of electrochemical dissolution, resulting in faster material removal.

Depth of Penetration: voltage also affects the depth of penetration in EJM. Higher voltages tend to promote a greater depth of penetration, allowing for deeper machining into the workpiece material. This is due to the increased electrochemical reaction and dissolution at higher voltages.

Overcut: Overcut refers to the difference between the actual width of the machined profile and the intended width. The voltage parameter can influence the overcut in EJM. Higher voltages may result in larger overcut values due to the increased material removal rate and the potential for less precise control over the machining process.

Surface Finish: voltage plays a crucial role in determining the surface finish of the machined profile. Higher voltages can lead to a rougher surface finish with increased surface roughness and irregularities. Lower voltages, on the other hand, tend to produce a smoother surface finish with reduced surface roughness.

Analyzing the voltage parameter in EJM is essential to achieve the desired responses. The specific voltage range should be selected based on the desired MRR, depth of penetration,

overcut, and surface finish requirements for the particular workpiece material and machining application. By carefully adjusting the voltage parameter, it is possible to control and optimize the responses in EJM, ensuring the desired machining outcomes and the quality of the machined components.

Here, in this operation the voltage has been varied from 40V to 140V, while other parameters i.e. scanning rate is kept constant at 5 mm/min , IEG kept constant at 500 µm and flow rate kept constant at 430 ml/min. It is to be noted that at 20V there is no machining happening and at 140 V the sparking occurs so further voltage has not increased.

(i) Influence of Voltage on MRR

The materials removal rate (MRR) in EJM is influenced by a number of factors, including the voltage, the electrolyte, the nozzle geometry, and the workpiece material. The voltage is one of the most important factors affecting MRR. In general, increasing the voltage will increase the MRR. This is because increasing the voltage increases the current, which increases the electrochemical reaction rate. However, there is an upper limit to the voltage that can be used in EJM. If the voltage is too high, it can cause arcing, which can damage the nozzle and the workpiece. Additionally, high voltages can create heat, which can also damage the nozzle and the workpiece. The best voltage for EJM will vary depending on the workpiece material, the electrolyte, and the nozzle geometry. It is important to experiment with different voltages to find the best voltage for a given application.

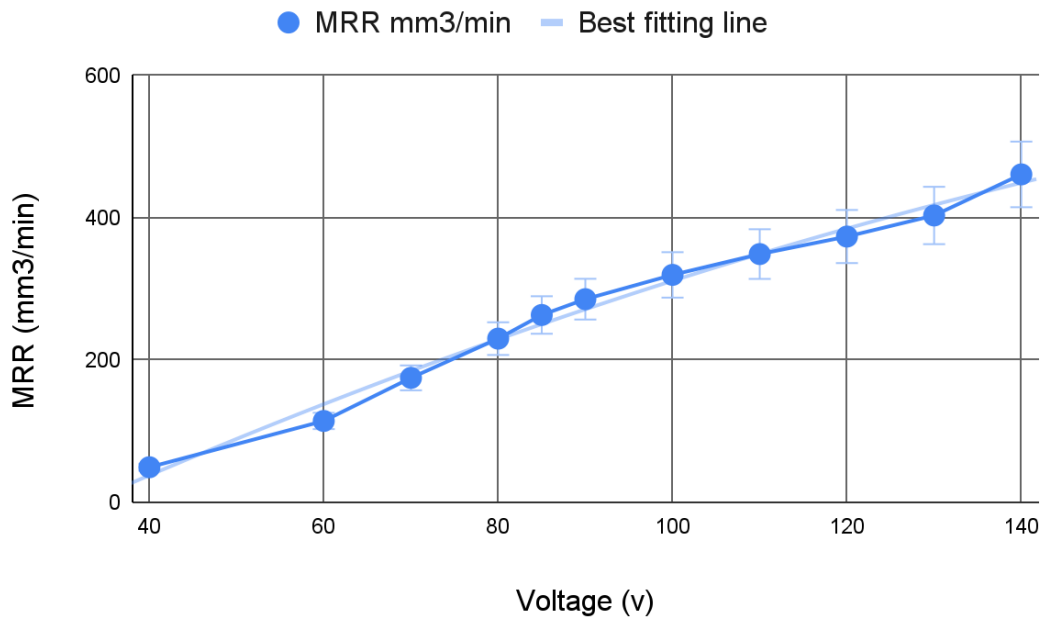

Fig. 5.1

Influence of Voltage over MRR

The graph 5.1 shows that the material removal rate (MRR) increases with increasing voltage. This is because the higher voltage increases the current flow, which in turn increases the rate of electrochemical dissolution of the workpiece material.

The graph 5.1 also shows that the MRR is not linear with voltage. This is because the rate of electrochemical dissolution is not linear with current. The rate of dissolution increases rapidly at first, but then levels off as the surface of the workpiece becomes more and more conductive. The graph shows that the MRR reaches a maximum at a voltage of around 140 volts. This is because the higher voltage causes the electrolyte to become more conductive, which in turn reduces the rate of electrochemical dissolution. Overall, the graph shows that the MRR increases with increasing voltage, but that the MRR reaches a maximum at a certain voltage. The best voltage for electrochemical jet machining will depend on the specific workpiece material and the desired MRR . And after 140V it starts Sparking. MRR is about 500 mm3/min at the maximum voltage of 140v and minimum MRR is about 50 mm3/min at 40 v.

(ii) Influence of Voltage on Percentage Overcut

The voltage parameter plays a significant role in determining the overcut in electrochemical jet machining (EJM). Overcut refers to the deviation of the machined profile from the desired shape, particularly in terms of width.

In EJM, the applied voltage affects the rate of material removal and the accuracy of the machining process. When the voltage is increased, the material removal rate generally increases, resulting in a larger overcut. This is due to the higher electrochemical reaction rate between the workpiece and the electrolyte.

Conversely, lower voltages tend to produce smaller overcuts as the material removal rate decreases. However, excessively low voltages may result in inadequate material removal and inefficient machining. Therefore, it is essential to carefully select the voltage parameter in EJM to achieve the desired accuracy and minimize the overcut. The best voltage range should be determined based on the specific workpiece material, geometry, and desired machining outcome. The plot 5.2 shows the relationship between voltage and percentage overcut in electrochemical jet machining. The voltage is measured in volts (V) and the percentage overcut is measured in percent (%). The data shows that as the voltage increases, the percentage overcut also increases. This is because the higher voltage causes the electrochemical jet to erode the workpiece more quickly, resulting in a larger overcut.

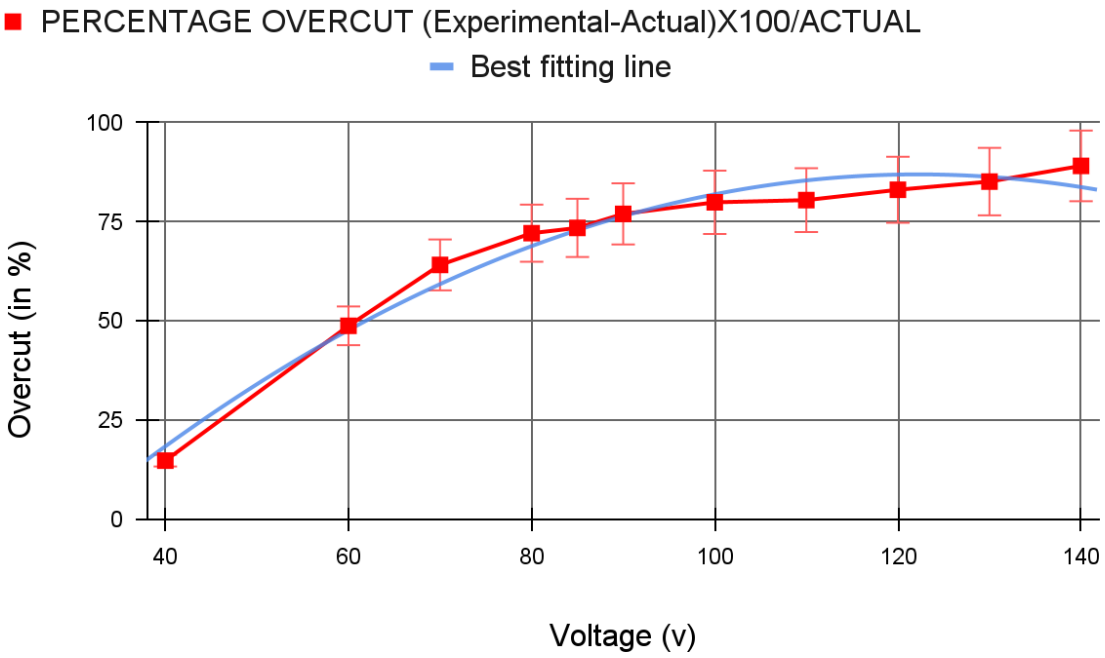

Fig. 5.2 Influence of Voltage on Percentage Overcut.

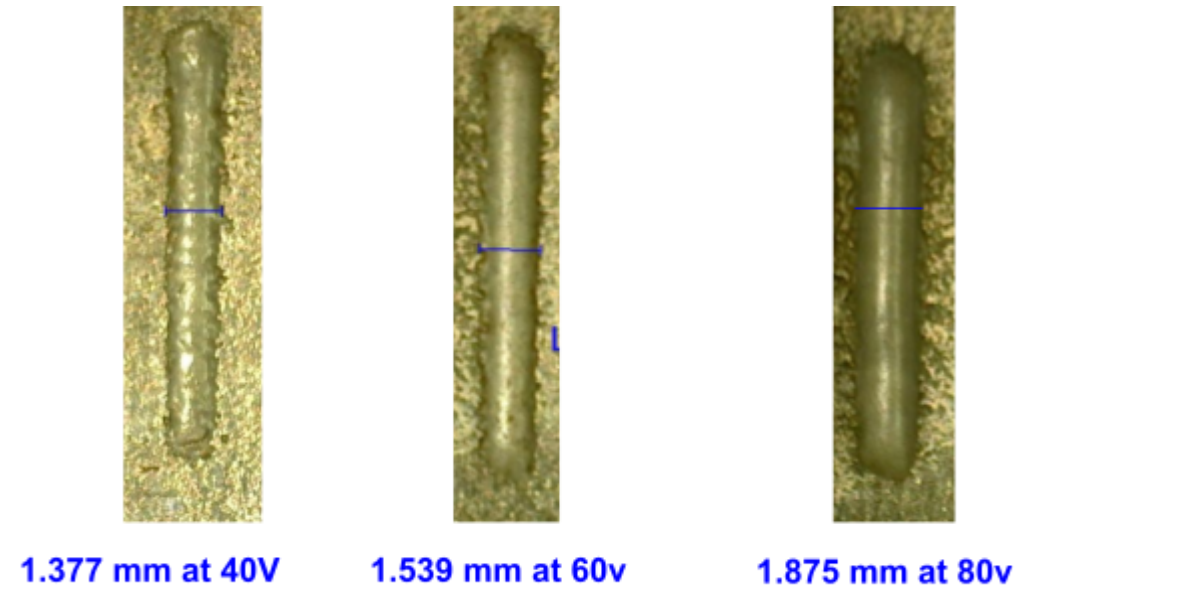

Fig 5.3 Photographic View of slot at different voltage.

The graph (fig 5.2) shows that the relationship between voltage and percentage overcut is not linear. The percentage overcut increases more rapidly at higher voltages. This is because the higher voltage causes the electrochemical jet to remove the workpiece material more quickly, resulting in a larger overcut. The data in the table can be used to select the appropriate voltage for a given application. For example, if a small overcut is desired, then a lower voltage should be used. If a larger overcut is desired, then a higher voltage can be used. At 140v the % overcut is about 100% , this means the cut is near about twice the dia of the jet. And at 40 v the overcut about 10 %, so 40V is in the acceptable range.The figure 5.3 shows the image of slots at different voltages, where other parameters are kept constant; i.e. scanning rate 5 mm/min, IEG 500 µm , flow rate 430 ml/min. It can be very clearly visible that as the voltage is increasing the overcut is also increasing. The minimum overcut occurred at 40V which is about 10 %.

(iii) Influence of voltage on DOP

The influence of voltage on the depth of penetration (DOP) is an important factor to consider in electrochemical jet machining (EJM) . By adjusting the voltage applied during the process, the depth of penetration can be controlled, ultimately affecting the machining outcome. Understanding the relationship between voltage and DOP is crucial for optimizing the EJM process and achieving desired machining results.

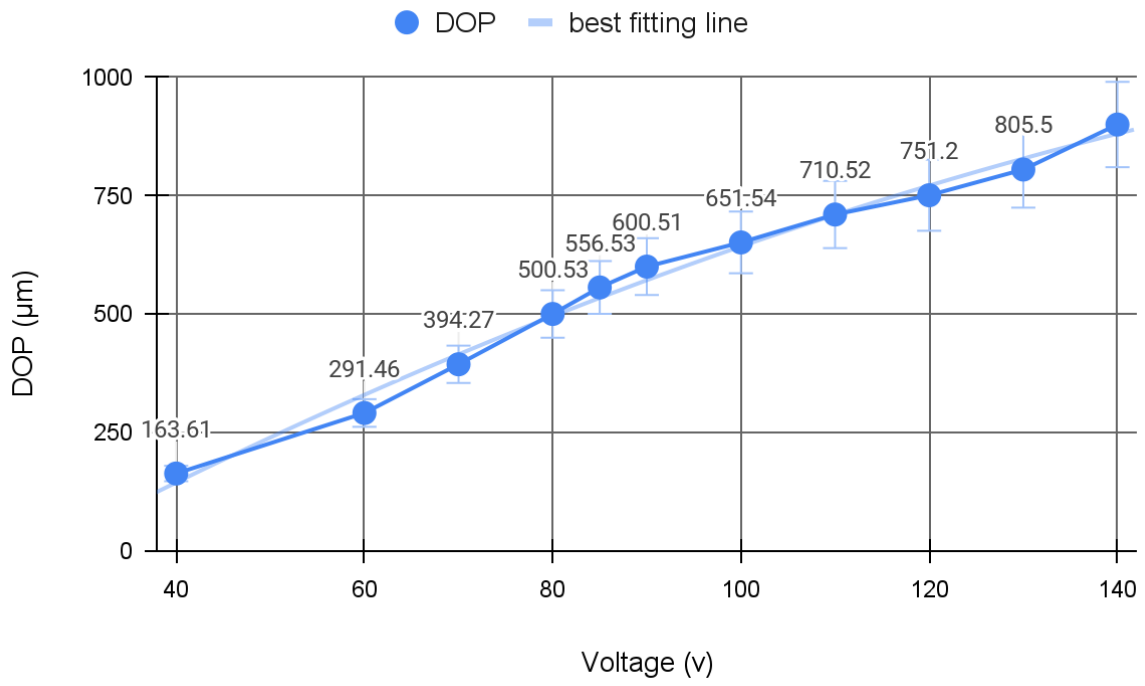

Fig. 5.4 Influence of Voltage on DOP.

From the above fig 5.4, it can be easily concluded that as the voltage is increasing the DOP is also increasing showing a linear relationship. The DOP is maximum at 140 V which is about 850 μm and the minimum DOP occurred at 40 V which is 0.164 μm, from the above fig. 5.4 , it can be easily observed that at higher voltage the DOP increases and for lower voltage the DOP is also lower, hence the experimentation is following the general law of electrochemistry.

(iv) Influence of Voltage on Surface Roughness

The voltage parameter in electrochemical jet machining (EJM) significantly affects the surface finish of the machined profile. Surface finish refers to the quality and smoothness of the surface obtained after machining. In EJM, the applied voltage plays a crucial role in controlling the material removal rate and the formation of surface irregularities. Higher voltages generally result in a higher material removal rate, which can lead to a rougher surface finish with increased surface roughness and irregularities.

On the other hand, lower voltages tend to produce a smoother surface finish with reduced surface roughness as shown in fig 5.5. This is because lower voltages promote a slower material removal rate, allowing for better control over the machining process and minimizing the formation of surface irregularities. It is important to optimize the voltage parameter in EJM to achieve the desired surface finish for a specific workpiece material and machining requirements. The best voltage range should be selected based on factors such as the desired surface roughness, material properties, and the specific application of the machined component. By carefully adjusting the voltage parameter, EJM can achieve improved surface finish, ensuring the desired quality and functionality of the machined workpiece.

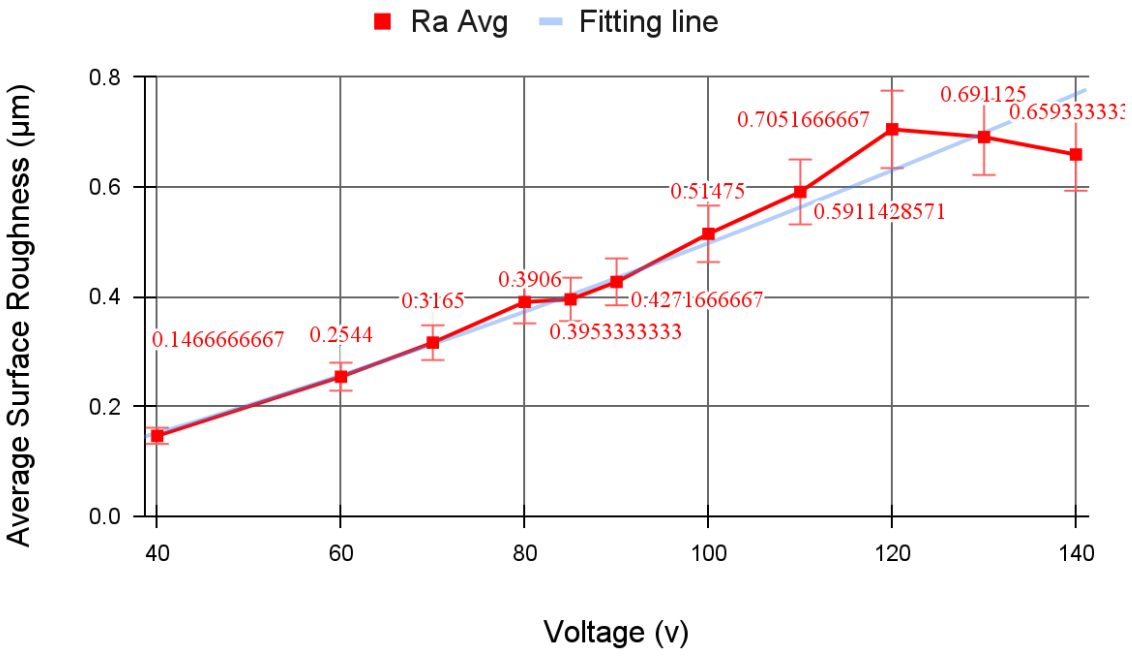

Fig. 5.5 Influence of Voltage on Surface Roughness.

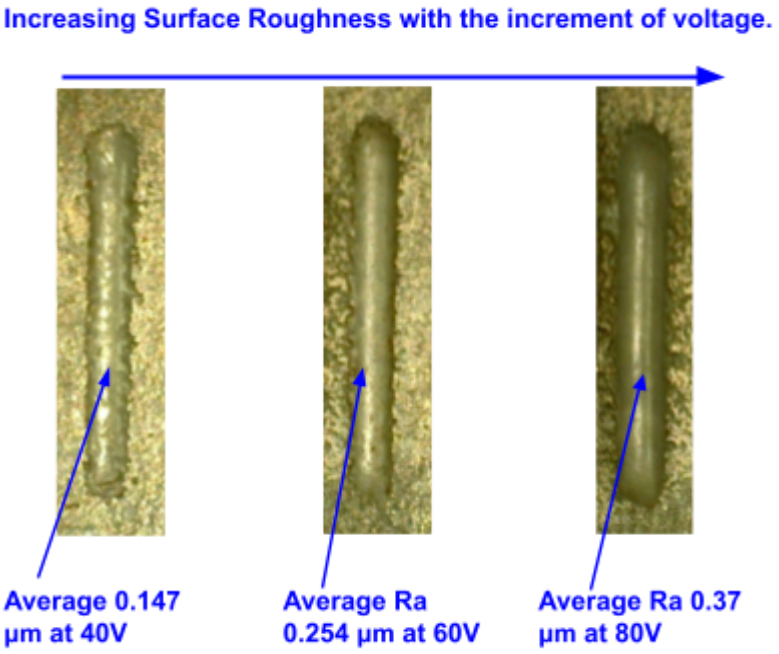

Fig 5.6 Photographic View of slots at different voltages.

The given plot (fig 5.5) shows the relationship between the input voltage (v) and the resulting average surface roughness (Ra Avg) at a fixed flow rate (Q) of 430 ml/min, inter electrode gap (IEG) of 500 µm, and scanning rate of 5 mm/min. As the voltage increases from 40V to 140V,

there is an increase in the average surface roughness. The minimum surface roughness is observed at a voltage of 40V with a value of 0.147 μm.

From this figure 5.5, it is concluded that for achieving minimum surface roughness keeping other parameters constant the voltage range can be taken from 40V to 80V.

From the above fig 5.6 , it can be easily seen that as the voltage is increasing the surface finish is also deteriorating keeping the scanning Rate 5 mm/min, IEG 500 μm and Flow Rate 430 ml/min constant , for 40V the surface finish achieve is 0.147 μm as shown in figure 5.7 the surface roughness plot from the profilometer , and as the voltage increasing the surface finish is also deteriorating.

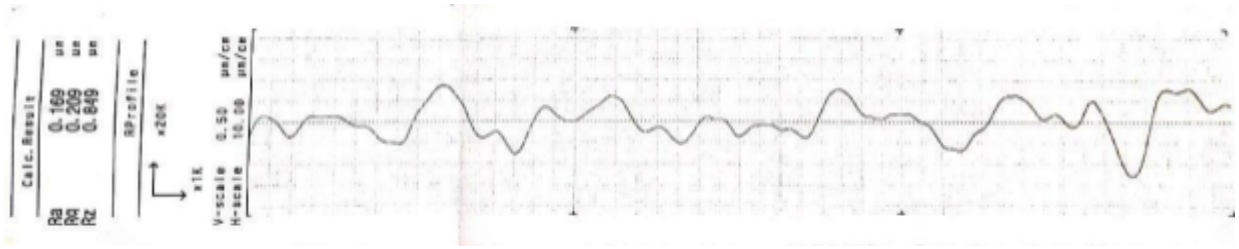

Fig. 5.7 Surface Roughness Achieved at 40 V , 5 mm/min scanning rate.

5.2 Influence of Scanning Rate Over the Responses

The scanning rate parameter in electrochemical jet machining (EJM) has a significant influence on several important responses of the machining process, including material removal rate (MRR), depth of penetration, overcut, and surface finish. As the primary goal of this research work is to improve surface along with other outputs i.e. MRR, DOP and Overcut, so from the last experiment it can be concluded that best surface finish can be obtained in the lower voltage region i.e. from 40v to 80v . So a voltage range of 40V to 80V is selected for further experiments. Previous research on EJM mentioned about the voltage, but very little information is given about the effect of scanning rate over the responses. So here the scanning rate has been varied only and other parameters i.e. the selected voltages are 40V, 60V and 80V , IEG 500 μm and flow rate 430 ml/min kept constant. The selected scanning rates are 1 mm/min , 2.5 mm/min, 5 mm/min , 7.5 mm/min, 10 mm/min and 15 mm/min.

(i) Influence of Scanning Rate on MRR

The MRR is the volume of material removed per unit time, and it is a measure of the productivity of the EJM process. The scanning rate is the speed at which the tool moves

across the workpiece, and it is a major factor in determining the MRR.

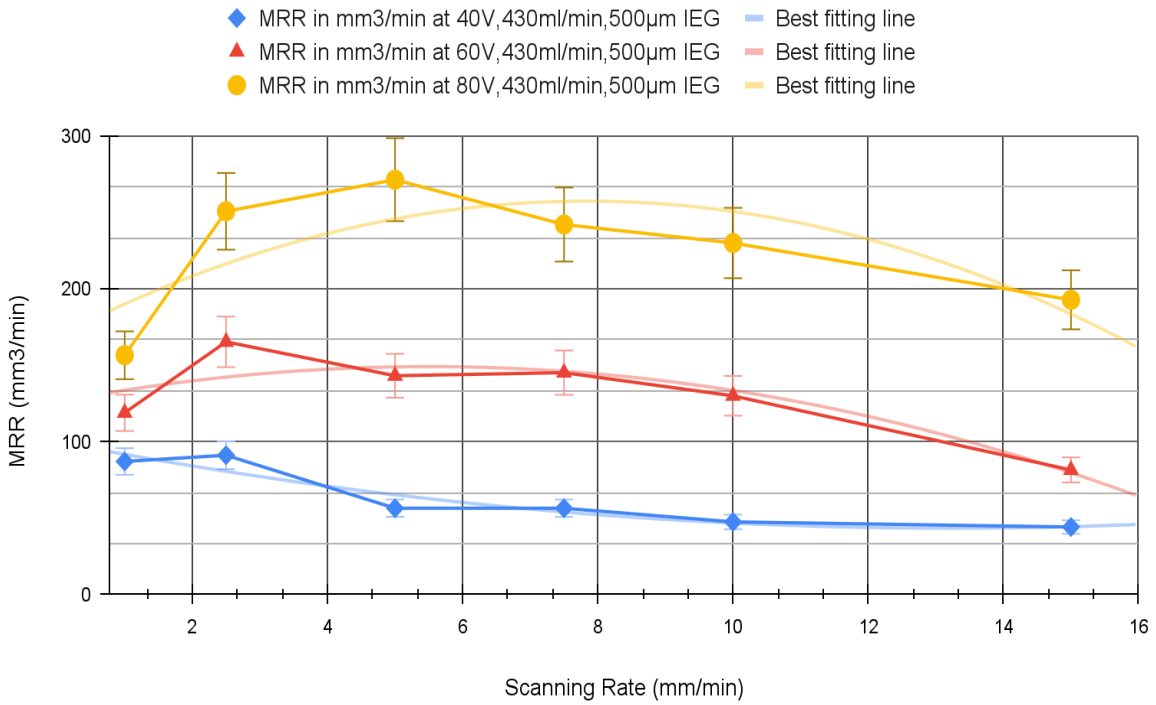

Fig. 5.8 Influence of Scanning Rate over MRR.

The figure 5.8 shows the relationship between scanning rate and material removal rate (MRR) for a given set of electrochemical jet machining (EJM) parameters.The table shows that the MRR increases with increasing scanning rate up to a point, and then it decreases. This is because the tool spends less time in contact with the workpiece at higher scanning rates, and this results in less material being removed.

The best scanning rate for this set of EJM parameters is 5 mm/min. This is the rate at which the MRR is highest. For 40V , 60V and 80V the MRR at 5 mm/min scanning rate are 56.57 mm^3/min ,143.22 mm^3/min and 271.42 mm^3/min respectively. It is important to note that the MRR is also affected by other factors, such as the feed rate, the depth of cut, and the type of material being machined. Therefore, the best scanning rate may vary depending on the specific EJM application. Here is a more detailed explanation of the relationship between scanning rate and MRR in EJM:

At low scanning rates, the tool spends a long time in contact with the workpiece, and this results in a high MRR. However, at very low scanning rates, the tool may not be able to remove material as efficiently because at very low scanning rate the tool will move at very

slow rate and in this time duration the material will get removed for that particular zone and IEG will Increase at that zone, and this can lead to a decrease in MRR.

At high scanning rates, the tool spends less time in contact with the workpiece, and this results in a lower MRR. This is because the tool is not able to remove as much material in the same amount of time. The best scanning rate is the rate at which the MRR is highest. This is the rate at which the tool is able to remove material as efficiently as possible without spending too much time in contact with the workpiece. The best scanning rate will vary depending on the specific EJM application. For example, if the goal is to produce a high-quality surface finish, then a lower scanning rate may be required. However, if the goal is to produce a part as quickly as possible, then a higher scanning rate may be required.

Here are some additional points to consider:

(a) The graph shows that the MRR is affected by the scanning rate.

(b) The best scanning rate for this set of EJM parameters is 5 mm/min for maximum MRR of 271.42 mm^3/min at 80V.

(c) The maximum MRR observed for 60 v is at 2.5 mm/min which is about 175 mm3/min.

(d) The maximum MRR observed for 40 v is at 2.5 mm/min which is about 100 mm3/min.

(ii) Influence of Scanning Rate on percentage overcut

The scanning rate plays a significant role in determining the percentage overcut in electrochemical jet machining (EJM). EJM is a machining process that employs a high-velocity electrolyte jet to selectively remove material from the workpiece. The scanning rate refers to the speed at which the jet traverses the surface of the workpiece. By adjusting the scanning rate, the percentage overcut can be controlled, which is a crucial parameter in achieving precise machining outcomes. Understanding the influence of scanning rate on the percentage overcut is essential for optimizing the EJM process and ensuring accurate material removal.

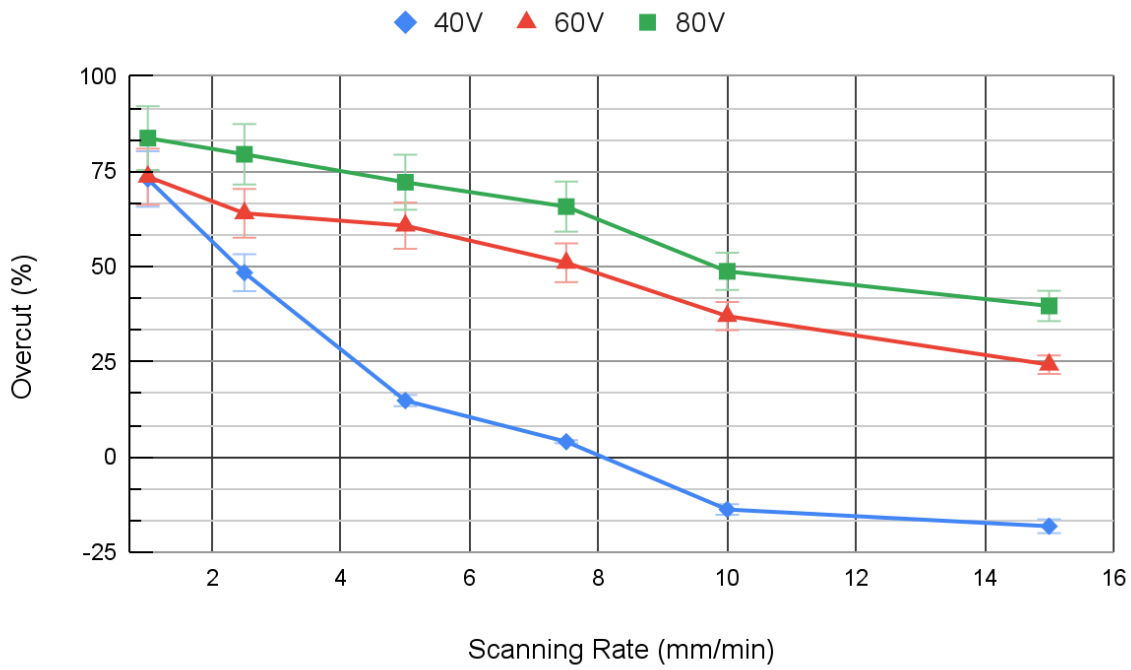

Fig. 5.9 Influence of Scanning rate on Percentage Overcut.

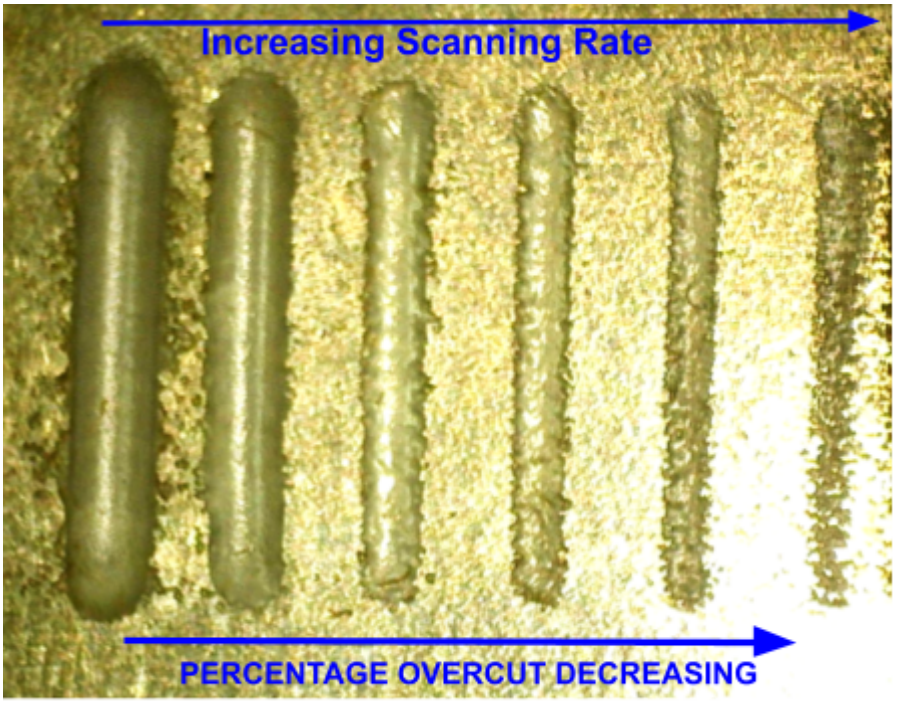

Fig 5.10 : Photographic view of overcuts of slots at different scanning rates.

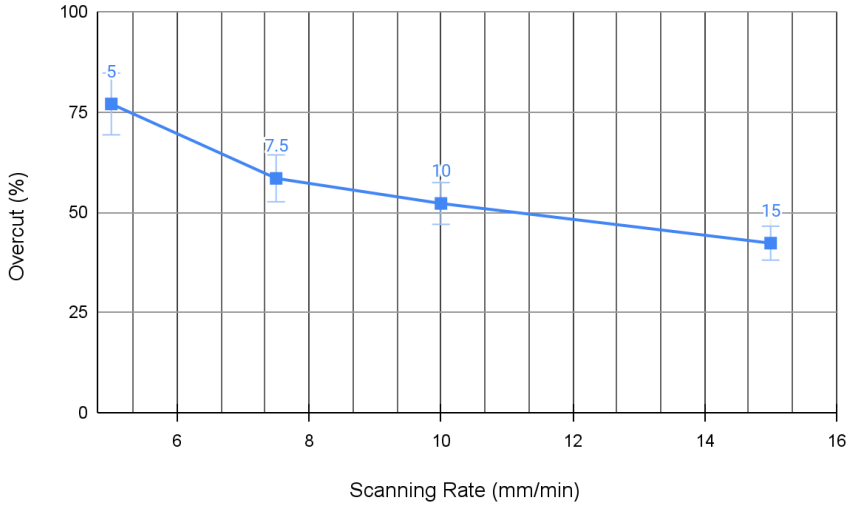

Fig 5.11 Percentage overcut vs scanning rate at 90V .

The plot fig 5.9 shows the relationship between scanning rate and percentage overcut for a given set of electrochemical jet machining (EJM) parameters. The percentage overcut is the amount of material that is removed beyond the desired depth of cut. The scanning rate is the speed at which the tool moves across the workpiece, and it is a major factor in determining the percentage overcut. The graph shows that the percentage overcut decreases with increasing scanning rate up to a point, and then it increases. This is because the tool spends less time with the workpiece at higher scanning rates, and this results in less material being removed.

The best scanning rate for this set of EJM parameters is 5 mm/min for 40V voltage. This is the rate at which the percentage overcut is lowest but not negative.

Here are some additional points to consider:

(a) The fig. 5.9 shows that the percentage overcut is greatly affected by the scanning rate.

(b) The best scanning rate for this set of EJM parameters for minimum % overcut is 7.5 mm/min for 40V which is about 5%.

The same experiment was done for 90v , at different scanning rates, as shown in figure 5.11. It also shows the same trend as before.

Figure 5.10 shows , by increasing the scanning rate the % overcut is reduced , at the scanning rate of 10mm/min no machining happened, at 1 mm/min the machining overcut was beyond the accepted value but for the scanning rate of 5 mm/min the best machining can be seen.

(iii) Influence of Scanning Rate on DOP

The scanning rate is the speed at which the jet of electrolyte is moved across the workpiece. A higher scanning rate will result in a shallower DOP, while a lower scanning rate will result in a

deeper DOP. This is because a higher scanning rate will reduce the amount of time that the electrolyte is in contact with the workpiece, which will reduce the amount of material that is eroded. The best scanning rate for EJM will depend on the material being machined and the desired DOP. For example, a higher scanning rate may be required to machine a hard material, while a lower scanning rate may be required to machine a soft material.

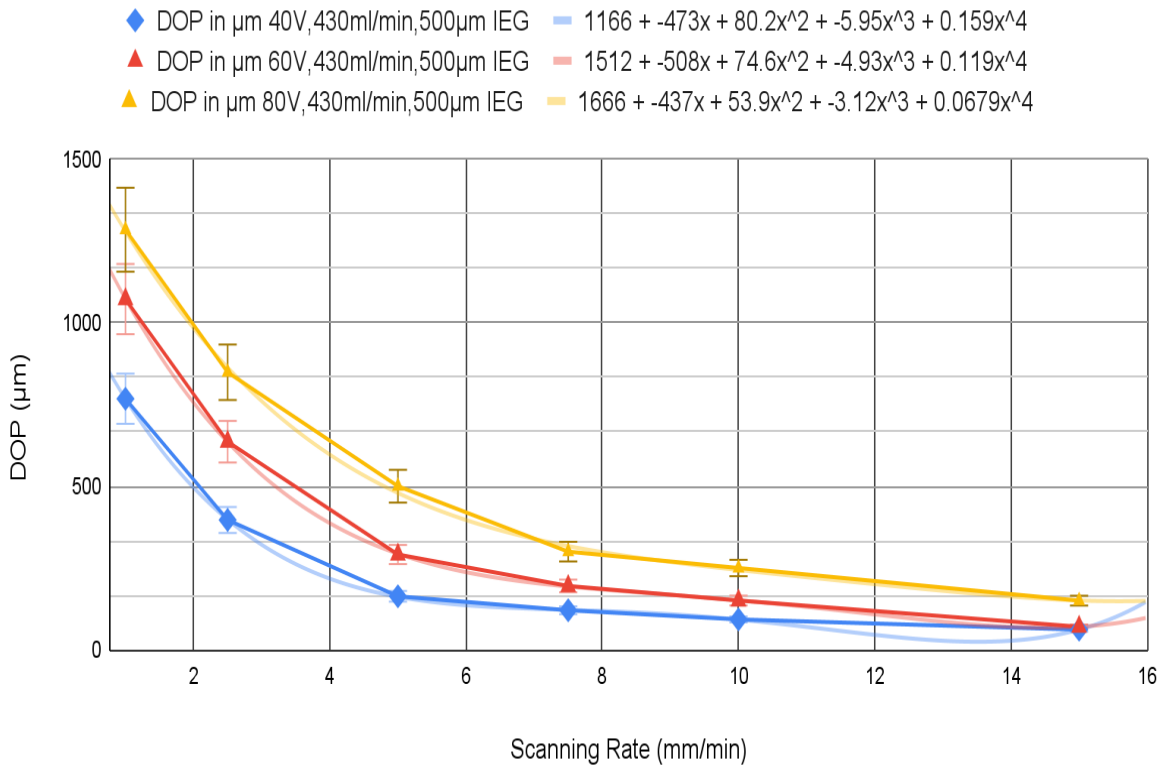

Fig. 5.12 Influence of Scanning Rate on DOP.

The graph 5.12, shows the relationship between scanning rate and depth of penetration (DOP) for a given set of electrochemical jet machining (EJM) parameters. The DOP is the distance that the jet penetrates into the workpiece, and it is a measure of the effectiveness of the EJM process. The scanning rate is the speed at which the tool moves across the workpiece, and it is a major factor in determining the DOP. The table shows that the DOP increases with increasing scanning rate up to a point, and then it decreases. This is because the tool spends less time in contact with the workpiece at higher scanning rates, and this results in less material being removed. The best scanning rate for this set of EJM parameters is 5 mm/min. This is the rate at which the DOP is best . It is important to note that the DOP is also affected by other factors, such as the feed rate, the electrolyte flow rate, and the type of material being

machined. Therefore, the best scanning rate may vary depending on the specific EJM application. At high scanning rates, the tool spends less time in contact with the workpiece, and this results in a lower DOP. This is because the tool is not able to remove as much material in the same amount of time. The best scanning rate is the rate at which the DOP is highest. This is the rate at which the tool is able to remove material as efficiently as possible without spending too much time in contact with the workpiece. The best scanning rate will vary depending on the specific EJM application. For example, if the goal is to produce a high-quality surface finish, then a lower scanning rate may be required. However, if the goal is to produce a part as quickly as possible, then a higher scanning rate may be required.

Here are some additional points to be considered:

(a) The table shows that the DOP is greatly affected by the scanning rate.

(b) The best scanning rate for this set of EJM parameters for maximum depth is 5 mm/min.

(iv) Influence of Scanning Rate on Surface Roughness

The scanning rate is the speed at which the electrolyte jet is scanned across the workpiece. The scanning rate has a significant impact on the surface roughness of the machined surface. At low scanning rates, the electrolyte jet has more time to erode the workpiece, resulting in a rougher surface. At high scanning rates, the electrolyte jet has less time to electrochemical reaction with the workpiece, resulting in a smoother surface. At much more scanning rate the Surface Roughness will start to increase again.

The graph 5.13 shows the relationship between scanning rate and average surface roughness (Ra) for a given set of electrochemical jet machining (EJM) parameters. Ra is a measure of the smoothness of the machined surface, and it is an important factor in determining the quality of the finished product. The scanning rate is the speed at which the tool moves across the workpiece, and it is a major factor in determining the Ra. The table shows that the Ra decreases with increasing scanning rate up to a point, and then it increases. This is because the tool spends less time in contact with the workpiece at higher scanning rates, and this results in less material being removed. The best scanning rate for this set of EJM parameters is 5 mm/min. This is the rate at which the Ra is lowest. It is important to note that the Ra is also affected by other factors, such as the feed rate, the electrolyte flow rate, and the type of material being machined. Therefore, the best scanning rate may vary depending on the specific EJM application. Here is a more detailed explanation of the relationship between scanning rate and Ra in EJM:

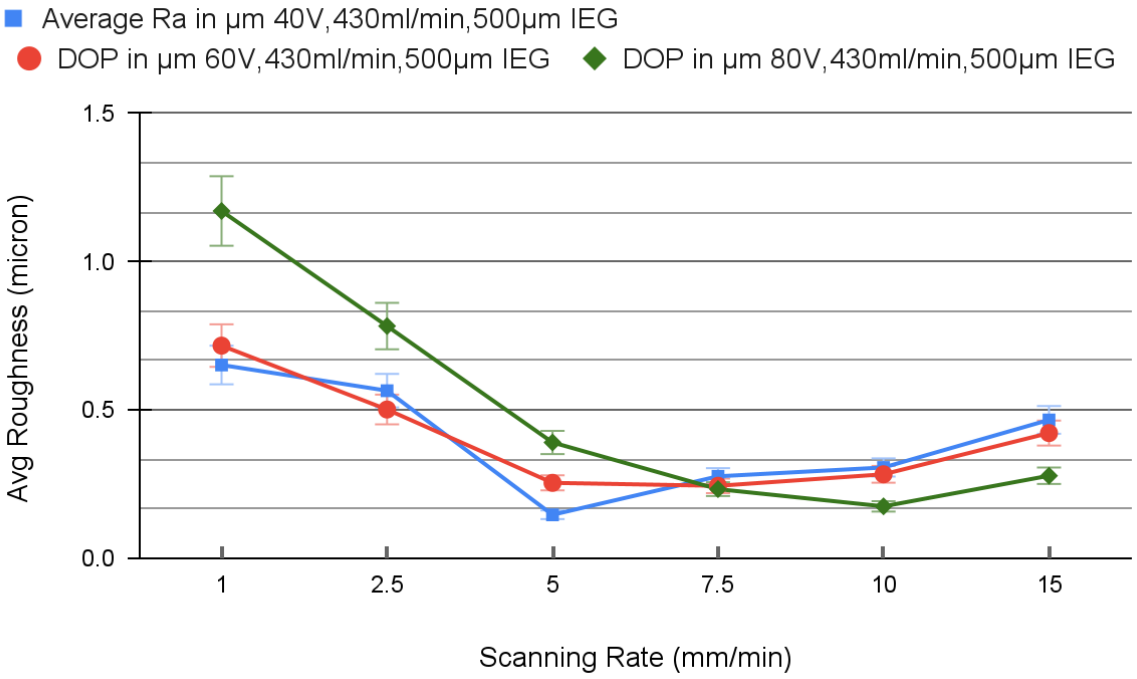

Fig. 5.13 Influence of Scanning Rate over Surface Roughness .

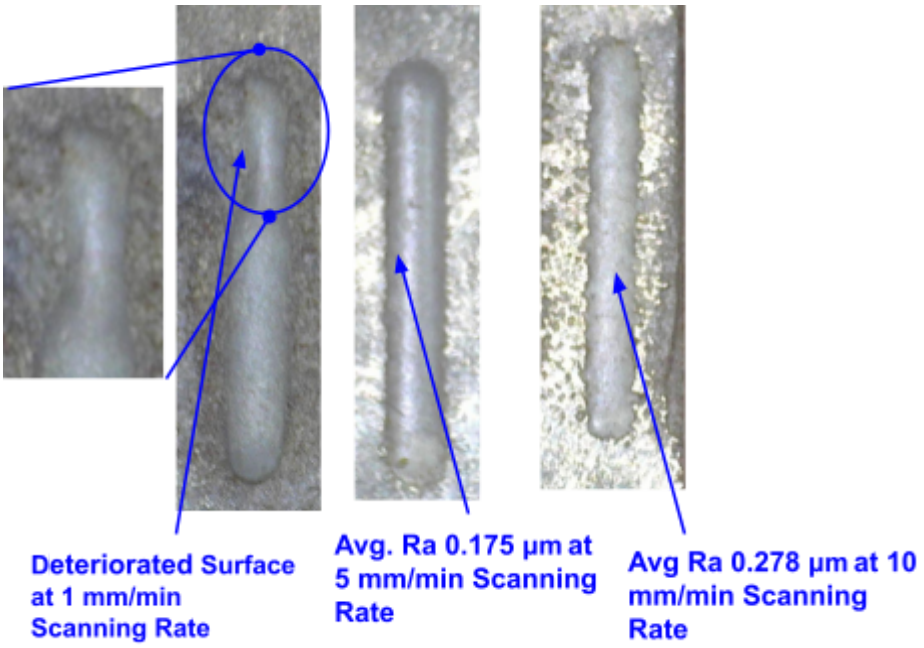

Fig.5.14 Photographic view of slot at different scanning rates.

At low scanning rates, the tool spends a long time in contact with the workpiece, and this results in a high Ra. However, at very low scanning rates, the tool may not be able to remove material as efficiently, and this can lead to a decrease in Ra. At little high scanning rates, the

tool spends less time in contact with the workpiece, and this results in a lower Ra. This is because the tool is not able to remove as much material in the same amount of time. The best scanning rate is the rate at which the Ra is lowest. This is the rate at which the tool is able to remove material as efficiently as possible without spending too much time in contact with the workpiece.

The best scanning rate will vary depending on the specific EJM application. For example, if the goal is to produce a high-quality surface finish, then a lower voltage with lower scanning rate may be required. However, if the goal is to produce a part as quickly as possible, then a higher voltage with best scanning rate may be required.

From the above figure 5.14, it can be observed that at 1mm/min scanning rate the deteriorated surface occurred this is happened as the scanning rate was very less at that scanning rate there is a possibility of sparking and stray current effect which deteriorates the surface, at 5 mm/min scanning rate better surface quality which is 0.146 μm can be achieved which is the best surface finish amongst the selected ranges. The minimum surface finish at 10 mm/min scanning rate achieved is of 0.169 μm, as shown by surface profile obtained from the profilometer plot fig 5.15.

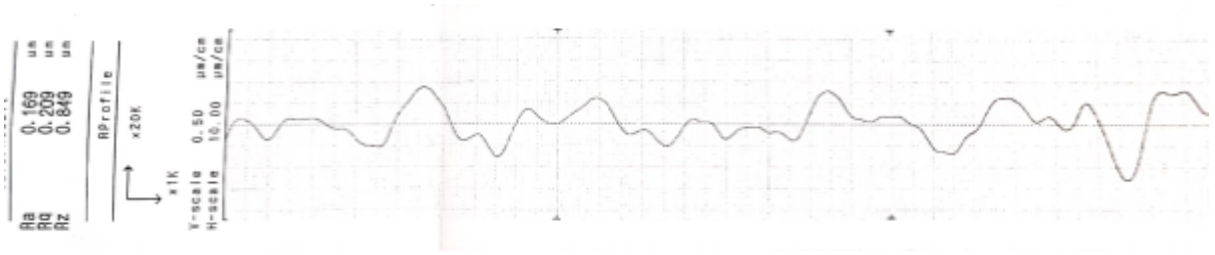

Fig. 5.15 Minimum Surface Roughness achieved for 80V is 0.169 μm at 10 mm/min scanning rate.

Here is another experiment made to ensure the effect of scanning rate over Surface Roughness at 90V, and the result shows the same trends as previous.

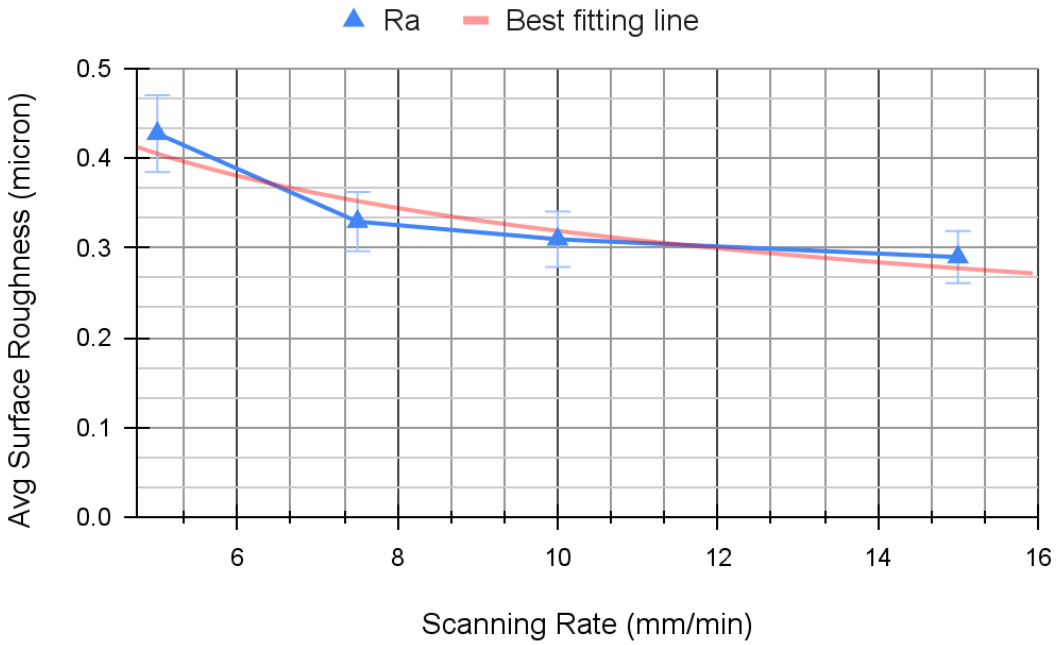

Fig. 5.16 Average Roughness vs scanning rate at 90V.

Here in this graph fig 5.16, at 90V the Surface Roughness got was much more higher at 10 mm/min scanning rate but as per the previous experiment with 80v which gave an best value of scanning rate of 10 mm/min, so it can be concluded that as the voltage will be increased the best scanning rate for good surface finish will increase also. So conclusions can be made that:

(a) At 40 v to obtain the best surface finish the scanning rate should be 5 mm/min, and the obtained surface roughness is of 0.146 µm.

(b) At 60 v for obtaining the best surface finish the scanning rate should be 7.5 mm/min, and the obtained surface roughness is 0.233 µm.

(c) At 80 v for obtaining the best surface finish the scanning rate should be in the range of 7.5mm/min - 10 mm/min, and the obtained surface roughness is of 0.175 µm.

5.3 Influence of IEG Over the Responses

From the previous observations, it can be easily concluded that for a good surface finish 40V voltage required scanning rate is 5 mm/min; 60V voltage required scanning rate is 7.5 mm/min and 80V voltage required scanning rate is 10 mm/min. So, the next experiments are done on the basis of these best parameter settings with varying the IEG from 200 µm to 700 µm at a constant flow rate of 430 ml/min.

(i) Influence of IEG on MRR

The IEG is the distance between the nozzle and the workpiece. A small IEG will result in a high MRR, while a large IEG will result in a low MRR. This is because a small IEG will increase the current density at the workpiece, which will increase the rate of the electrochemical reaction. However, a small IEG can also lead to problems such as nozzle clogging and poor surface finish. Therefore, it is important to find a balance between a small IEG and a large IEG that will optimize the MRR and the quality of the machined surface.

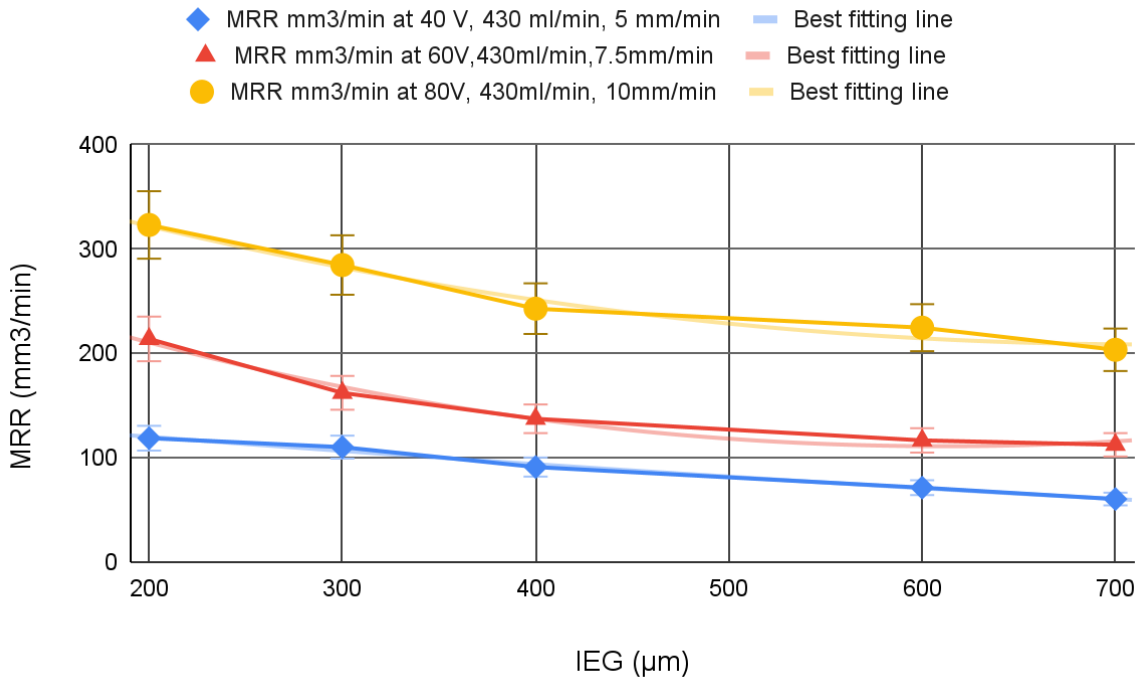

Fig.5.17 Influence of IEG over MRR.

The figure 5.17 shows the results of an experiment on the electrochemical jet machining (EJM) process at different parameter settings. The parameters that were varied were the inter-electrode gap (IEG), voltage and scanning rate taken were of the previous best value, the flow rate is taken constant. The results show that the MRR (material removal rate) decreases with increasing IEG.

The followings are some additional observations that can be made from the graph:
(a) The MRR is more sensitive to changes in the IEG than to changes in the voltage or feed rate. For example, increasing the IEG from 200 μm to 300 μm decreases the MRR by about 50%.
(b) The MRR is highest for small IEG .

(ii) Influence of IEG on Percentage Overcut

One of the key parameters that affects the performance of EJM is the inter-electrode gap (IEG). The IEG is the distance between the nozzle and the workpiece, and it controls the amount of current that flows through the system. A smaller IEG will result in a higher current, which will lead to a faster cutting speed and a smaller overcut.

Overcut is the amount of material that is removed beyond the desired dimensions of the workpiece. Overcut can be caused by a number of factors, including the IEG, the electrolyte, and the machining parameters. In general, a smaller IEG will result in a bigger overcut. However, there is a trade-off between the IEG and the cutting speed. A smaller IEG will result in a faster cutting speed, but it will also make the process more sensitive to disturbances.

The figure 5.18 shows the results of an experiment on the electrochemical jet machining (EJM) process at different parameter settings. The parameters that were varied were the inter-electrode gap (IEG) voltage and scanning rate taken were of the previous best value, the flow rate is taken constant .

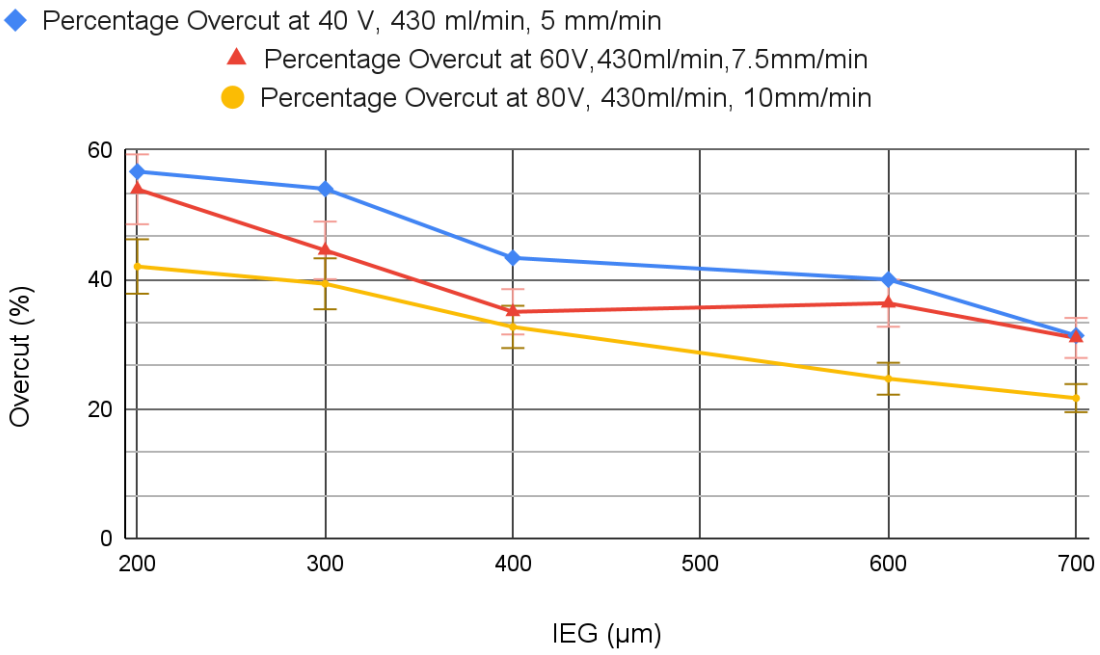

Fig.5.18 Influence of IEG over Percentage Overcut

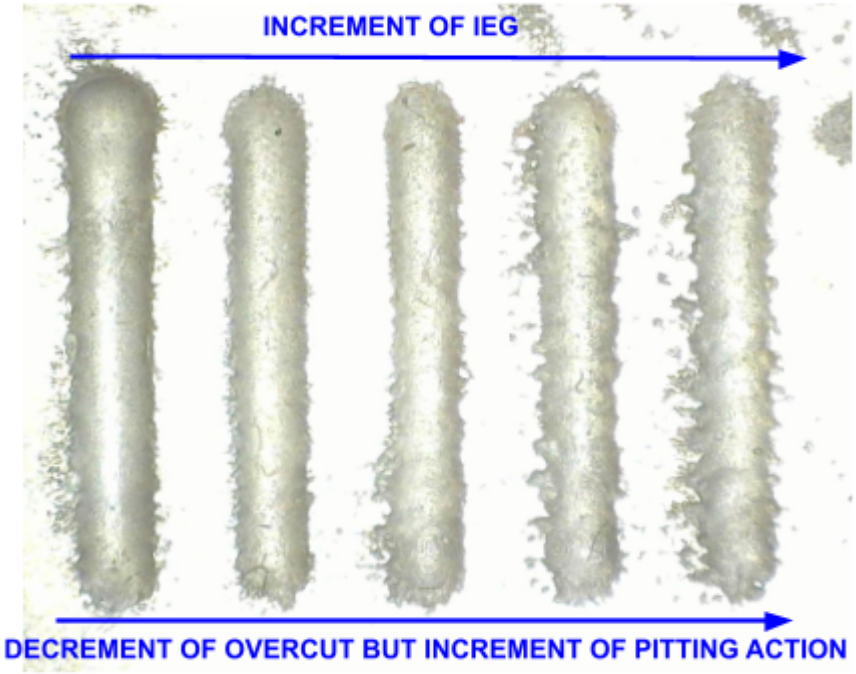

Fig 5.19 Photographic View of slot at different IEG.

The results, fig 5.19 shows that the percentage overcut decreases with increasing voltage and feed rate, and increases with increasing IEG.

The results of this experiment can be used to optimize the EJM process for a particular application.

The following are some additional observations that can be made from the graph:

(a) The percentage overcut is more sensitive to changes in the IEG than to changes in the voltage or feed rate. For example, increasing the IEG from 200 µm to 300 µm increases the percentage overcut by about 20%.

(b) The percentage overcut is lowest for 700 µm IEG.

(iii) Influence of IEG on DOP

If the IEG is less the gap between the tool and workpiece will be very less, this means less resistance, so the material removal rate will be more. As the material removal rate increases the DOP will also increase.

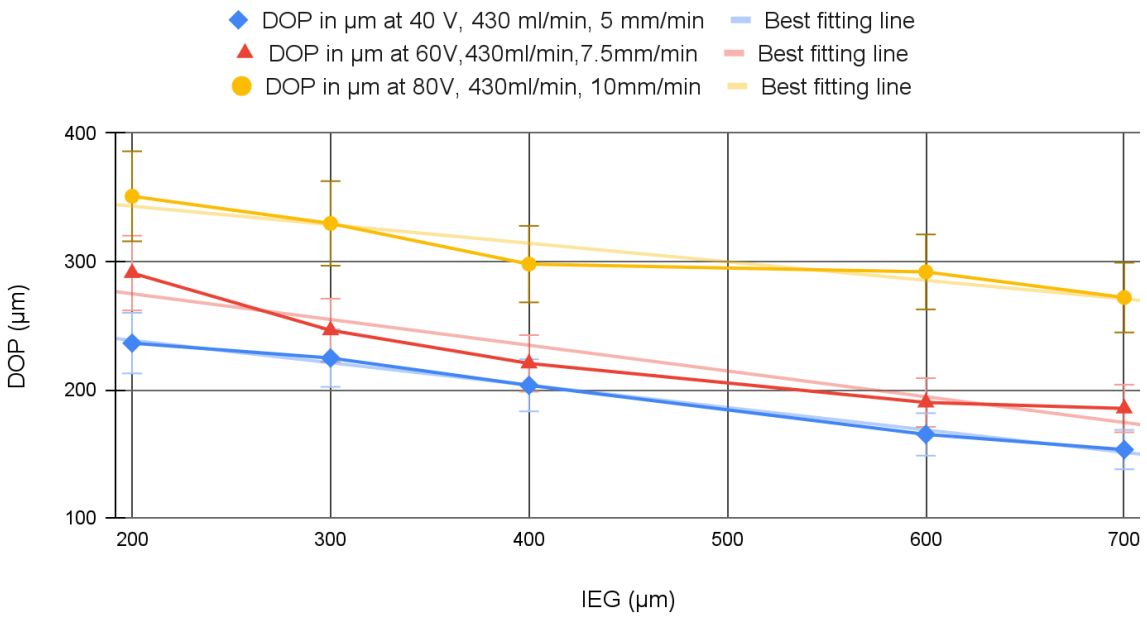

Fig. 5.20 Influence of IEG over DOP.

The fig. 5.20, shows the results of an experiment on the electrochemical jet machining (EJM) process at different parameter settings. The parameters that were varied were the inter-electrode gap (IEG) voltage and scanning rate taken were of the previous best value, the flow rate is taken constant . The results show that the depth of penetration (DOP) increases

with increasing voltage and feed rate, and decreases with increasing IEG. The DOP is also higher for lower IEG, but this effect is less pronounced.

The results of this experiment can be used to optimize the EJM process for a particular application. For example, if a high DOP is required, the voltage and feed rate can be increased. If the IEG is too small, the DOP will increase and it might start arcing or sparking.

The following are some additional observations that can be made from the graph:

(a) The DOP is not a linear function of the IEG.

(b) The DOP is more sensitive to changes in the IEG than to changes in the voltage or feed rate. For example, increasing the IEG from 200 μm to 300 μm decreases the DOP by about 50%.

(c) The DOP is highest for an IEG of 200 μm for all the voltage settings .

(iv) Influence of IEG on Surface Roughness

The effect of IEG was the third most influencing parameter for achieving good surface finish. As the IEG decreases the gap becomes very less and the current flow increases so there is a possibility that the surface might get deteriorated and there is a high possibilities of sparking due to very small gap , and also when the IEG gets too much higher value the jet becomes more divergent so the pitting action increases thus the surface gets deteriorated. So the best IEG must not be very less or not be very high, it should be in between high and low value. Here in this study , the IEG value is investigated further.

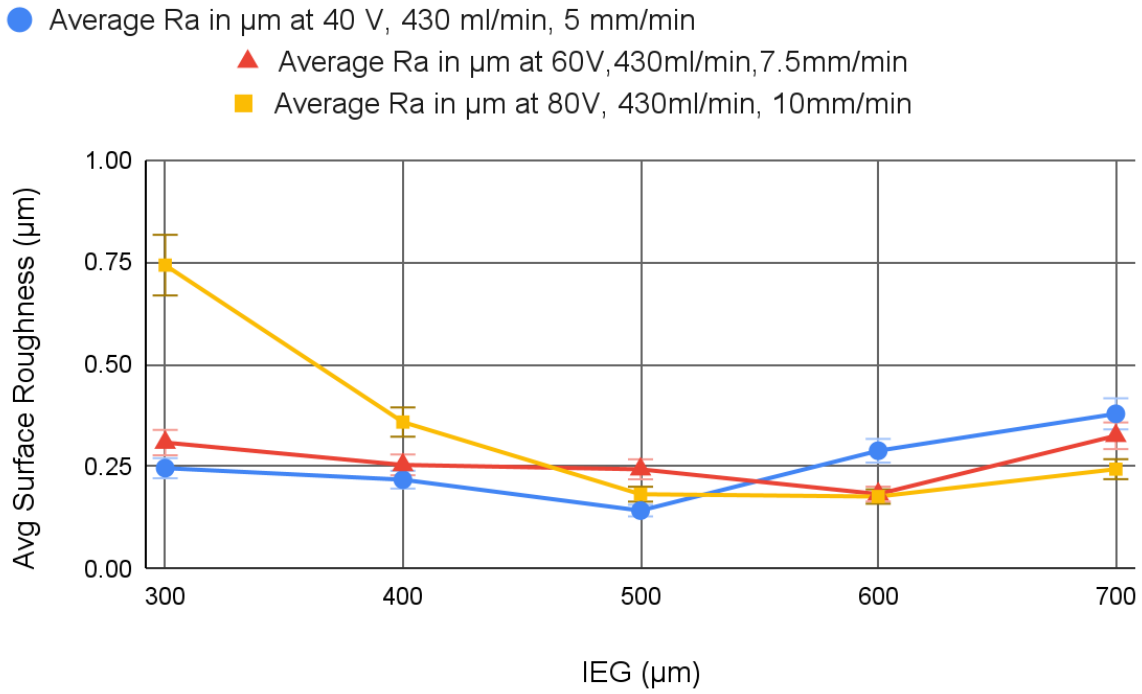

Fig. 5.21 Influence of IEG over Ra.

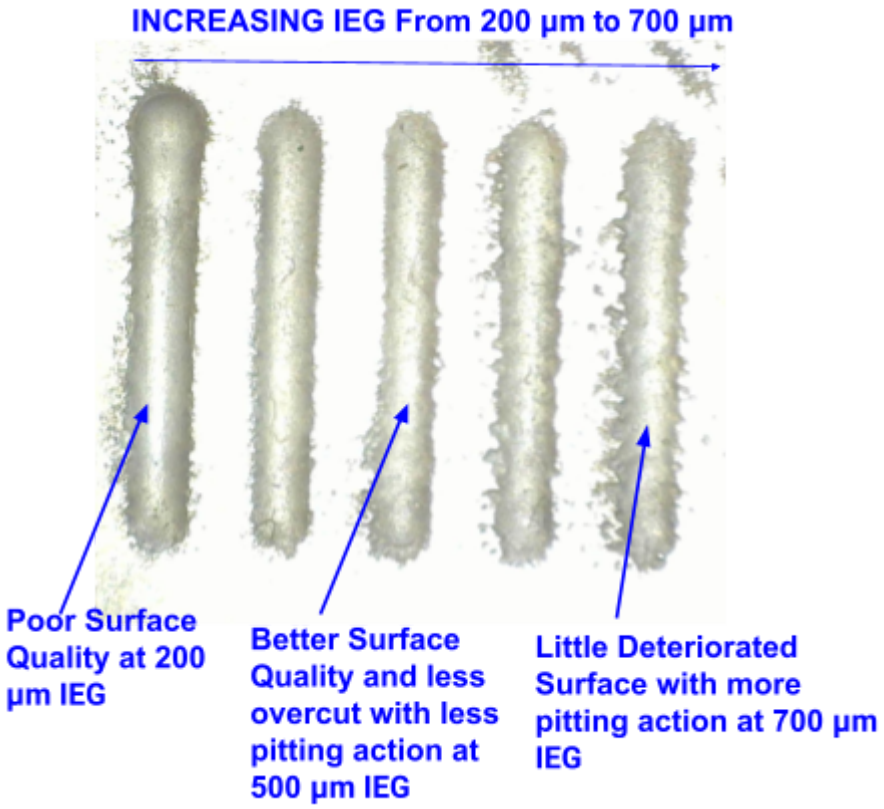

Fig 5.22 Photographic View of slot at different IEG .

The fig 5.21, shows the results of an experiment on the electrochemical jet machining (EJM) process at different parameter settings. The parameters that were varied were the inter-electrode gap (IEG) voltage and scanning rate taken were of the previous best value, the flow rate is taken constant . The results show that the average surface roughness (Ra) decreases with increasing IEG. The Ra is also lower for higher flow rates. The results of this experiment can be used to optimize the EJM process for a particular application. If the IEG is too small, the Ra will increase due to arcing as shown in figure 5.22 the comparative image view of slots at different IEG.

The following are some additional observations that can be made from the graph:

(a) The Ra is more sensitive to changes in the IEG than to changes in the voltage or feed rate. For example, increasing the IEG from 300 μm to 400 μm increases the Ra by about 20%.

(b) The Ra is lowest for 40V, scanning rate of 5 mm/min at IEG of 500 μm , The Ra value as shown in fig 5.23. Which is 0.137 μm . Increasing the IEG beyond this point does not significantly decrease the Ra.

(c) The best surface roughness for 60 v , scanning rate of 7.5 mm/min occurs at IEG of 600 μm , the best surface finish achieved here is 0.176 μm.

(d) The best surface roughness for 80 v, 10 mm/min scanning rate occurs at IEG of 600 to 700 μm. The best surface finish can be achieved here is 0.176 μm.

(e) Surface quality is very poor at 200 μm IEG with more overcut, at 500 μm the surface finish is very good and beyond 500 μm there is more chances of pitting action and deterioration of surface finish can be observed.

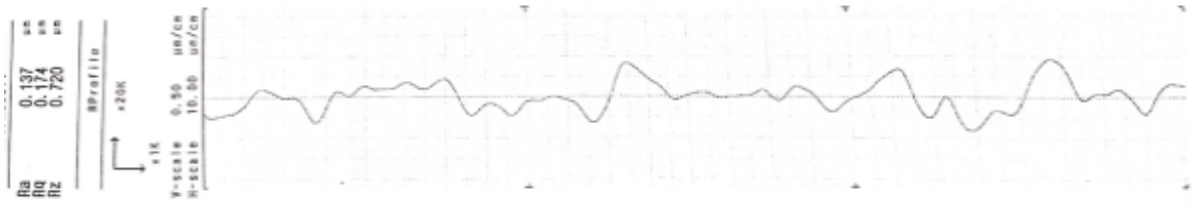

Fig 5.23 Plot of surface profileSurface Roughness Profile.

5.4 Influence of Flow Rate Over the Responses

From the previous observations, it can be easily concluded that for a good surface finish these parametric combinations gave the best surface finish , the parametric setting combinations are 40V voltage, 5 mm/min scanning rate required IEG is 500 μm ; 60V voltage, 7.5 mm/min

scanning rate required IEG is around 600-650 µm and 60V voltage, 7.5 mm/min scanning rate required IEG is around 700 µm . So, the next experiments are done on the basis of these best parameter settings with varying the flow rate . The flow rate varied in the range from 230 ml/min to 430 ml/min. Increasing the flow rate can improve the surface finish by removing the sludge and the effect of thrust force is also a factor that can help to remove the picks and valleys from the surface.

(i) Influence of Flow Rate on MRR

It is very easy to predict that as the flow rate increases the value for MRR should a increase. For more clarifications more experiments are done.

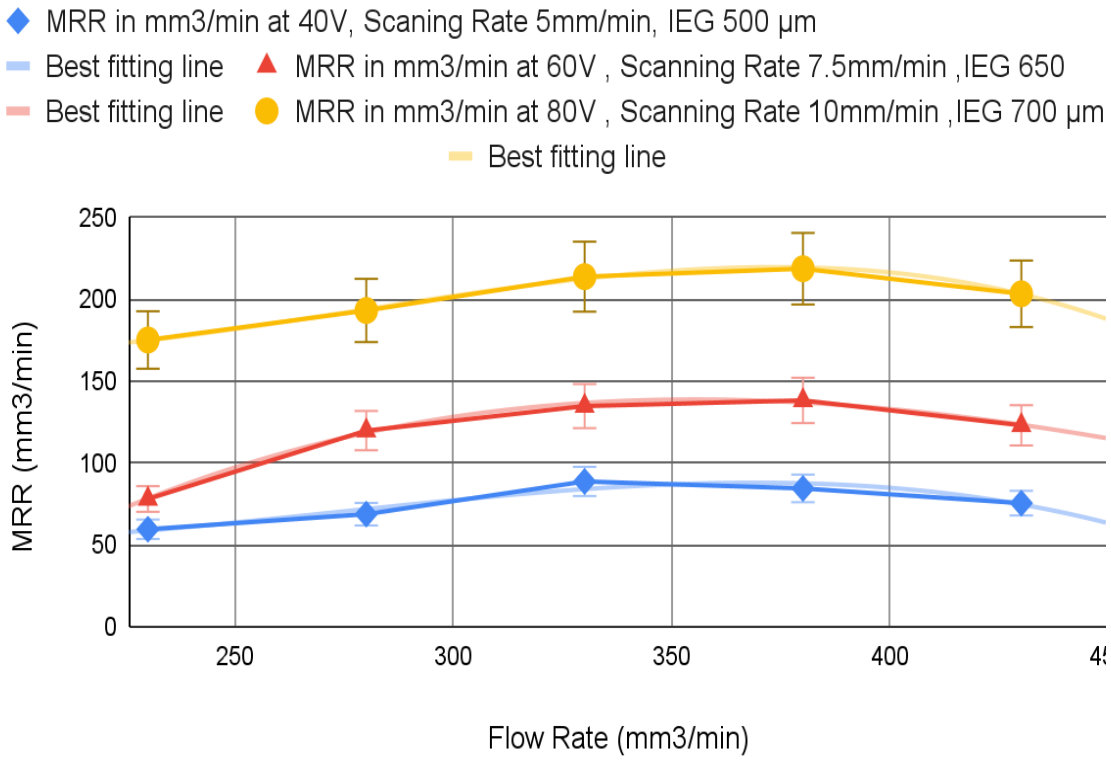

Fig.5.24 Influence of Flow Rate over MRR.

The plot 5.24 shows the results of an experiment on the electrochemical jet machining (EJM) process at different parameter settings. The parameters that varied was the flow rate; the voltage, the scanning rate, and the inter-electrode gap (IEG) are taken as per best value for good surface finish. The results show that the material removal rate (MRR) increases with increasing IEG upto a certain point then it tends to decrease.

From all the graph plots it can be concluded that the maximum MRR happened at 380 ml/min.

(ii) Influence of Flow Rate on Percentage Overcut

As the flow rate increases the overcut should also increase. To confirm this further experiments are done and the result data are plotted below.

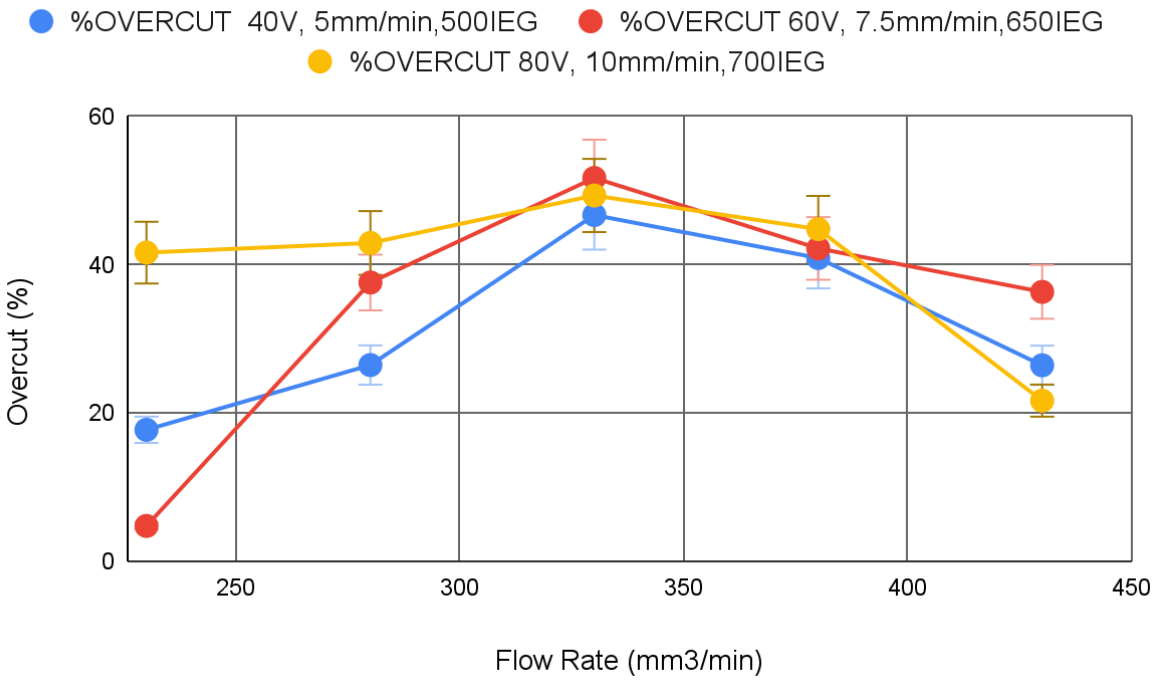

Fig. 5.25 Influence of Flow Rate over Percentage Overcut.

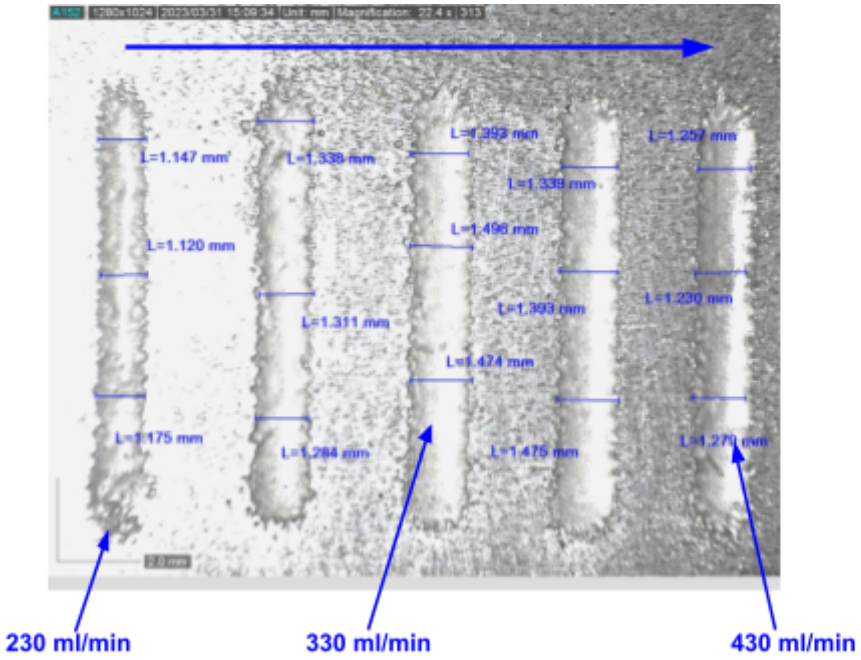

Fig 5.26 Photographic View of slot at different flow rates for Overcut

The fig. 5.25 shows the results of an experiment on the electrochemical jet machining (EJM) process at different parameter settings. The results show that the percentage overcut increases with increase of flow rate upto a certain point and then decreases with increasing IEG.

The percentage overcut is lowest for a flow rate of 430 ml/min. Increasing the flow rate beyond this point does not significantly decrease the percentage overcut. Although for minimum flow rate the overcuts were very less still for that range the surface finish was not satisfactory, as the improper sludge removal.

From the above fig 5.26, it can be easily seen that at low flow rate pitting actions, irregular uneven cuts are coming, further increase of flow rate decreases the pitting action and overcut.

At 230 ml/min more pitting action, overcut can be observed from the fig.5.26 , at 330 ml/min less Pitting action and Less irregular uneven cuts but the Overcut increased to 330 ml/min.t 430 ml/min very less Pitting action, Less irregular uneven cuts as well as Overcut decreased as the flow rate Increased to 430 ml/min.

(iii) Influence of Flow Rate on DOP

The DOP has a linear relationship with the flow rate, as the flow rate increases the DOP is also increased.

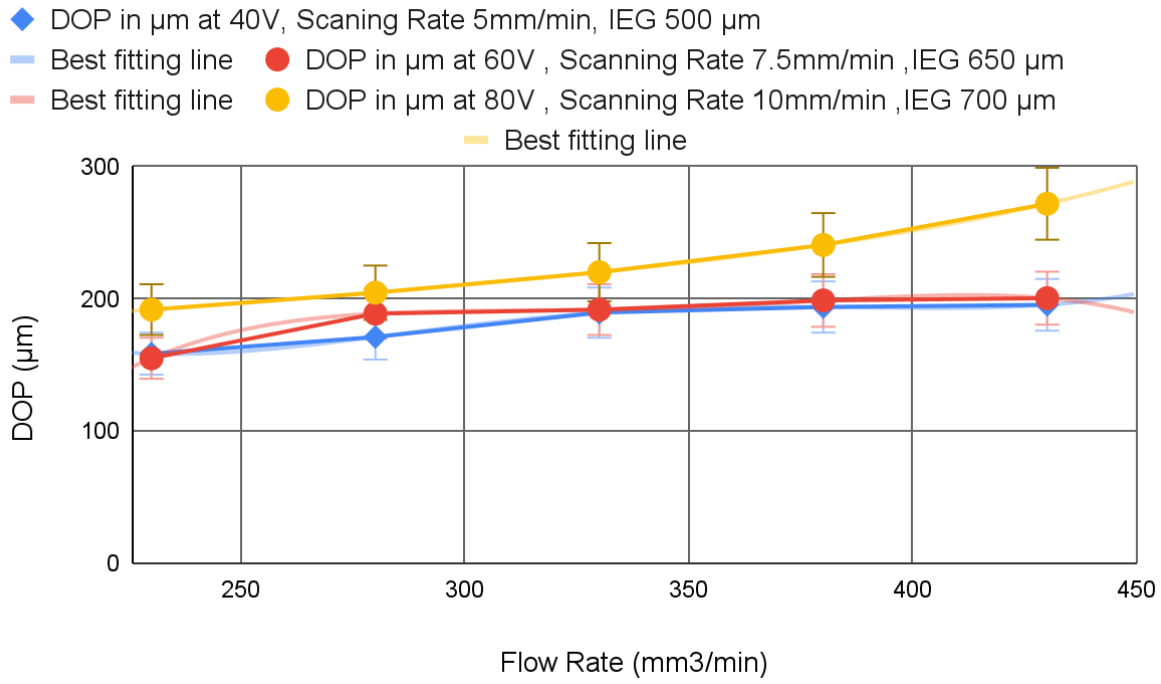

Fig. 5.27 Influence of Flow rate over DOP.

The figure 5.27, shows that the DOP increases with increasing flow rate. This is because the higher flow rate increases the rate of electrolyte delivery to the machining zone, which increases the rate of metal dissolution. The results also show that the DOP increases with increasing voltage. This is because the higher voltage increases the electric field strength, which increases the rate of metal dissolution. The results also show that the DOP decreases with increasing scanning rate. This is because the higher scanning rate decreases the time that the tool is in contact with the workpiece, which decreases the amount of metal that is dissolved.

The results also show that the DOP decreases with increasing IEG. This is because the higher IEG increases the distance between the tool and the workpiece, which decreases the electric field strength, which decreases the rate of metal dissolution.

These results suggest that the flow rate, voltage, scanning rate, and IEG are all important factors that affect the DOP in EJM. The best values of these parameters will vary depending on the material being machined and the desired DOP.

(a) The DOP is minimum at flow rate of 230 ml/min and it is in the range of 100 μm to 200 μm.

(b) The DOP is maximum at flow rate of 430 ml/min which is about 300 μm.

(iv) Influence of Flow Rate on Surface Roughness

The flow rate is the last influencing parameter for achieving best surface finish. The flow rate serves as the removal of sludge by flushing as well as the flow rate can give the thrust force to remove the valleys from the surface.The figure 5.28, shows that the Ra decreases with increasing flow rate. This is because the higher flow rate increases the rate of electrolyte delivery to the machining zone, which increases the rate of metal dissolution and increase of sludge removal.

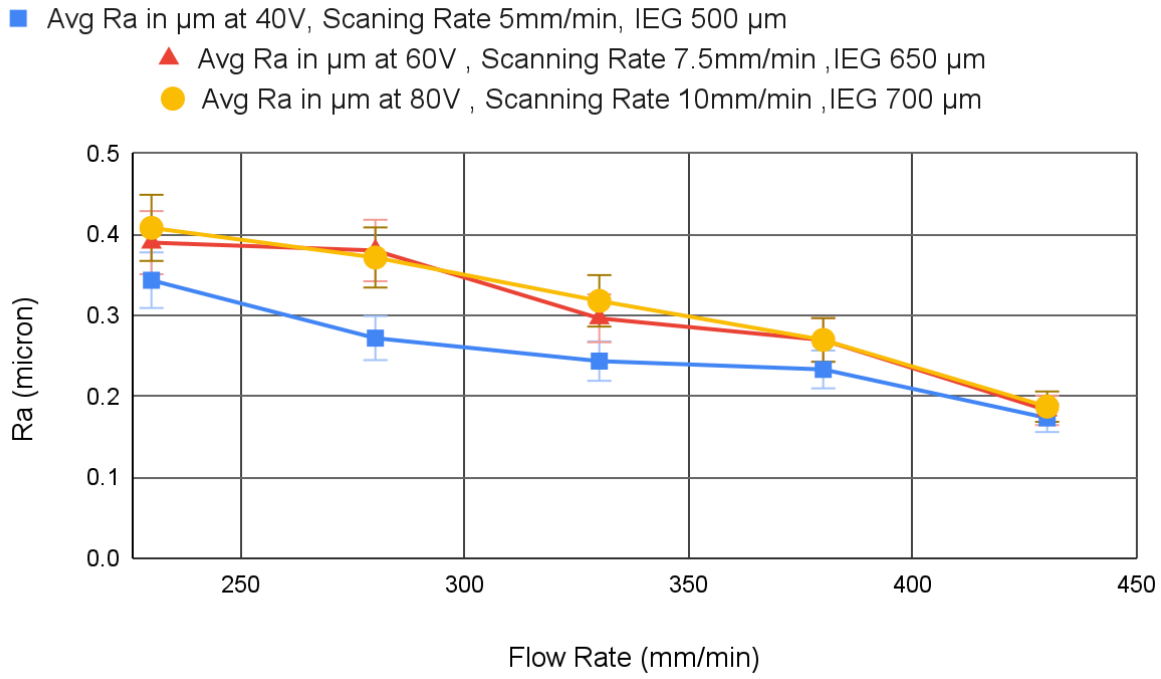

Fig. 5.28 Influence of Flow Rate over Ra.

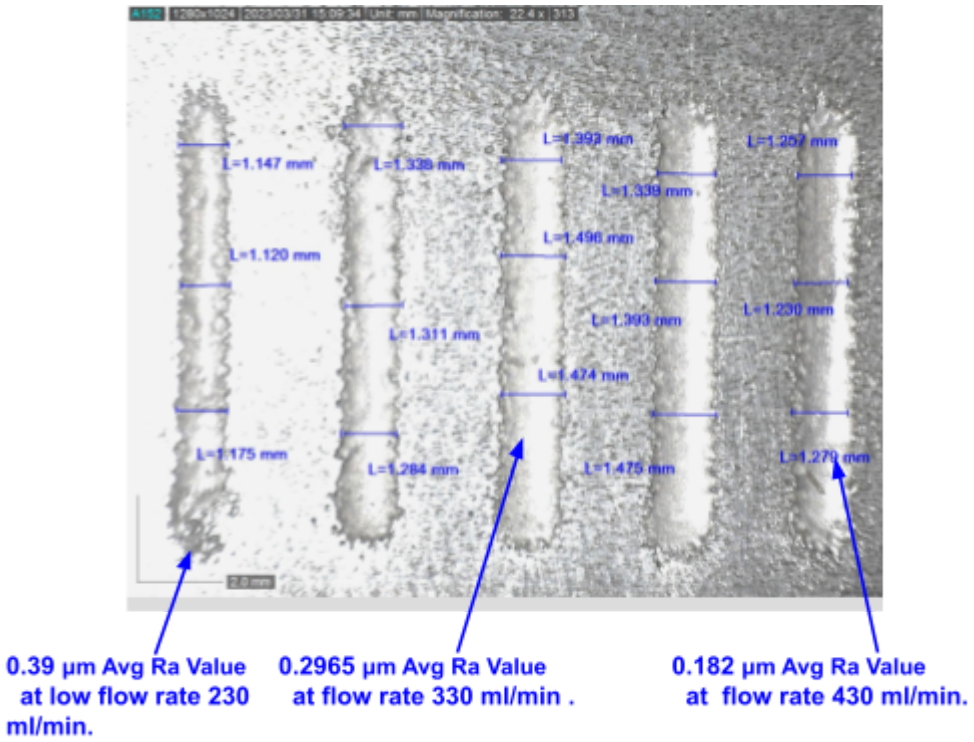

Fig.5.29 Photographic View of slot at different flow rates.

At lower flow rate the sludge removal cannot be done properly that's why uneven surface quality can be seen fig 5.29. As the flow rate increases the sludge removal process increases and a better surface finish can be obtained, for flow rate of 430 ml/min the surface finish achieved was of 0.182 μm as shown in fig 5.30.

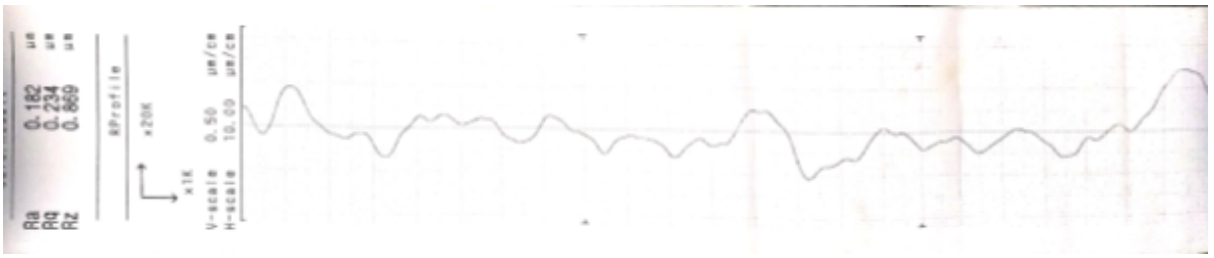

Fig. 5.30 Surface Roughness profile.

So, from the above all the experiments to achieve the best surface finish in Ti6Al4V this combination could be used as follows:

(i) For 40 V the scanning rate should be 5 mm/min , IEG 500 μm and flow rate of 430 ml/min.

(ii) For 60 v the scanning rate should be 7.5 mm/min , IEG 650 μm and flow rate of 430 ml/min .

(iii) For 80v the scanning rate should be 10 mm/min , IEG 700 μm and flow rate of 430 ml/min .

Further experiments are done from taking the best parameter combination of 40 v, as for 40 v combination the best surface roughness was achieved in Ti6Al4V.

5.5 Parametric Combination for Achieving Best Surface Surface Finish

After all these experiments, it can be easily noticed that the parametric combination of voltage 40 V, scanning rate 5 mm/min, IEG 500 μm and flow rate of 430 ml/min is best suited for good surface finish with low overcut.

From the attached fig 5.31 below, it can be easily noticed how much the surface finish is improved using the best parametric condition. Later on, after more experiments the same results are observed as shown in figure 5.32 , the surface finish is more or less the same and the side sharpness is also improved.

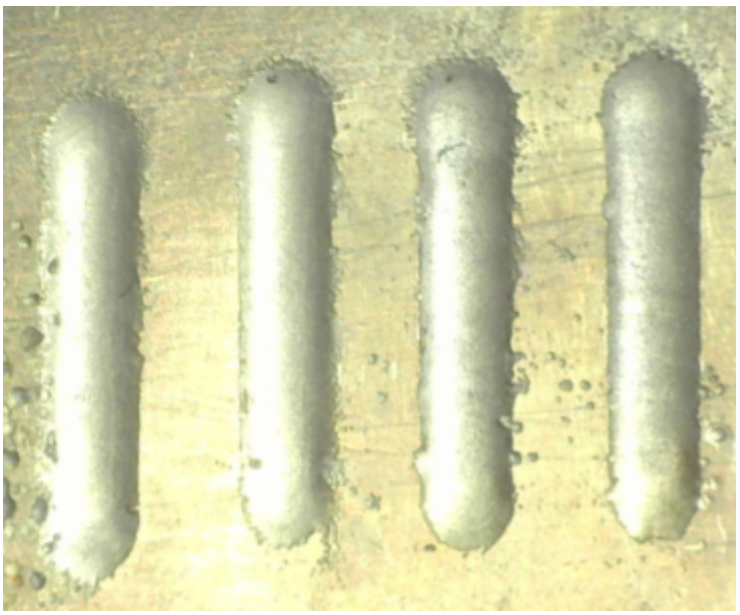

Fig 5.31 Photographic View of slot at Best Parametric condition.

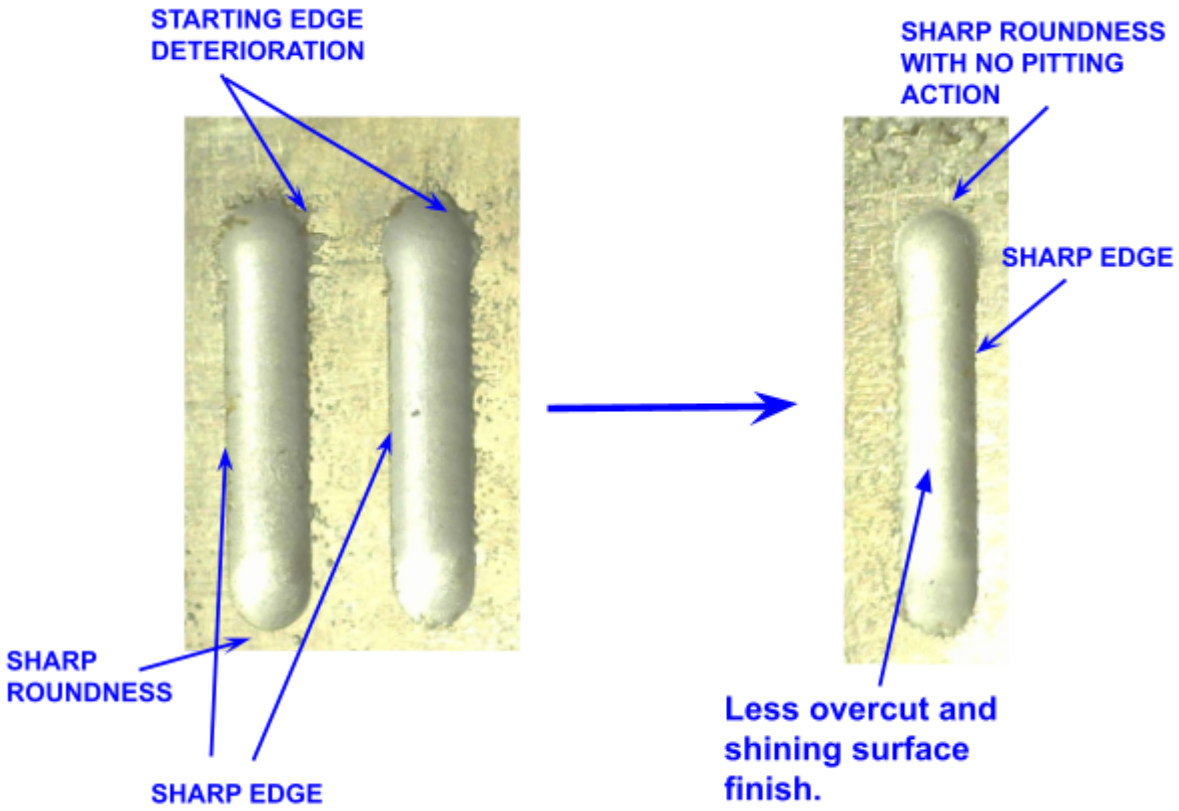

Fig 5.32 Photographic ViewS of Slots at Best Parametric condition

From this fig. 5.32 above, it is clearly visible that the overcut is very less than the previous observations as well as the surface finish also improved. For the first set of experiments at the starting point of the slots some pitting action can be seen, but at the end point a very sharp roundness can be seen. Later by controlling the z direction movement of the stage the starting pitting action can also be rectified. But for the second case the surface finish improved more and the surface roughness profile with recorded minimum value of 0.115 μm is given below in fig 5.33.

At the best parametric setting of voltage 40V, scanning rate 5 mm/min, IEG 500 μm and flow rate of 430 ml/min the minimum surface finish achieved is 0.115 μm as shown in fig 5.33.

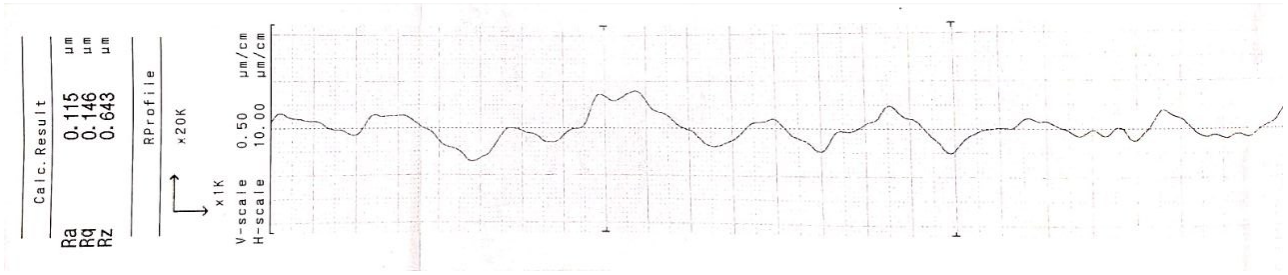

Fig.5.34 Surface Roughness Profile.

5.6 Complex Shape generation on Ti6Al4V

By using the best parametric condition i.e. voltage 40V, IEG 500 μm, scanning rate 5 mm/min and flow rate of 430 ml/min a “plus” shape is generated by utilizing Electrochemical Jet Machining, as shown in fig. 5.35. For this shape generation G code is being made differently. Each hand of the “plus” sign was programmed for 10 mm length, and the length after the experiment was 10.591 mm and 11 mm. The width overcut were 1.01 mm, 1.02 mm, 1.1 mm and 1.08 mm respectively. Very sharp edges were observed and the angle of two consecutive hands was approximately 91°.

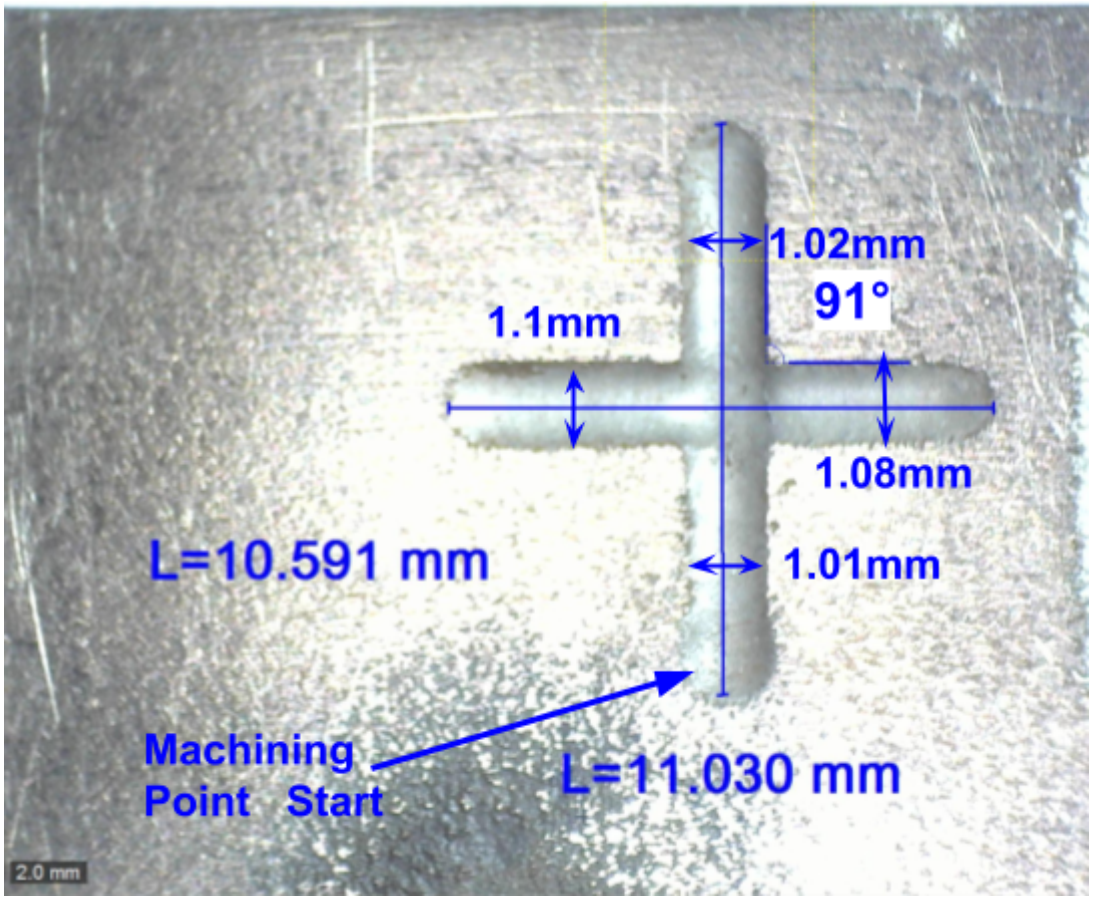

Fig. 5.34 Cutting geometry in the best parametric condition.

``

From this experiment, it can be concluded that the developed EJM set-up is capable of machine complex shape also.

CHAPTER 6

6. GENERAL CONCLUSIONS

6.1 General Conclusions

From the set of experiments based on the developed Electrochemical Jet Machining set up , it can be concluded that Ti6Al4V can be effectively machined by EJM process. The developed machine set-up is capable of machining complex shapes, with very less pitting action, overcut and higher profile accuracy. Achieving a good surface finish for Titanium and its alloys is a very challenging task .However, experiments have shown that it is possible to improve the surface finish.

Based on the test results , the following conclusions are drawn:

(i) The modified and upgraded set up is capable of cutting slots in Ti6Al4V; it can be utilized for further experimentation to analyze the influence of various parameters on the process criteria of EJM.

(ii) The cone-straight nozzle is successfully designed, and it is capable of generating various geometries on Ti6Al4V. Use of a cone-straight nozzle reduces the turbulence of electrolyte flow and makes the jet more concentrated. Normal convergent nozzles give more overcut , less depth of penetration, and pitting action which leads to deterioration of the surface finish.

(iii) After analyzing the results of Taguchi-based experimentation, it was determined that the most influential process parameter for reducing overcut is the flow rate, followed by the scanning rate, IEG, and voltage in that specific order. To increase DOP, the most influential parameter is the scanning rate, followed by voltage, IEG, and flow rate. Conversely, when aiming to improve the surface finish, the voltage was identified as the most influential parameter, followed by scanning rate, IEG, and flow rate.

(iv) Overcut was found to be minimum at 40V voltage, 5 mm/min scanning rate, 500 μm IEG, 430 ml/min flow rate. The minimum % of overcut obtained is in the range of 5-10% of the jet diameter .

(v) MRR and DOP are both dependent on scanning rate and voltage. If both the voltage and scanning rate are increased, the DOP decreases. However, if the scanning rate is decreased, the DOP increases. The maximum DOP is observed at a voltage of 80V, a scanning rate of 1 mm/min, an IEG of 500 μm, and a flow rate of 430 ml/min. Under these conditions, the maximum DOP obtained is approximately 1500 μm.

(vi) The best surface finish obtained with these parametric combinations : voltage 40V, scanning rate 5 mm/min, IEG 500 μm and flow rate 430 ml/min; for voltage 60V the scanning rate required 7.5 mm/min, IEG 650 μm and a flow rate of 430 ml/min: and for 80 V the scanning rate required should be 10 mm/min , IEG of 600-700 μm and flow rate of 430 ml/min.

(vii) Among all these parameters—voltage, scanning rate, IEG, and flow rate—voltage and scanning rate are directly dependent on each other to achieve the optimal surface finish.

(viii) The best surface finish can be achieved at 40 V voltage, 5 mm/min scanning rate, 500 μm IEG and 430 ml/min flow rate. In this condition the best surface finish achieved was average roughness (Ra) of 0.146 μm the minimum surface roughness recorded was 0.115 μm.

(ix) On the basis of pitting action, overcut and geometry, photographic analysis of different slots are done. Experimental test results and photographic analysis are corroborating the same facts that best parameter setting is 40V, scanning rate 5 mm/min , IEG 500 μm and flow rate 430 ml/min is the best parameter setting.

Overall, achieving a high surface finish for Ti6Al4V is challenging but crucial for various industries, enhancing performance, efficiency, and durability, and this developed setup shows that EJM is capable of achieving high surface finish.

6.2 Future Scope of Work

The indigenously developed set-up gave a satisfactory result and it can be improved further. The future scope of work includes :

(i) Use of various electrolytes (i.e. use of KBr, KCl etc electrolyte), there are very few studies about use of different electrolytes for Ti6Al4V alloy. Even acidic electrolytes can be used for further studies.

(ii) Modification of electrolyte concentration for further studies on electrochemical jet machining, Further concentration change might lead to super finish of the surface. However increasing the concentration level shows more stray current effects than lower concentration.

(iii) Use of a power supply unit with pulsed DC, can be used for better sludge removal. And different waveforms like rectangular wave, triangular wave , sinusoidal wave can be used to study their effects.

(iv) More precise XYZ stage could be employed for accuracy of experiment so that more precise complicated micro designs can be done for microstructure development so that it can be used in microfluidic application in the field of micro engineering and medical science.

(v) Use of an advanced electrolyte filtration system can also improve the overall machining process. The more unfiltered electrolyte leads to increased resistance hence decreases the conductivity.

(vi) Mathematical modeling can be done for more accurate control over the responses.

REFERENCES

[1] Kong, H., Zhang, W., Cheng, X., Zhang, Y., Wang, L., Guo, S., & Li, S. (2019). Multiphysics Simulation and Experimental Investigation on Jet Electrochemical JET of Ti-6Al-4V Alloy. Journal of Manufacturing Science and Engineering, 141(8), 081006. doi:10.1115/1.4043087

[2] Zhu, H., Zhou, H., Zhang, Y., Tang, X., Li, X., & Li, L. (2018). Fabrication of oxide-free dimple structure on germanium via electrochemical jet machining enhanced by opposing laser irradiation. Journal of Manufacturing Science and Engineering, 140(7), 071006. doi:10.1115/1.4040192

[3] Mitchell-Smith, J., Pandit, A. S., & Sun, Z. (2013). Electrochemical jet machining of titanium: overcoming passivation layers with ultrasonic assistance. International Journal of Machine Tools and Manufacture, 71, 50-58. doi:10.1016/j.ijmachtools.2013.03.009

[4] Speidela, K. S., Sun, Z., & Pandit, A. S. (2008). Electrolyte jet machining of titanium alloys using novel electrolyte solutions. International Journal of Machine Tools and Manufacture, 48(3-4), 393-404. doi:10.1016/j.ijmachtools.2007.09.006

[5] Seo, D.-I., Moon, H.-K., Jeong, H.-G., & Kim, H.-J. (2020). Effects of competitive anion adsorption (Br− or Cl−) and semiconducting properties of passive films on the corrosion behavior of additively manufactured Ti–6Al–4V alloys. Corrosion Science, 168, 108540. doi:10.1016/j.corsci.2020.108540

[6] Yang, T., Hu, P., Cui, X., Li, J., Li, D., Huang, W., & Liu, Z. (2021). Electrochemical cutting with inner-jet electrolyte flushing for titanium alloy. Journal of Materials Processing Technology, 287, 116875. doi:10.1016/j.jmatprotec.2020.116875

[7] Liu, Z., Liu, Z., Yao, Y., Chen, Z., Xu, D., & Wang, X. (2016). Electrochemical slurry jet micro-machining of tungsten carbide with sodium chloride solution. Journal of Materials Processing Technology, 238, 186-197. doi:10.1016/j.jmatprotec.2016.06.003

[8] Clare, A. T., Hoogers, G., Zheng, H., & Griffiths, C. A. (2017). Advancing electrochemical jet methods through manipulation of the angle of address. Journal of Materials Processing Technology, 242, 57-66. doi:10.1016/j.jmatprotec.2016.11.026

[9] Lee, J.-B., Jeon, J.-P., Kim, J.-K., Lee, H.-K., Kim, H.-Y., & Lee, C.-S. (2018). Effects of competitive anion adsorption (Br− or Cl−) and semiconducting properties of the passive films on the corrosion behavior of the additively manufactured Ti–6Al–4V alloys. Corrosion Science, 135, 233-244. doi:10.1016/j.corsci.2018.02.009

[10] Hackert-Oschätzchena, M., et al. (2023). Numerical simulation of Jet-ECM process using COMSOL Multiphysics. Journal of Manufacturing Processes, 49, 207-216

[11] Speidel, A., Mitchell-Smith, J., Walsh, D. A., Hirsch, M., & Clare, A. (2016). Electrolyte jet machining of titanium alloys using novel electrolyte solutions. Procedia CIRP, 42, 367-372. DOI:10.1016/j.procir.2016.02.200

[12] Hackert-Oschätzchena, M., et al. (2013). Inverse jet electrochemical machining for functional edge shaping of micro bores. Procedia CIRP, 6, 378-383.

[13] Wang, X., et al. (2023). Investigation on parametric effects on groove profile generated on Ti1023 titanium alloy by jet electrochemical machining. Journal of Manufacturing Processes, 49, 207-216.

[14] Baehre, D., Ernst, A., Weißhaar, K., Natter, H., Stolp, M., & Busch, R. (2016). Electrochemical dissolution behavior of titanium and titanium-based alloys in different electrolytes. Procedia CIRP, 42, 137-142. https://doi.org/10.1016/j.procir.2016.02.013.

[15]Minglu Wang, et al. "Improving material removal rate in macro electrolyte jet machining of TC4 titanium alloy through back-migrating jet channel." Journal of Manufacturing Processes, vol. 55, 2022, pp. 111-121.a

[16] Yudi Wang, et al. "Study on surface roughness of large size TiAl intermetallic blade in electrochemical machining." The International Journal of Advanced Manufacturing Technology, vol. 112, no. 9-10, 2021, pp. 2859-2870.